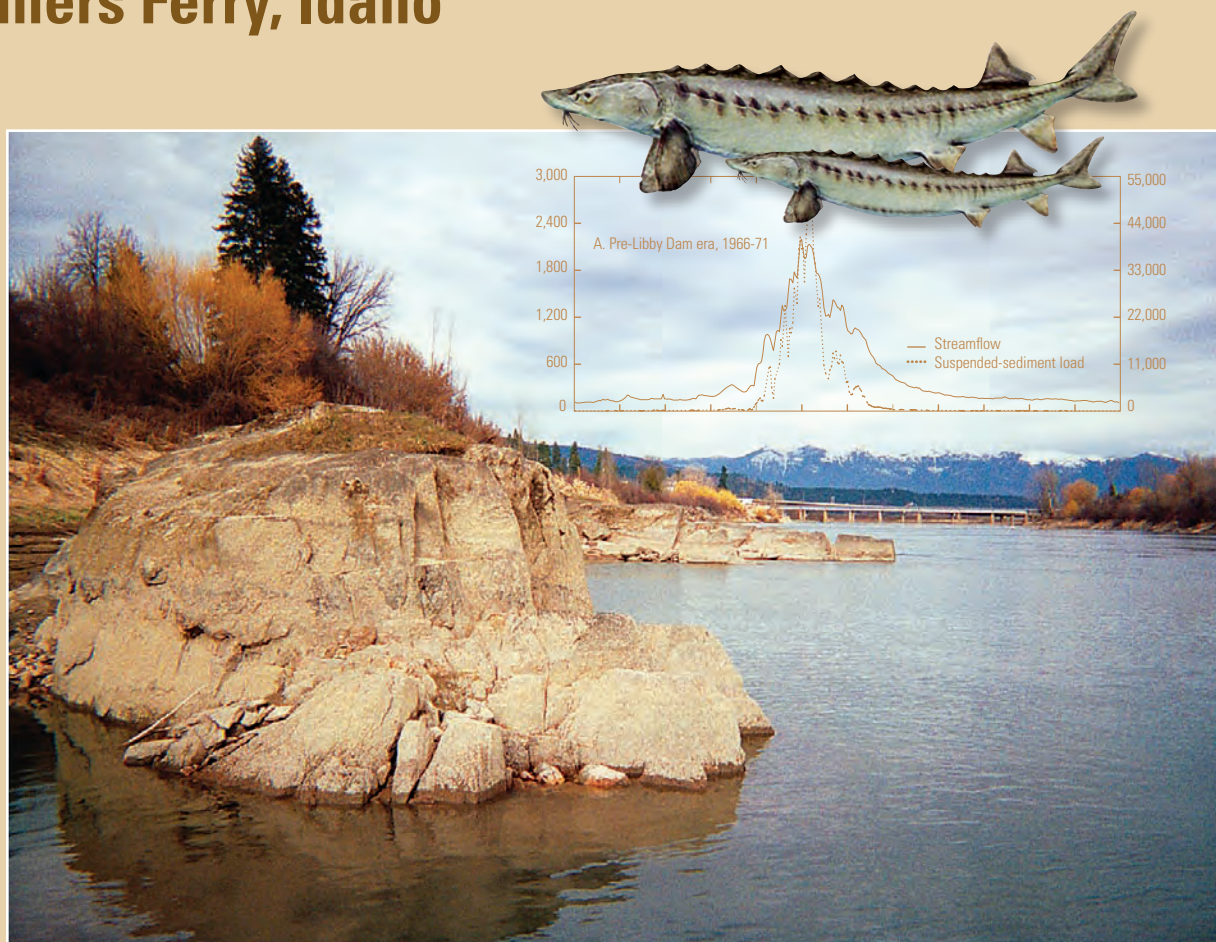


Prepared in cooperation with the
Kootenai Tribe of Idaho and
Bonneville Power Administration



Simulation of Flow and Sediment Mobility Using a Multidimensional Flow Model for the White Sturgeon Critical-Habitat Reach, Kootenai River near Bonners Ferry, Idaho



Scientific Investigations Report 2005–5230

Cover: Photograph of Kootenai River at Bonners Ferry, photograph taken near river kilometer 245. View facing upstream with bedrock outcropping in the foreground and the Union Pacific Railroad bridge in the background. (Photograph by Gary Barton, U.S. Geological Survey, April 2005.)

Simulation of Flow and Sediment Mobility Using a Multidimensional Flow Model for the White Sturgeon Critical-Habitat Reach, Kootenai River near Bonners Ferry, Idaho

By Gary J. Barton, Richard R. McDonald, Jonathan M. Nelson, and
Randal L. Dinehart

Prepared in cooperation with the Kootenai Tribe of Idaho and
Bonneville Power Administration

Scientific Investigations Report 2005-5230

U.S. Department of the Interior
U.S. Geological Survey

U.S. Department of the Interior
Gale A. Norton, Secretary

U.S. Geological Survey
P. Patrick Leahy, Acting Director

U.S. Geological Survey, Reston, Virginia: 2005

For sale by U.S. Geological Survey, Information Services
Box 25286, Denver Federal Center
Denver, CO 80225

For more information about the USGS and its products:
Telephone: 1-888-ASK-USGS
World Wide Web: <http://www.usgs.gov/>

Any use of trade, product, or firm names in this publication is for descriptive purposes only and does not imply endorsement by the U.S. Government.

Although this report is in the public domain, permission must be secured from the individual copyright owners to reproduce any copyrighted materials contained within this report.

Suggested citation:

Barton, G.J., McDonald, R.R., Nelson, J.M., and Dinehart, R.L., 2005, Simulation of flow and sediment mobility using a multidimensional flow model for the white sturgeon critical-habitat reach, Kootenai River near Bonners Ferry, Idaho: U.S. Geological Survey Scientific Investigations Report 2005-5230, 54 p.

Contents

Abstract	1
Introduction	2
Purpose and Scope	2
Acknowledgments	2
Description of the Study Reach	5
Physical Characteristics of the White Sturgeon Critical-Habitat Reach of the Kootenai River	7
Streamflow	7
Composition of Channel Substrate	10
Sediment-Transport Regime	13
River Channel Geometry	14
Bathymetry and Streambank Topography	14
Dunes and Other Bedforms	16
River Channel Degradation and Aggradation	16
Construction of the Multidimensional Flow Model	20
Computational Grid and Bathymetric Interpolation	20
Streamflow Velocity at the Upstream Model Boundary	22
Water-Surface Elevation at the Downstream Model Boundary	22
Model Calibration	22
Model Boundary Conditions for Calibration Runs	25
Drag Coefficient	25
Results	25
Model Validation	26
Model Sensitivity Analysis	31
Simulation of Flow and Sediment Mobility in the White Sturgeon Critical-Habitat Reach	34
Water-Surface Elevation Profiles and Free-Flowing and Backwater Streamflow	35
River Depth	36
Streamflow Velocity	37
Sediment Mobility	46
Model Limitations	49
Summary	49
References Cited	51
Appendix A. Processing Acoustic Doppler Current Profiler Data	53

Figures

Figure 1. Map showing location of study area, near Bonners Ferry, Idaho, and selected streamflow-gaging stations and dams in the Kootenai River drainage basin, Idaho, Montana, and British Columbia, Canada	3
Figure 2. Map showing location of the white sturgeon critical-habitat reach and upstream and downstream boundaries for the multidimensional flow model on the Kootenai River near Bonners Ferry, Idaho	4
Figure 3. Graph showing location and number of white sturgeon spawning events and spawning events per unit effort on the Kootenai River near Bonners Ferry, Idaho, 1994 to 2001	6
Figure 4. Graphs showing annual median daily streamflow and suspended-sediment load for the pre-Libby Dam era (1966–71) and Libby Dam era (1973–82) and annual streamflow and suspended-sediment load, 1966–82, Kootenai River at Copeland, Idaho.....	8
Figure 5. Graphs showing streamflow, water-surface elevation, and water-surface slope of the white sturgeon critical-habitat reach of the Kootenai River, Bonners Ferry, Idaho, and water-surface elevation of Kootenay Lake, 1965–2003	9
Figure 6. Map showing location of sediment core sites sampled in 2000 and 2004 on the white sturgeon critical-habitat reach of the Kootenai River near Bonners Ferry, Idaho	11
Figure 7. Map showing location of streambed-sediment sampling sites on the white sturgeon critical-habitat reach of the Kootenai River near Bonners Ferry, Idaho	12
Figure 8. Graph showing particle-size distribution for streambed sediment samples taken between river kilometers 228.4 and 245.8 on the white sturgeon critical-habitat reach of the Kootenai River near Bonners Ferry, Idaho	13
Figure 9. Graph showing daily mean flow and water-surface elevation for the white sturgeon critical-habitat reach of Kootenai River near Bonners Ferry, Idaho, 2002 and 2003.....	15
Figure 10. Map showing location of acoustic Doppler current profiler cross sections and longitudinal profiles for monitoring riverbed stability and bedforms on the white sturgeon critical-habitat reach of the Kootenai River near Bonners Ferry, Idaho	17
Figure 11. Graphs showing changes in bedforms along longitudinal profiles measured with an acoustic Doppler current profiler in the white sturgeon critical-habitat reach of the Kootenai River near Bonners Ferry, Idaho, 2002	18
Figure 12. Graphs showing aggradation and degradation of streambed at five cross sections of the white sturgeon critical-habitat reach of the Kootenai River near Bonners Ferry, Idaho, 2002	19
Figure 13. Aerial photographs showing nodes forming an approximately 5.0-by-5.0-meter grid in the multidimensional flow model at the upstream end of Shorty Island in the white sturgeon critical-habitat reach of the Kootenai River near Bonners Ferry, Idaho.....	21
Figure 14. Graph showing streamflow-velocity measurements at the upstream model boundary on the white sturgeon critical-habitat reach of the Kootenai River at Bonners Ferry, Idaho, June 1996 and April 2002	23

Figures—Continued

Figure 15. Graph showing drag and lateral eddy-viscosity coefficients for the calibrated multidimensional flow model of the white sturgeon critical-habitat reach of the Kootenai River near Bonners Ferry, Idaho	26
Figure 16. Map showing location of acoustic Doppler current profiler cross sections for validating the multidimensional flow model for the white sturgeon critical-habitat reach of the Kootenai River near Bonners Ferry, Idaho	27
Figure 17. Cross sections showing measured cross sections of vertically averaged velocities and corresponding simulated velocities on the white sturgeon critical-habitat reach of the Kootenai River near Bonners Ferry, Idaho, for a steady flow that averaged 538 cubic meters per second on August 12–14, 2003	28
Figure 18. Graph showing functional dependence of the drag coefficient on depth, used to improve simulated vertically averaged velocity at cross section 2313 on the Kootenai River near Bonners Ferry, Idaho	30
Figure 19. Cross sections showing measured vertically averaged velocity and simulated vertical velocity based on a constant drag coefficient and variable drag coefficient for cross-section 2313 on the white sturgeon critical-habitat reach of the Kootenai River near Bonners Ferry, Idaho, for a steady flow that averaged 538 cubic meters per second on August 12–14, 2003	30
Figure 20. Cross sections showing measured and simulated vertical profiles of downstream velocity and cross-stream velocity at section 2370 on the white sturgeon critical-habitat reach of the Kootenai River near Bonners Ferry, Idaho, for a steady flow that averaged 538 cubic meters per second on August 12–14, 2003	32
Figure 21. Graph showing simulated average water-surface elevation for five streamflows at cross sections positioned every 100 meters along the white sturgeon critical-habitat reach of the Kootenai River near Bonners Ferry, Idaho, and spawning event locations	36
Figure 22. Graph showing simulated average and maximum depth for five streamflows at cross sections positioned every 100 meters along the white sturgeon critical-habitat reach of the Kootenai River near Bonners Ferry, Idaho, and spawning event locations	37
Figure 23. Graph showing simulated average and maximum velocity for five streamflows at cross sections positioned every 100 meters along the white sturgeon critical-habitat reach of the Kootenai River near Bonners Ferry, Idaho, and spawning event locations	38
Figure 24. Graph showing standard deviation of simulated velocity for five streamflows at cross sections positioned every 100 meters along the white sturgeon critical-habitat reach of the Kootenai River near Bonners Ferry, Idaho, and spawning event locations	39
Figure 25. Aerial photographs showing distribution of simulated velocity for five streamflows in the white sturgeon critical-habitat reach of the Kootenai River near Bonners Ferry, Idaho	40
Figure 26. Graph showing simulated sediment mobility and critical shear stress for five streamflows at cross sections positioned every 100 meters along the white sturgeon critical-habitat reach of the Kootenai River near Bonners Ferry, Idaho, and spawning event locations	48

Tables

Table 1. Amplitude and wavelength of dune bedforms in the white sturgeon critical-habitat reach of the Kootenai River, near Bonners Ferry, Idaho	16
Table 2. Calibration summary for the multidimensional hydraulic flow model for the white sturgeon critical-habitat reach of the Kootenai River, near Bonners Ferry, Idaho	24
Table 3. Sensitivity analysis and results of the multidimensional flow model for the white sturgeon critical-habitat reach of the Kootenai River near Bonners Ferry, Idaho, for five streamflows	34
Table 4. Upstream and downstream boundary conditions in the multidimensional flow model for the white sturgeon critical-habitat reach of the Kootenai River near Bonners Ferry, Idaho	35
Table 5. Sediment grade scale and critical shear stress for determining approximate condition for sediment mobility at 20 degrees Celsius	46

Conversion Factors and Datums

Conversion Factors

Multiply	By	To obtain
centimeter (cm)	0.3937	inch
cubic meter per day (m ³ /d)	35.31	cubic foot per day
cubic meter per day (m ³ /d)	264.2	gallon per day
cubic meter per second (m ³ /s)	70.07	acre-foot per day
cubic meter per second (m ³ /s)	35.31	cubic foot per second
kilometer (km)	0.6214	mile
meter (m)	3.281	foot
meter per second (m/s)	3.281	foot per second
metric ton per day (mt/d)	1.102	ton per day
millimeter (mm)	0.03937	inch
square kilometer (km ²)	247.1	acre
square kilometer (km ²)	0.3861	square mile
square meter (m ²)	0.0002471	acre

Pressure: 1 Pascal (Pa) = 1N/m² = 6.895 kPa.

Temperature in degrees Celsius (°C) may be converted to degrees Fahrenheit (°F) as follows:

$$^{\circ}\text{F}=(1.8\times^{\circ}\text{C})+32.$$

Datums

Vertical coordinate information is referenced to the North American Vertical Datum of 1988 (NAVD 88).

Horizontal coordinate information is referenced to the North American Datum of 1983 (NAD 83), Idaho Transverse Mercator—North American Datum 1983/1998 Idaho West, in meters.

Simulation of Flow and Sediment Mobility Using a Multidimensional Flow Model for the White Sturgeon Critical-Habitat Reach, Kootenai River near Bonners Ferry, Idaho

By Gary J. Barton, Richard R. McDonald, Jonathan M. Nelson, and Randal L. Dinehart

Abstract

In 1994, the Kootenai River white sturgeon (*Acipenser transmontanus*) was listed as an Endangered Species as a direct result of two related observations. First, biologists observed that the white sturgeon population in the Kootenai River was declining. Second, they observed a decline in recruitment of juvenile sturgeon beginning in the 1950s with an almost total absence of recruitment since 1974, following the closure of Libby Dam in 1972. This second observation was attributed to changes in spawning and (or) rearing habitat resulting from alterations in the physical habitat, including flow regime, sediment-transport regime, and bed morphology of the river. The Kootenai River White Sturgeon Recovery Team was established to find and implement ways to improve spawning and rearing habitat used by white sturgeon. They identified the need to develop and apply a multidimensional flow model to certain reaches of the river to quantify physical habitat in a spatially distributed manner. The U.S. Geological Survey has addressed these needs by developing, calibrating, and validating a multidimensional flow model used to simulate streamflow and sediment mobility in the white sturgeon critical-habitat reach of the Kootenai River. This report describes the model and limitations, presents the results of a few simple simulations, and demonstrates how the model can be used to link physical characteristics of streamflow to biological or other habitat data. This study was conducted in cooperation with the Kootenai Tribe of Idaho along a 23-kilometer reach of the Kootenai River, including the white sturgeon spawning reach near Bonners Ferry, Idaho that is about 108 to 131 kilometers below Libby Dam.

U.S. Geological Survey's MultiDimensional Surface-Water Modeling System was used to construct a flow model for the critical-habitat reach of the Kootenai River white sturgeon, between river kilometers 228.4 and 245.9. Given streamflow, bed roughness, and downstream water-surface elevation, the model computes the velocity field, water-surface elevations, and boundary shear stress throughout the modeled reach. The 17.5 kilometer model reach was subdivided into two segments on the basis of predominant grain size: a straight reach with a sand, gravel, and cobble substrate located between the upstream model boundary at river kilometer 245.9

and the upstream end of Ambush Rock at river kilometer 244.6, and a meandering reach with a predominately sand substrate located between upstream end of Ambush Rock and the downstream model boundary at river kilometer 228.4. Model cell size in the x and y (horizontal) dimensions is 5 meters by 5 meters along the computational grid centerline with 15 nodes in the z (vertical) dimension. The model was calibrated to historical streamflows evenly distributed between 141.6 and 2,548.9 cubic meters per second. The model was validated by comparing simulated velocities with velocities measured at 15 cross sections during steady streamflow. These 15 cross sections were each measured multiple (7–13) times to obtain velocities suitable for comparison to the model results. Comparison of modeled and measured velocities suggests that the model does a good job of reproducing flow patterns in the river, although some discrepancies were noted.

The model was used to simulate water-surface elevation, depth, velocity, bed shear stress, and sediment mobility for Kootenai River streamflows of 170, 566, 1,130, 1,700, and 2,270 cubic meters per second (6,000, 20,000, 40,000, 60,000, and 80,000 cubic feet per second). The three lowest streamflow simulations represent a range of typical river conditions before and since the construction of Libby Dam, and the highest streamflow simulation (2,270 cubic meters per second) is approximately equal to the annual median peak streamflow prior to emplacement of Libby Dam in 1972. Streamflow greater than 566 cubic meters per second were incrementally increased by 570 cubic meters per second. For each of the five streamflow simulations, the average, maximum, and standard deviation of water-surface elevation, depth, velocity, and sediment mobility were quantified at 174 cross sections of the river channel (positioned every 100 meters along the length of the model reach). Simulated conditions along the critical-habitat reach were compared with locations of white sturgeon spawning events, based on the number of spawning events per unit of effort during 1994–2001, to demonstrate how the model can be used to relate observed spawning or other observed habitat-related behavior to local physical characteristics of the river. With further applications focused on specific spawning or rearing habitat questions, the model potentially is a useful tool for relating river flows to quantitative assessments of habitat quality and quantity.

Introduction

Many local, State, and Federal agencies are concerned about the declining population of white sturgeon (*Acipenser transmontanus*) in the Kootenai River in Idaho (fig. 1). In 1994, Kootenai River white sturgeon was listed as an Endangered Species, and fishing for this species was prohibited. The decrease in the white sturgeon population apparently is driven by an overall decline in spawning success, as reflected by the presence of few juvenile sturgeon (U.S. Fish and Wildlife Service, 1999). Observations suggest that a decline in recruitment of white sturgeon began in the 1950s and the last successful recruitment was in 1974 (Paragamian and others, 2005). (Recruitment refers a spawning event that produces juvenile fish that survive to create a new year-class of fish in sufficient numbers to maintain fish population.) Lack of Kootenai River white sturgeon recruitment has been attributed, at least in part, to changes in the natural streamflow regime of the Kootenai River after emplacement of Libby Dam, near Libby, Montana, in 1972 (U.S. Fish and Wildlife Service, 1999). The reservoir upstream of the dam, Lake Koocanusa, completely filled in 1974. Accompanying changes in the flow hydrograph, sediment supply, and bed morphology downstream of the dam are hypothesized to have adversely affected distribution of channel substrate and other elements of sturgeon spawning habitat near Bonners Ferry, Idaho (fig. 2; Collier and others, 1996). Other changes in the Kootenai River that could have affected sturgeon recruitment include the construction of dikes on natural levees, changes in backwater conditions near Bonners Ferry caused by changes in the level of Kootenay Lake, loss of wetlands in the river valley, reduction of the river's nutrient load, and fishing.

The Kootenai River White Sturgeon Recovery Team, composed of scientists and engineers from the Kootenai Tribe of Idaho (KTOI), Idaho Department of Fish and Game, and several local, State, Federal, and Canadian agencies, is trying to reestablish recruitment of white sturgeon by developing a better understanding of the physical factors affecting quality and quantity of spawning and rearing habitat, and by using that understanding to design and implement ways to improve that habitat. In view of these goals, the Recovery Team has a need to relate observed biological behavior (for example, spawning) to local physical characteristics of the river. Establishing these relations requires riverine-flow and sediment-transport models that provide spatially distributed (at a point) simulation of physical characteristics of the river. In response to this need, the U.S. Geological Survey (USGS), in cooperation with the KTOI, during a 4-year study collected hydraulic, topographic, and sediment data that were used to develop a multidimensional flow model and a 1-dimensional sediment-transport model of the white sturgeon critical-habitat reach near Bonners Ferry, Idaho (fig. 2). These models can be used as tools to quantify the local characteristics of the flow and sediment transport and can also serve to assess the feasibility of various habitat-enhancement scenarios to

re-establish recruitment of white sturgeon. For example, modeling assessments might be used to (1) determine whether a proposed spawning substrate structure will be susceptible to erosion or deposition, (2) test that streamflow velocity at a proposed spawning-substrate structure will be high enough to minimize egg predation for a given flow, or (3) identify potential hydraulic cues used by white sturgeon to initiate spawning. Although both models simulate water-surface elevation, depth, velocity, shear stress, and sediment-transport characteristics, the 1-dimensional model provides only a single cross-sectionally averaged value at each river cross section, whereas the multidimensional model provides those values at every location in the river. The 1-dimensional model is described in detail by Berenbrock and Bennett (2005).

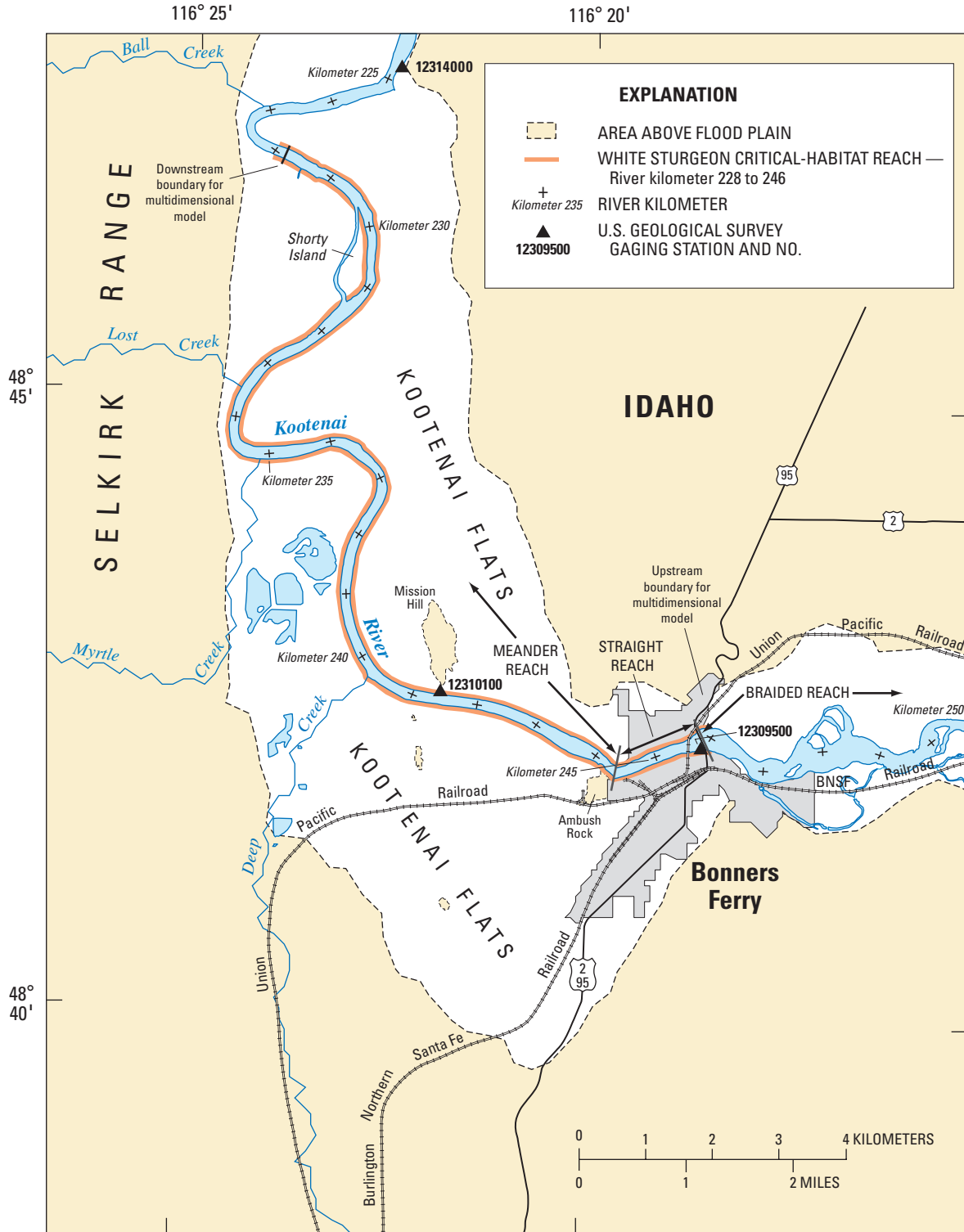
Purpose and Scope

The purposes of this report are to (1) discuss construction, calibration, and validation of the multidimensional flow model used to simulate streamflow and sediment mobility in the white sturgeon critical-habitat reach of the Kootenai River; (2) present results of a few simple simulations and demonstrate how the model can be used to link physical characteristics of streamflow to biological or other habitat data; and (3) discuss limitations of the model. Data needed for the study included general channel characteristics, channel topography and bathymetry, particle grain-size distributions making up the channel bed, bedform presence and geometry, water-surface elevations, and streamflow velocity.

Acknowledgments

The authors thank the people of the Kootenai River Valley in Idaho, Montana, and British Columbia who provided access to the Kootenai River for surveying. Sue Ireland of the KTOI provided storage facilities for USGS boats and equipment. Vaughn Paragamian, Diane Wakkinen, and Peter Rust of Idaho Department of Fish and Game (IDFG) provided white sturgeon spawning location and egg location data. The authors also appreciate that the KTOI collected suspended-sediment samples from the Kootenai River at Bonners Ferry and provided logistical support for field work. Rick Backsen, John Gralow, and Russ Christensen of USGS in Post Falls, Idaho, Edward Moran of USGS in Anchorage, Alaska, and Charles Berenbrock of USGS in Boise, Idaho, worked long hours collecting data on the Kootenai River for this project. Sandra Ball of USGS in Post Falls, Idaho, helped with many logistic issues. Kimberly Mueller, student, and Theresa Olsen, with USGS in Tacoma, Washington, entered survey control field measurements into the National Geodetic Survey database and provided geographical information systems support. Mary Donato of USGS in Boise, Idaho, provided a graphical illustration of IDFG's white sturgeon spawning and egg location data.

4 Simulation of Flow and Sediment Mobility Using Multidimensional Model, Kootenai River near Bonners Ferry, Idaho



Base from U.S. Geological Survey digital data, 1:100,000, 1983
 Universal Transverse Mercator projection, Zone 13

Figure 2. Location of the white sturgeon critical-habitat reach and upstream and downstream boundaries for the multidimensional flow model on the Kootenai River near Bonners Ferry, Idaho.

Description of the Study Reach

Kootenai River begins in British Columbia, Canada, flows through Montana and Idaho, and then turns northwest back into British Columbia ([fig. 1](#)). Kootenai River is referred to as the Kootenay River in British Columbia. For the purpose of this report and as a matter of convenience, the United States spelling (Kootenai) will be used when referring to the river and the Canadian spelling (Kootenay) will be used when referring to the lake, which is located entirely within British Columbia, Canada. The drainage basin is within the Northern Rocky Mountains physiographic province, which is characterized by north- to northwest-trending mountain ranges. The Rocky Mountains form much of the eastern basin boundary, the Selkirk Mountains form the western basin boundary, and the Cabinet Mountains form the southern basin boundary. Kootenai River is 721 kilometers (km) long and drains an area of 45,584 square kilometers (km²). The study area is a reach of Kootenai River near Bonners Ferry, Idaho, which comprises the spawning habitat for the Kootenai River population of endangered white sturgeon ([figs. 1](#) and [2](#)). The designated critical habitat for white sturgeon ranges from river kilometer (RKM) 225.0 to 246.7 ([fig. 2](#); U.S. Fish and Wildlife Service, 2000). Litigation may result in extending the critical-habitat reach further upstream (Bob Hallock, U.S. Fish and Wildlife Service, oral commun., 2006).

The altitude at the headwaters of the river in British Columbia is 3,618 meters (m). Kootenai Falls, where the river loses 61 m of altitude over a distance of about 100 m, is the only waterfall between Libby Dam and Kootenay Lake and is 46 km downstream of the dam. Kootenai Falls forms a natural fish-migration barrier. At Bonners Ferry, 111 km downstream of Libby Dam near the upstream end of the white sturgeon critical habitat, Kootenai River flows westward into a nearly straight, northwest-trending, 480-km-long trough known as the Purcell Trench. The Purcell Trench is flanked by the Selkirk Mountains on the west and by the Purcell Mountains on the east. Here, the river meanders northwest through the broad, flat bottomlands referred to as Kootenai Flats ([figs. 1](#) and [2](#)) for about 80 km to Kootenay Lake near Creston, British Columbia. Kootenai River then flows from the lower end of the West Arm of Kootenay Lake for about 32 km and empties into the Columbia River at Castlegar, British Columbia. Bonnington Falls, with its series of four dams, including Corra Lynn Dam, isolates white sturgeon from other populations of fish in the Columbia River Basin. This disconnection apparently is not recent; a natural barrier at Bonnington Falls has isolated the Kootenai River white sturgeon for approximately 10,000 years (Northcote, 1973).

Snyder and Minshall (1996) classified three geomorphic reaches in the Kootenai River between Libby Dam and Kootenay Lake: a canyon reach, a braided reach, and a meander reach. The canyon reach extends from Libby Dam to 2 km downstream of the mouth of Moyie River. Here, the valley broadens and the river forms a low-gradient braided reach as it courses over gravel and cobbles. This braided reach extends downstream into the study area to a bedrock constriction near the U.S. Highway 95 Bridge over Kootenai River at Bonners Ferry. A straight reach between RKM 245.9 and 244.5 forms a transition zone between the meandering reach and the braided reach. This straight reach was first described by Tetra Tech, Inc. (2003). The meander reach is sandy and extends from RKM 244.5, about 4.5 km upstream of the mouth of Deep Creek, to its confluence with Kootenay Lake ([figs. 1](#) and [2](#)).

The white sturgeon critical-habitat reach includes the lower part of the braided and entire straight reach, but known spawning sites are within the straight and meandering reaches. During the initial years of monitoring white sturgeon over the spawning season (1992-93), mats used by biologist for egg collection were placed upstream, within, and downstream of the critical-habitat reach, but spawning was seldom detected in the upstream and downstream areas. Since 1994, egg mats were placed over most of the critical-habitat reach. Since 1996, egg collection has been limited to the deepest areas of the river (V.L. Paragamian, Idaho Department of Fish and Game, oral commun., 2005). Paragamian and others (2001, 2002) identified five primary white sturgeon spawning reaches in the Kootenai River in the meandering reach between RKM 228.0 to 240.0 and concluded that spawning occurs mostly in the outsides of meander bends in the thalweg ([fig. 3](#)). However, during 2001 these same investigators observed spawning in the straight reach at RKM 245.1 and 245.7.

The multidimensional flow model was developed for the 17.5-km critical-habitat reach between RKM 228.4 and RKM 245.9, and includes all observed spawning sites ([fig. 2](#)). The model reach was subdivided into two reaches to reflect the distinct type of sediment forming the river substrate: (1) the straight reach which has a sand, gravel, cobble substrate between the upstream model boundary (RKM 245.9) and the upstream end of Ambush Rock (RKM 244.6); and (2) the meandering reach which primarily consists of a sand substrate between upstream end of Ambush Rock and the downstream model boundary (RKM 228.4). In addition, the model reach was divided into three velocity zones based on the velocity structure characteristics within each zone, as discussed in the section Streamflow Velocity.

6 Simulation of Flow and Sediment Mobility Using Multidimensional Model, Kootenai River near Bonners Ferry, Idaho

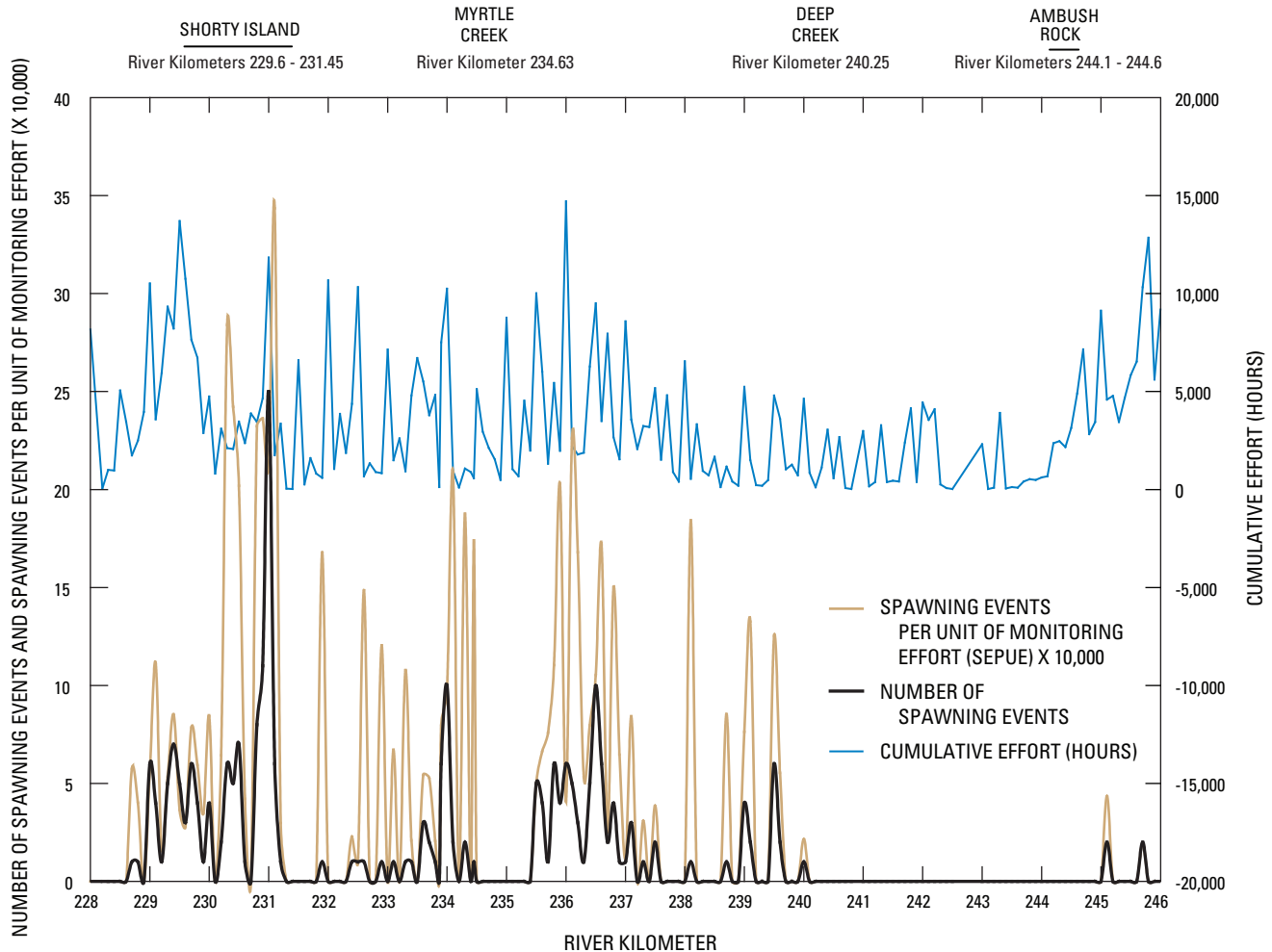


Figure 3. Location and number of white sturgeon spawning events and spawning events per unit effort on the Kootenai River near Bonners Ferry, Idaho, 1994 to 2001. (Paragamian and Wakkinen, Idaho Department of Fish and Game, written commun., 2005.)

The width of Kootenai River in the model reach ranges from about 65 to 255 m when streamflow is below flood stage. This reach includes two major tributaries, Deep Creek at RKM 240.25 and Myrtle Creek at RKM 234.63. Channel geometry in the reach varies greatly. The channel is shallow and straight between the U.S. Highway 95 Bridge and Ambush Rock and a few gravel bars are exposed at low flow; downstream of Deep Creek, it meanders and divides around Shorty Island, between RKM 229.6 and RKM 231.45. Morphology of the Kootenai River near the mouth of Myrtle Creek and at Shorty Island is distinct. Near Myrtle Creek, the river forms an S-shaped meander and has a maximum width of 200 m. Shorty Island is in a gentle meander and divides the flow into a main and a secondary channel over its 1,400-m length. Kootenai River

near Myrtle Creek displays morphology typical of meander bends, with the thalweg along the outside of the bend and point bars along the inside of the river bend (Henderson, 1966, figs. 10-25). In contrast, near the upstream end of Shorty Island between RKM 229.97 and RKM 230.45, the thalweg is in the center of the channel and is incised in lacustrine clay and silt (Barton, 2004, fig. 23P). The thalweg is on the outside of the river bend in the rest of this reach. Variations in channel curvature, morphology, and grain size over the model reach are important considerations in constructing a flow model that can provide spatially distributed information for linkage to biological data. The multidimensional model used here is sufficiently general to address these variations.

Physical Characteristics of the White Sturgeon Critical-Habitat Reach of the Kootenai River

Application of a 2- or 3-dimensional flow model to a river like the Kootenai requires streamflow information, topography and bathymetry with sufficient detail to characterize the channel, water-surface elevations for boundary conditions, substrate grain-size, and bedform information for characterization of roughness, and, ideally, measurements of water-surface elevation and velocity to calibrate and validate the model. Physical characteristics used in this study are based on data from previous studies, historical USGS data, and data collected by USGS in the critical-habitat reach during 2000-04 as part of this study. Most of the historical data on streamflow and sediment regime are from 1965 through 2004; therefore, the construction and calibration of the flow model for the critical-habitat reach are based on data from that period.

Streamflow

One of the most essential model inputs both for determining model results and for relating results to biological observations is discharge in the river, or streamflow. A significant part of streamflow information used for model construction is based on records from the Bonners Ferry stage-gaging station (12309500) at RKM 245.9, the Tribal Hatchery stage, velocity, and streamflow-gaging station (12310100) at RKM 241.3, the Klockmann Ranch stage-gaging station (12314000) at RKM 224.0, the Copeland stage and streamflow-gaging station (12318500) at RKM 198.2, the Boundary Creek stage and streamflow-gaging station (12321500), which empties into Kootenai River at RKM 170.6, and the Porthill stage and streamflow-gaging station (12322000) at RKM 170.3. Typically, model runs can be constructed based on streamflow and water-surface elevation from a single measurement site on the mainstream and appropriate streamflow information from major tributaries, but the influence of backwater effects from Kootenay Lake on the study reach makes multiple gaging station locations important for this model.

The operation of Corra Linn Dam and Libby Dam also affect backwater conditions. The altitude of the river is about 532 m at its confluence of Kootenay Lake, located behind Corra Linn Dam and about 235 km downstream of Libby Dam (fig. 1). Corra Linn Dam was completed in 1931 and is operated for hydroelectric power, which affects water levels in

Kootenay Lake and, consequently, in the backwater-affected reach of Kootenai River (Duke and others, 1999). The river channel upstream of the dam at Grohman Narrows was deepened in 1939 to help maintain a lower lake water-surface elevation at Nelson and, thus, a lower river water-surface elevation at Bonners Ferry (Pacific Watershed Institute, written commun., 1999). Kootenay Lake creates backwater conditions in Kootenai River to a variable point upstream of the mouth of Deep Creek (RKM 240.25) near Bonners Ferry. During May, June, and early July, when lake water-surface elevation and river discharge are high, backwater conditions can extend several kilometers upstream of the U.S. Highway 95 Bridge (RKM 245.9) at Bonners Ferry (fig. 2). During periods of low streamflow, backwater conditions diminish and free-flowing water may extend a few kilometers downstream of the U.S. Highway 95 Bridge. A detailed analysis of the contact location between the free-flowing river and backwater under a range of streamflow conditions is presented in Berenbrock (2005). Construction of Libby Dam began in 1966, and Lake Koocanusa was officially impounded behind the dam on March 21, 1972. Libby Dam is operated for flood protection, hydroelectric power, and recreation. Streamflow and water-surface elevation boundary conditions used in the model depend significantly on the operation of both dams.

The pre-Libby Dam-era flow regime for Kootenai River during the period of suspended sediment record at the Copeland gaging station (12318500), 1966-71, is characterized by peak streamflows resulting from spring snowmelt from late April through mid-July (fig. 4). During the pre-Libby Dam era, median annual peak streamflow was about 2,237 m³/s. A slow recession of streamflow generally started in mid-June and stabilized in September. The annual median base streamflow during October through February was 88.0 m³/s. The average cross-sectional velocity for 62 measurements from the cableway at the Copeland gaging station ranged from 0.06 to 1.21 m/s.

The Libby Dam-era flow regime for Kootenai River during the period of suspended-sediment record at the Copeland gaging station, 1973-82 (fig. 4), is characterized by median annual peak streamflows of about 600 m³/s, less than one-third of the pre-Libby Dam value. Long periods of sustained higher flows were during the autumn and winter, reflecting the greater demand for hydroelectric power generation. Average cross-sectional velocity during 83 measurements from the cableway at the Copeland gaging station ranged from 0.11 to 0.80 m/s. The peak cross-sectional velocity during the Libby Dam era was about one-half that of the pre-Libby Dam era.

8 Simulation of Flow and Sediment Mobility Using Multidimensional Model, Kootenai River near Bonners Ferry, Idaho

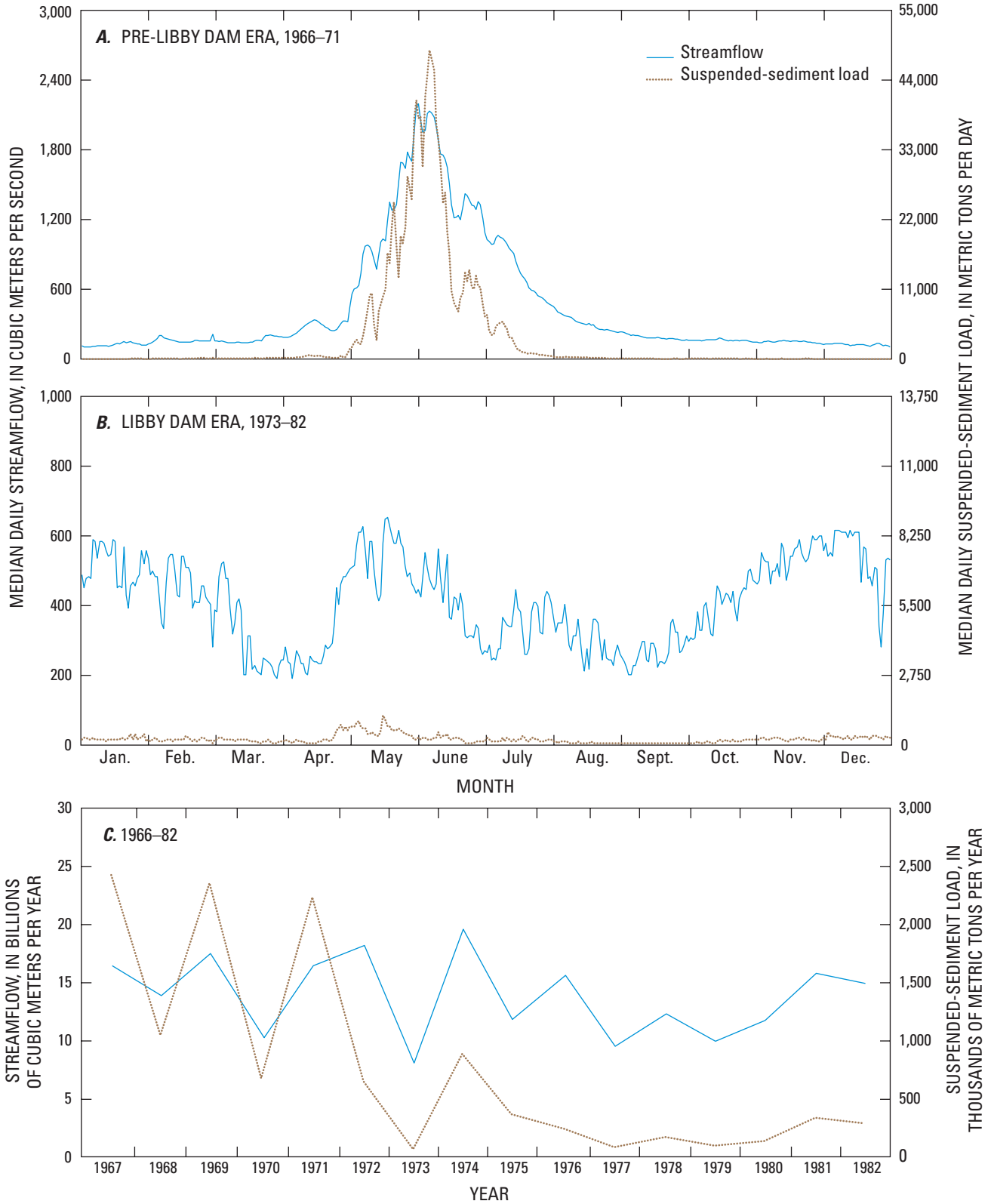


Figure 4. Annual median daily streamflow and suspended-sediment load for the pre-Libby Dam era (1966–71) and Libby Dam era (1973–82) and annual streamflow and suspended-sediment load, 1966–82, Kootenai River at Copeland, Idaho. (Data from U.S. Geological Survey streamflow-gaging station 12318500; from Barton, 2004.)

The difference in water-surface elevation between the gaging station at Klockmann Ranch (12314000), at the downstream model boundary of the critical-habitat reach of the Kootenai River, and Kootenay Lake (08NH064) remained small over the period of streamflow record, 1965–2003, at the Porthill gaging station (fig. 5). The slope of the reach was computed as the water-surface elevation at Bonners Ferry (12309500) minus water-surface elevation at Klockmann Ranch divided by the distance between the two gaging stations. Backwater conditions in the critical-habitat reach result in gentle water-surface slopes (fig. 5). Slope is reported as a reach average that approximates conditions in the critical-habitat reach. Median daily slope in the reach during the pre-Libby Dam era (1965–71) was 0.000018 and during the Libby-Dam era (1973–2003) was 0.000027. The difference in daily water-surface elevation between Klockmann Ranch and Queens Bay on Kootenay Lake during the pre-Libby Dam era was 0.59 m and during the Libby-Dam era was 1.13 m.

To augment existing water-surface elevation and streamflow data, the USGS began operating gaging station 12310100 at the KTOI Tribal Hatchery near Bonners Ferry

at RKM 241.5, in October 2002. The gaging station was equipped with an acoustic Doppler velocity meter. Streamflow at the gaging station during the period of record through April 12, 2004, ranged from 120 to 892 m³/s and average cross-sectional velocity ranged from 0.17 to 0.75 m/s.

Since the mid-1990s, the U.S. Fish and Wildlife Service has requested that Kootenai River flows be increased during white sturgeon spawning in May and June in an attempt to help re-establish recruitment. Kootenai River flows are augmented with additional release of water from Libby Dam; however, flow during spawning season is less than one-half that of the pre-Libby Dam era.

Additional information about streamflow, as well as sediment-transport regime, in Kootenai River can be obtained in reports by Berenbrock and Bennett (2005) who developed the 1-dimensional sediment-transport model of the white sturgeon critical-habitat reach, Berenbrock (2005), who developed a 1-dimensional hydraulic model of Kootenai River throughout Idaho, and Barton (2004), who analyzed streamflow and suspended-sediment load measured at the Copeland gaging station (12318500) during 1966–82.

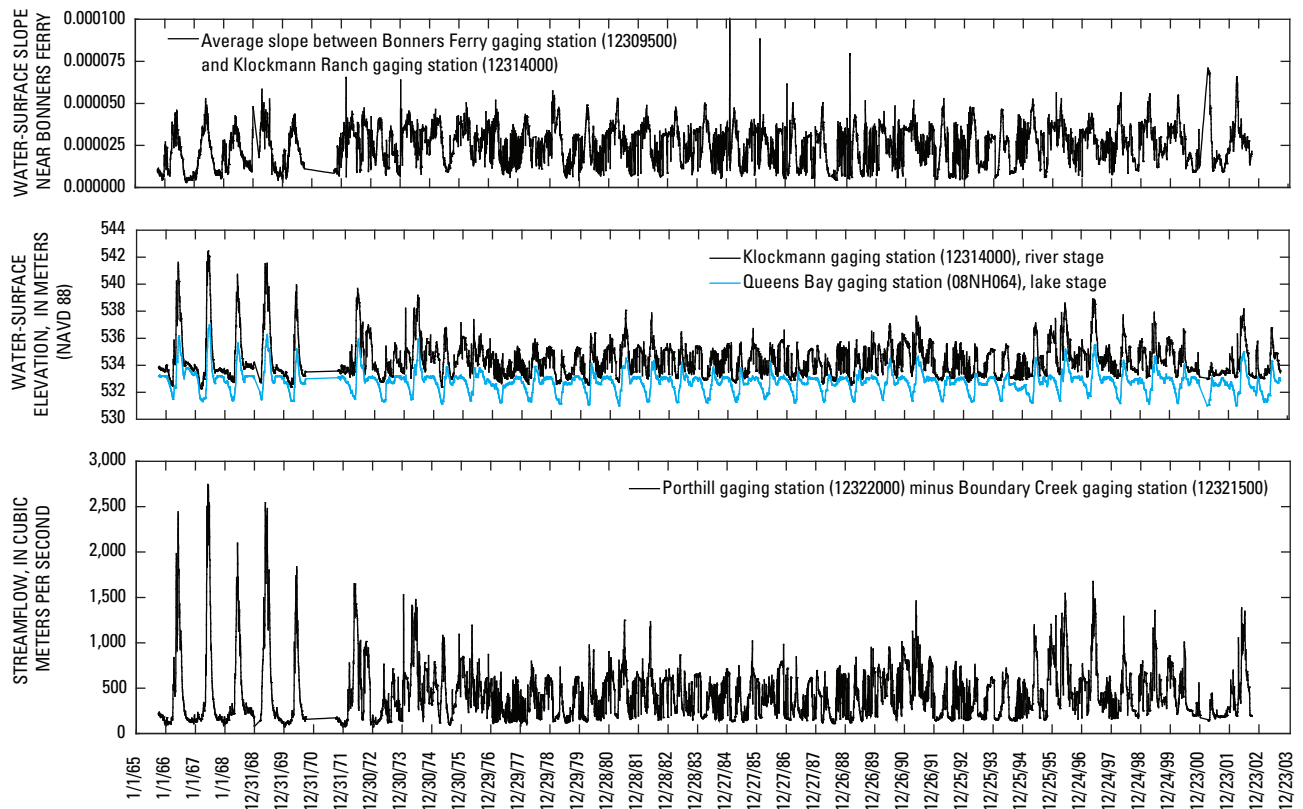


Figure 5. Streamflow, water-surface elevation, and water-surface slope of the white sturgeon critical-habitat reach of the Kootenai River, Bonners Ferry, Idaho, and water-surface elevation of Kootenay Lake, 1965–2003.

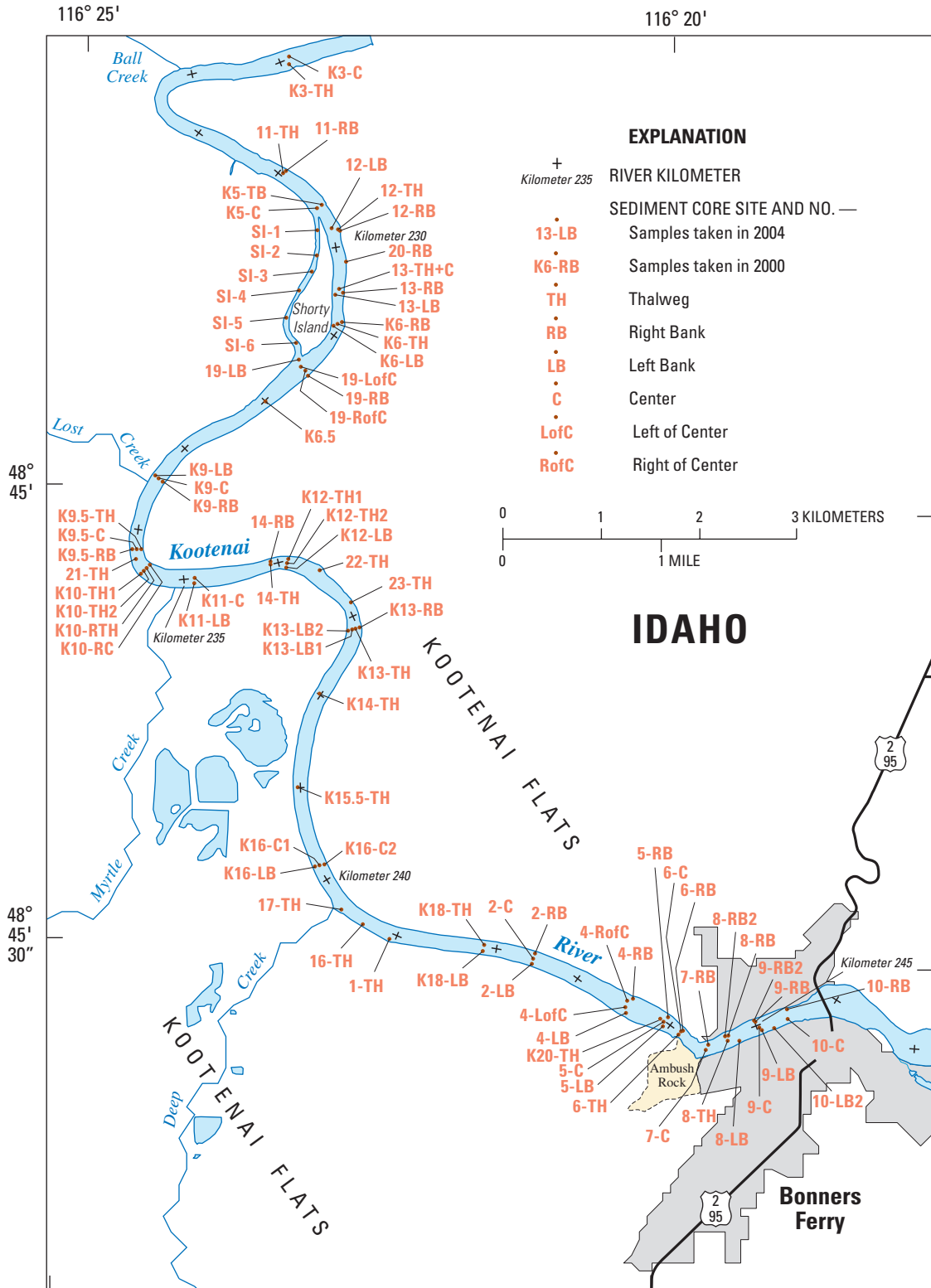
Composition of Channel Substrate

One goal of the modeling program was to demonstrate how the model can be used to link physical characteristics of streamflow to biological or other habitat data, such as predicting sediment movement for various streamflows. To obtain the required information, sediment cores and surface sediment samples were collected during this study to refine the characterization of the composition of the channel substrate. Fifty-one cores of riverbed sediment were collected from RKM 245.4 to RKM 228.0 during September 2004. (fig. 6). A 7.3-m pontoon coring boat was used for taking vibracores and piston cores of sediment beneath the riverbed. Core sites were referenced spatially using a global positioning system (GPS). Two to four sediment cores were usually taken at a cross section of the river. Generally, one core was taken from the thalweg and another in shallower water. The vibracoring system is equipped with a 0.08-m diameter core barrel that is 3.66 m long and can recover clay, silt, sand, gravel, and some cobble. The maximum substrate penetration by the core during data collection was 3.3 m.

Several gravel bars are in the upper half of the straight reach. The substrate is composed of gravel and some cobble, some alluvial sand, and a few bedrock outcrops. The river bed in the meandering reach is dominated by sand dunes, and the substrate consist mainly of fine to medium sand, with minor amounts of lacustrine clay and silt that typically are detected in the thalweg and along the outside bank of meanders. In a few cases, gravel, cobble, and riprap are on the riverbed in the meandering reach. Riprap is erosion resistant ground cover consisting of large, loose, angular stone. Sediments generally are in limited areas along the outside of meander bends, where velocities are highest in the bend. At least some of these sediments are not naturally occurring and were placed to protect the dikes that line the river. Some riprap has rolled down the toe of the dike into the channel. In addition, below the mouth of Myrtle Creek between RKM 234.20 and 234.60, Barton (2004) identified gravel, cobble, and riprap on the

riverbed that is exposed or buried by a thin layer of sand. The source of these gravels and cobbles may be an alluvial fan at the base of Cascade Ridge or the sediment that forms the dike. Small, isolated gravel lenses buried by a thin layer of sand also were identified at RKM 241.6 and 243.8, between Ambush Rock and Mission Hill.

Particle-size distribution of the sediment that forms the substrate in the critical-habitat reach was measured during this study. The Kootenai Tribe of Idaho collected bed-material samples between RKM 226 and 244.3 on June 20, 2000. These samples were taken with a ponar dredge sampler at 22 sites located near mid-channel and near the riverbanks (fig. 7). In addition, six grab samples were collected from exposed gravel bars in the straight reach during March 2002 (fig. 7). A subset of 12 samples from the 2000 sampling and 3 samples from the 2002 sampling were sent to the USGS Cascades Volcanic Observatory Sediment Laboratory for $\frac{1}{2}$ phi particle size analysis. Average particle sizes for the set of samples from the meandering reach are D_{16} , 0.15 millimeters (mm), D_{50} , 0.23 mm, and D_{84} , 0.33 mm, classified as fine to medium sand (0.063 to 0.25 mm, very fine to fine sand; 0.25 to 0.50 mm, medium sand). Particle-size distribution data (fig. 8), along with geologist logs from vibracores and piston cores, show that the riverbed in the meandering reach is covered with sediment of nearly consistent size. Particle-size distribution of these bed-sediment samples is much smaller than in the set of samples collected further upstream between U.S. Highway 95 Bridge and Ambush Rock, where D_{50} was 15.5 mm, which represents gravel- and cobble-size sediment. Studies on the white sturgeon in the Lower Columbia River (Parsley and Beckman, 1994), suggest that the particle size of substrate in the straight reach has poor to moderate suitability for egg incubation and in the meander reach has poor suitability. Isolated areas in the meander reach may be better suited for egg incubation where gravel is present and not buried by sand, such as below the mouth of Myrtle Creek between RKM 234.20 and 234.60 (Barton, 2004).



Base from U.S. Geological Survey digital data, 1:100,000, 1983
 Universal Transverse Mercator projection, Zone 13

Figure 6. Location of sediment core sites sampled in 2000 and 2004 on the white sturgeon critical-habitat reach of the Kootenai River near Bonners Ferry, Idaho.

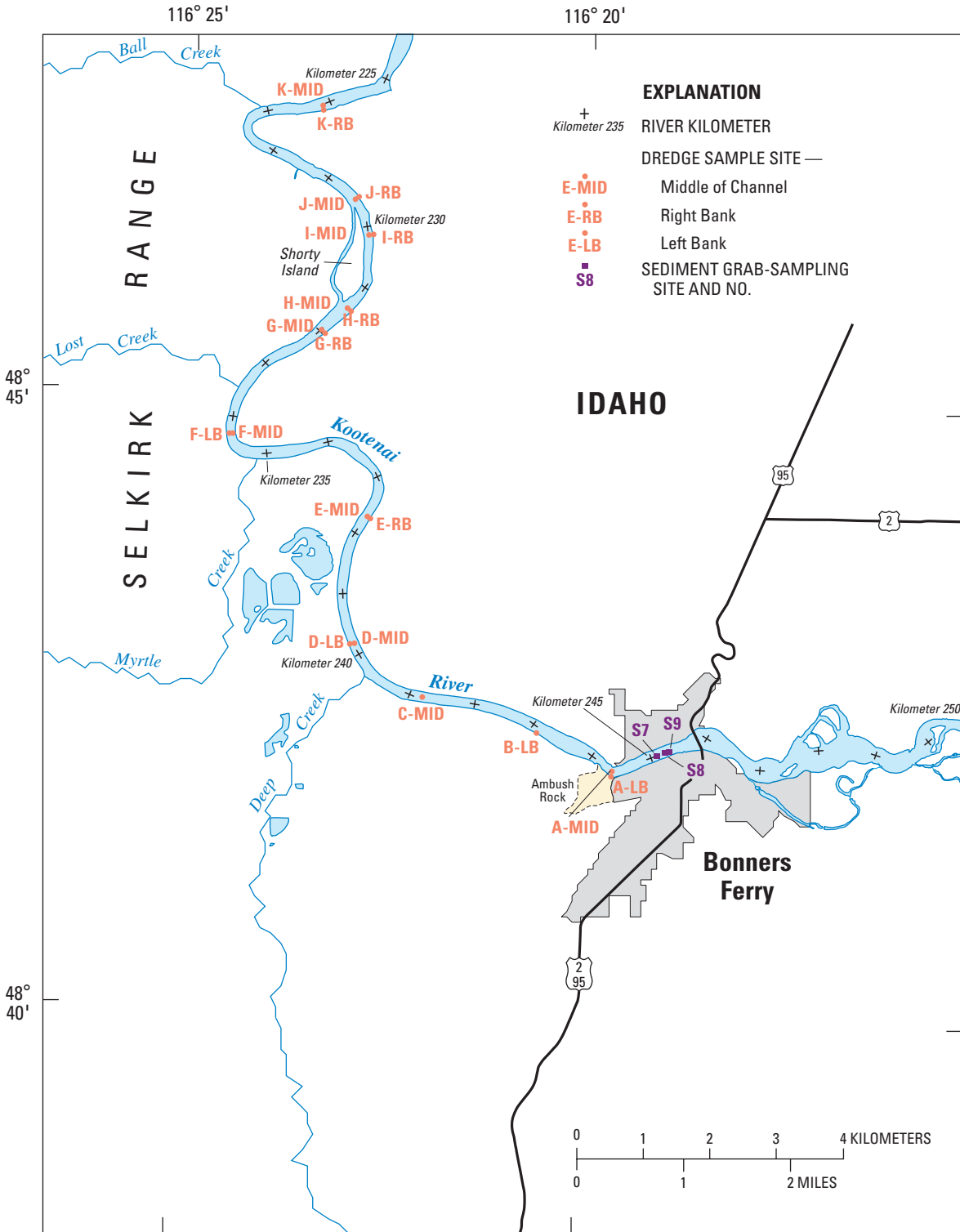


Figure 7. Location of streambed-sediment sampling sites on the white sturgeon critical-habitat reach of the Kootenai River near Bonners Ferry, Idaho.

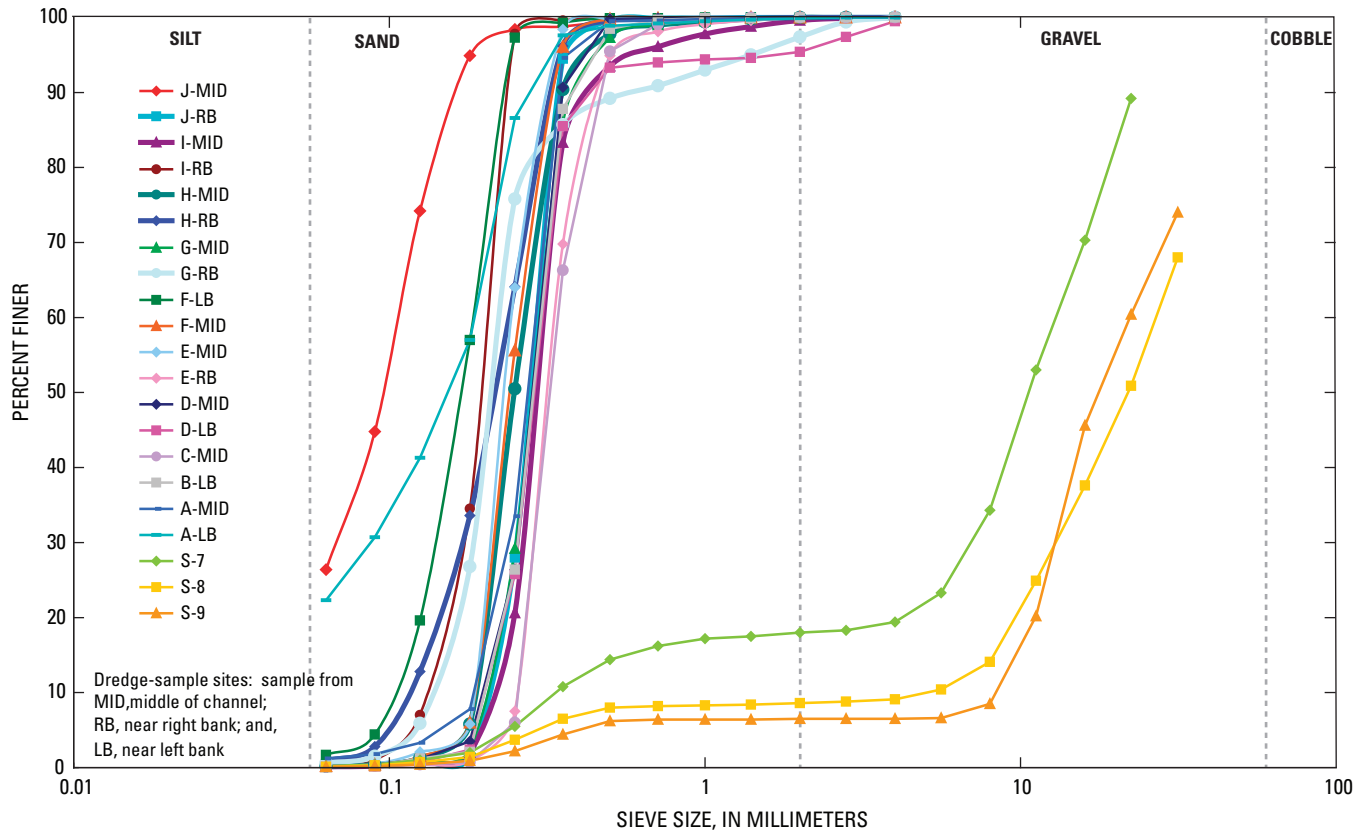


Figure 8. Particle-size distribution for streambed sediment samples taken between river kilometers 228.4 and 245.8 on the white sturgeon critical-habitat reach of the Kootenai River near Bonners Ferry, Idaho. (Kootenai Tribe of Idaho collected samples A through J with ponar dredge. Sample sites shown in [figure 7](#).)

Sediment-Transport Regime

Although information regarding the sediment-transport regime is not required for application of a multidimensional flow model, this information can be useful for understanding how changes in sediment supply during various streamflows might affect channel morphology or other physical characteristics of the system. During snowmelt runoff in the pre-Libby Dam era, sediment data collected at the USGS gaging station at Copeland (12318500) indicate that large amounts of suspended sediment were transported through the white sturgeon critical-habitat reach. The annual suspended-sediment load leaving the Kootenai River critical-habitat reach decreased dramatically after the closure of Libby Dam in 1972. During the pre-Libby Dam era, annual average load at the Copeland gaging station from 1966 to 1971 was 1,740,000 metric tons per day (mt/d) and annual median daily load ranged from 14 to 48,700 mt/d, but after dam closure, annual average load from 1973 to 1982 was 190,000 mt/d and annual median daily load ranged from 53 to 1,560 mt/d ([fig. 4](#)). Suspended-sediment transport during the Libby Dam era was minimal, about 11 percent of the average annual pre-Libby Dam era amount. This reduction was caused by the influence on the flow regime of dam regulation for flood control and

power demand, as discussed above. In addition to the effects of changes in streamflow, less sediment was available for transport because 70 percent of the basin is upstream of Libby Dam (Barton, 2004).

During 2002 and 2003, depth-integrated cross-sectional suspended-sediment samples were collected at the upstream end of the critical-habitat reach near Fry Creek and at the downstream end of the reach near Ball Creek, and are described in detail in Berenbrock and Bennett (2005). In addition, during 2002 and 2003 a series of single depth-integrated suspended-sediment samples was collected from the U.S. Highway 95 Bridge. Berenbrock and Bennett computed a suspended-sediment transport curve and a total-sediment transport curve for the upstream end of the modeling reach at the U.S. Highway 95 Bridge using these data. For streamflow simulations of 170, 547, 1,132, and 1,708 m^3/s , the suspended-sediment transport curve indicated estimated sediment loads of 132, 1,590, 6,670, and 15,400 mt/d, respectively; the total-sediment transport curve indicated estimated sediment loads of 148, 2,050, 9,260, and 22,400 mt/d, respectively. Berenbrock and Bennett (2005) also computed a sediment-transport curve for total suspended sediment for the downstream end of the white sturgeon critical-habitat reach near Ball Creek.

River Channel Geometry

Channel geometry data were collected for the critical-habitat reach of Kootenai River and then used to (1) map bathymetry for use in the flow modeling, (2) characterize bedform geometry, and (3) determine degradation and aggradation of the riverbed. River bathymetry was mapped during 2002, 2003, and 2004, and the data were used as input to the multidimensional flow model. Geometry, amplitude, and wavelength of dunes and other bedforms were monitored at five longitudinal-profile sites and channel degradation and aggradation were monitored at five cross-section sites on the reach. During collection of channel-geometry data, streamflow and river water-surface elevation fluctuated and generally represented unsteady flow conditions (fig. 9).

Bathymetry and Streambank Topography

Bathymetry for the modeling reach was based on mapping conducted during June 2002, April 2003, and August 2004. Bathymetric data collection details are provided in Barton and others (2004) and briefly summarized here. Prior to data collection, survey-control stations with a horizontal and vertical accuracy of less than 0.03 m were established along Kootenai River using survey-grade GPS equipment. Bathymetric data were obtained by interfacing real-time GPS equipment with a survey-grade echo sounder (Barton and others, 2004, fig. 4). Manufacturer-reported accuracy of real-time GPS surveying equipment is ± 0.020 m plus 1 part per million (ppm) in the vertical and ± 0.010 m plus 1 ppm in the horizontal, (<http://trl.trimble.com/docushare/dsweb/Get/Document-163620/>; accessed July 25, 2005), and the accuracy of the echo sounder

was consistently less than ± 0.031 m. Taking into account all sources of mapping error, the bathymetry and streambank topography was mapped with a horizontal accuracy of ± 0.050 m and ± 0.601 m and a vertical accuracy of ± 0.030 m and ± 0.091 m, respectively (Barton and others, 2004). Vertical coordinate information was referenced to the North American Vertical Datum of 1988 (NAVD 88). Horizontal coordinate information was referenced to the North American Datum of 1983 (NAD 83), Idaho Transverse Mercator—North American Datum 1983/1998 Idaho West, in meters.

During 2002 and 2003, water depth was measured with a single-beam echo sounder (Innerspace Technology, Inc., Model 448). About 260 cross sections and two to seven longitudinal lines were surveyed in the modeling reach. Spacing between cross sections ranged from less than 10 to about 50 m. During 2004, water depth was measured with a multi-beam echo sounder (Ross Model 875-4 with four channels). Spacing between each of the four sounding transducers was 2.8 m. A series of longitudinal lines was surveyed in the modeling reach between RKM 245.9 and RKM 236.8 and between RKM 232.5 and RKM 228.4. Longitudinal lines generally were parallel and spaced relatively close together. About 80 percent of the river bottom in these two reaches was surveyed. The multi-beam echo sounder provided a much more closely spaced set of bathymetric data than the single-beam system, allowing development of a model with smaller computational cells and greater detail.

Streambank shots were taken at breaks in topographic slope using a laser range-finder (Laser Technology Impulse 200LR) and angle encoder (Laser Technology Mapstar Angle Encoder System) interfaced with the Trimble 5700 GPS.

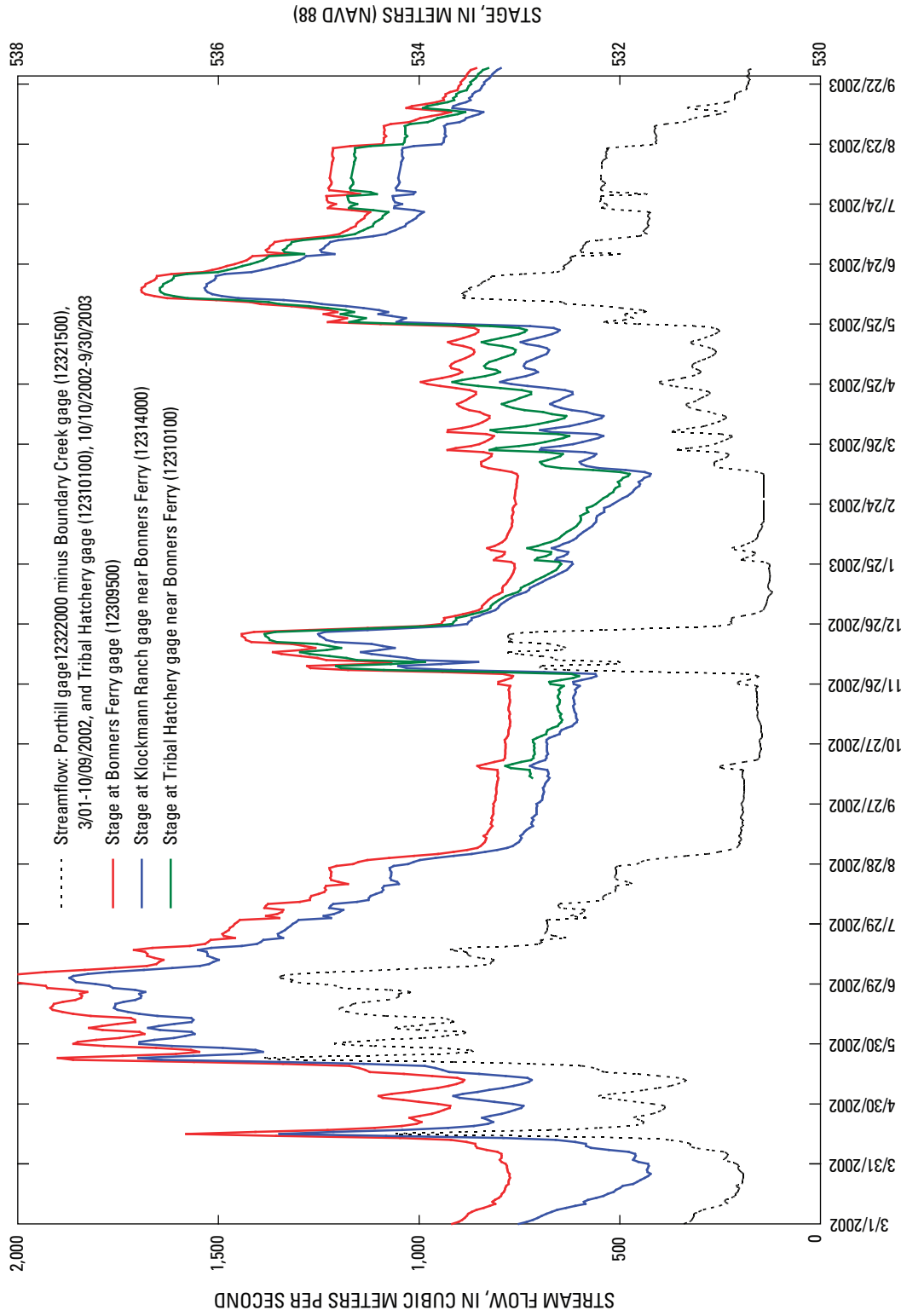


Figure 9. Daily mean flow and water-surface elevation for the white sturgeon critical-habitat reach of Kootenai River near Bonners Ferry, Idaho, 2002 and 2003.

Dunes and Other Bedforms

Geometry, amplitude, and wavelength of dunes and other bedforms were monitored at five sites in the modeled reach (fig. 10). The sites were monitored on May 24, June 6, July 23, and September 4, 2002, when streamflows were 1,150, 1,110, 663, and 229 m³/s. Each site consisted of a longitudinal profile in the center of the channel with lengths ranging from 216 to 329 m. An acoustic Doppler current profiler (ADCP, RD Instruments Rio Grande model) was mounted to a survey vessel and used to measure velocity, river depth, and distance traveled. The upstream end of each longitudinal profile was located with a general purpose GPS. Sites F-F', I-I', and J-J' are where the river forms a relatively straight channel and sites G-G' and H-H' are in the thalweg of meander bends (fig. 10). Sites G-G' and H-H' were not analyzed or included in the model because maintaining position on a profile was more difficult at sites in a meander bend as compared to sites in a straight channel.

Longitudinal-profile data indicate that Kootenai River bedform geometry is linked to streamflow. In general, dune bedforms have the greatest amplitude (vertical relief) at the low streamflow regime when flow is steady, and amplitude generally decreases with increasing streamflow until the dunes washout at the high streamflow regime and form a plane bed (fig. 11 and table 1). This observation is consistent with research on the evolution of sand bedforms and streamflow regime (Henderson, 1966, chap. 10.2; Simons and Richardson, 1961). Dunes exhibited the greatest amplitude during the 229 m³/s streamflow of September 4, 2002: the average amplitude for longitudinal profiles F-F', I-I', and J-J' was 0.7 m and the largest amplitude, 1.4 m, was observed at site I-I'. During high streamflow, dunes were washed out and a flat plane bed was formed along most of the longitudinal profile at sites F-F' and I-I' on May 24, 2002, and at site

J-J' on June 6, 2002. Average dune wavelength at profile F-F' was 12.2 m on May 24, 2002, and 14.2 m on July 23, 2002. In contrast, average dune wavelength at profile F-F', I-I', and J-J' was 20.42 m on September 4, 2002,. These data provide a generalized characterization of the relation between streamflow and bedform geometry; additional data would be needed to provide a more thorough understanding.

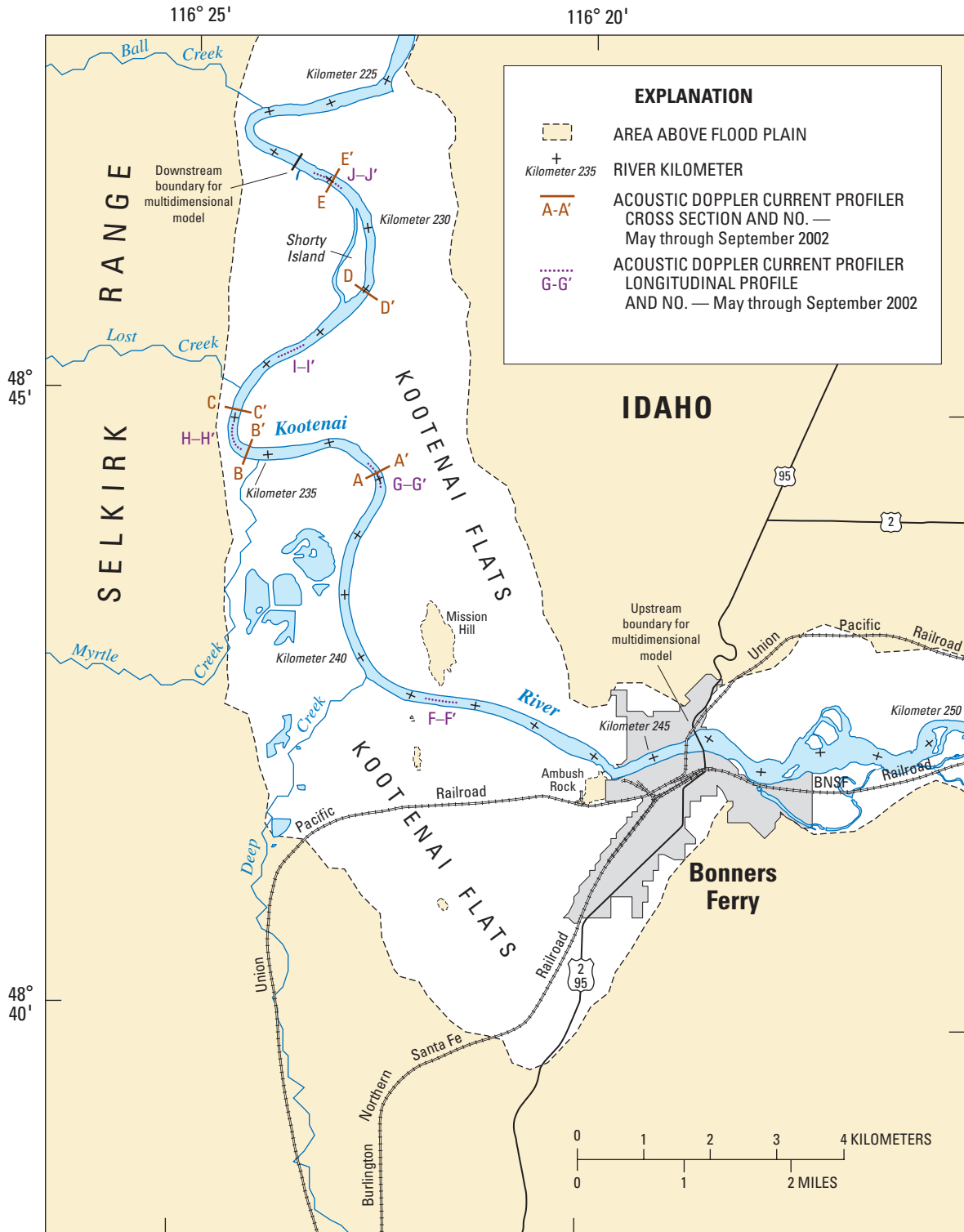
River Channel Degradation and Aggradation

Degradation and aggradation of the Kootenai River channel in the critical-habitat reach were monitored at five channel cross sections: A-A', B-B', C-C', D-D', and E-E' (figs. 10 and 12). The sites also were monitored on May 24, June 6, July 23, and September 4, 2002, when streamflows were 1,150, 1,110, 663, and 229 m³/s, respectively. Channel cross section were measured with an ADCP using data-collection methods discussed in the section Dunes and Other Bedforms. Channel cross section surveys show that the thalweg appears stable during low flows and high flows with little channel aggradation and degradation. In the thalweg of sections C-C', D-D', and E-E', less than 1, 1.2, and 0.6 m of change was measured in riverbed elevation, respectively (fig. 12). Changes in elevation at each cross section are on the order of measured bedform amplitudes, and because there is no systematic change in elevation along either the thalweg or the channel margins from low to high flow, changes likely represent migration of bedforms on the channel bottom. It appears that the river channel is fairly stable, at least for the range of observed streamflows. This observation can be used to justify merging topographic data sets that were measured over various streamflows. Furthermore, channel stability indicates that some justification exists for modeling flow patterns for streamflows other than when collecting bathymetric data.

Table 1. Amplitude and wavelength of dune bedforms in the white sturgeon critical-habitat reach of the Kootenai River, near Bonners Ferry, Idaho.

[Location of longitudinal profiles shown in figure 8. **Longitudinal profiles:** amplitude, dune vertical relief; wavelength, dune length; FI, flat to irregular bedforms; F, flat bedforms. **Abbreviations:** m³/s, cubic meter per second; ft³/s, cubic foot per second; m, meter; ft, foot; ND, no data]

Date	Streamflow		Longitudinal profile F-F'				Longitudinal profile I-I'				Longitudinal profile J-J'			
			Average amplitude		Average wavelength		Average amplitude		Average wavelength		Average amplitude		Average wavelength	
	(m ³ /s)	(ft ³ /s)	(m)	(ft)	(m)	(ft)	(m)	(ft)	(m)	(ft)	(m)	(ft)	(m)	(ft)
05-24-2002	1,150	40,700	0.20	0.64	12.2	40.0	FI	FI	F	F	0.21F	0.7F	F	F
06-06-2002	1,110	39,100	.30	.99	14.0	46.1	ND	ND	ND	ND	.12F	.4F	F	F
07-23-2002	663	23,400	.51	1.68	18.9	62.0	0.61	2.00	19.4	63.6	.23	.76	17.9	58.7
09-04-2002	229	8,070	.69	2.27	20.4	67.0	.84	2.75	22.4	73.4	.46	1.50	18.4	60.4



Base from U.S. Geological Survey digital data, 1:100,000, 1983
 Universal Transverse Mercator projection, Zone 13

Figure 10. Location of acoustic Doppler current profiler cross sections and longitudinal profiles for monitoring riverbed stability and bedforms on the white sturgeon critical-habitat reach of the Kootenai River near Bonners Ferry, Idaho.

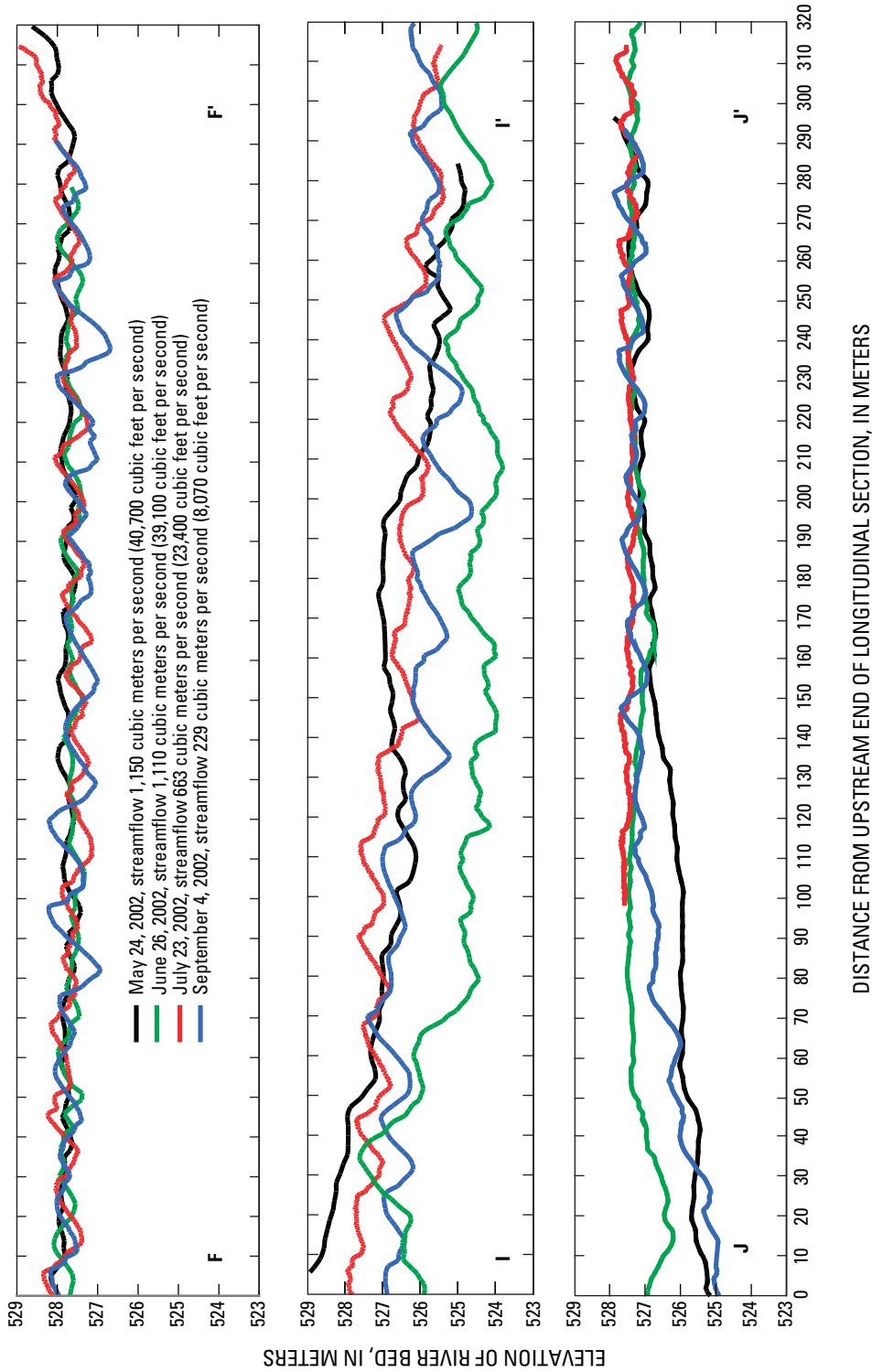
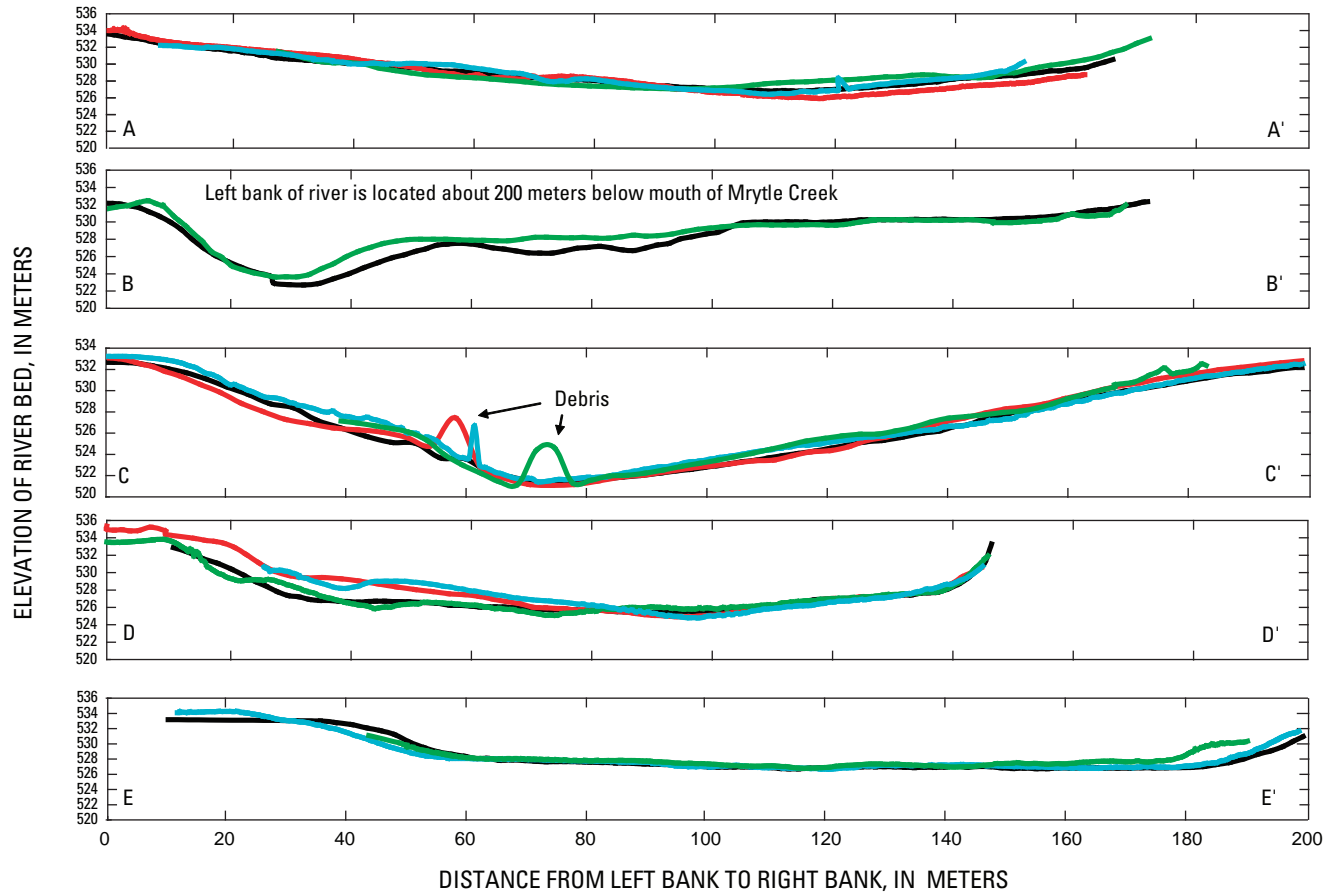


Figure 11 Changes in bedforms along longitudinal profiles measured with an acoustic Doppler current profiler in the white sturgeon critical-habitat reach of the Kootenai River near Bonners Ferry, Idaho, 2002. (Location of sections shown in [figure 8](#).)



EXPLANATION

- May 24, 2002, streamflow 1,150 cubic meters per second (40,700 cubic feet per second)
- July 23, 2002, streamflow 663 cubic meters per second (23,400 cubic feet per second)
- June 26, 2002, streamflow 1,110 cubic meters per second (39,100 cubic feet per second)
- September 4, 2002, streamflow 229 cubic meters per second (8,070 cubic feet per second)

Figure 12. Aggradation and degradation of streambed at five cross sections of the white sturgeon critical-habitat reach of the Kootenai River near Bonners Ferry, Idaho, 2002. (Location of sections shown in [figure 8](#).)

Construction of the Multidimensional Flow Model

The USGS multidimensional surface-water modeling system (MD_SWMS) was used in this study to simulate water-surface elevation, velocity, and boundary (bed) shear stress. When used with subsidiary methods, the flow model also can simulate the motion of sediment on the riverbed and morphologic evolution of the bed. Potential uses for the model include simulations of (1) flow and sediment-transport conditions at known or inferred spawning locations, and (2) sediment mobility and the potential for erosion or deposition in the channel near proposed stable substrate enhancements (Barton and Ireland, 2000).

MD_SWMS is a Graphical User Interface (GUI) developed by the USGS (McDonald and others, 2001; McDonald, Nelson, and Bennett, in press; McDonald, Nelson, Kinzel, and Conaway, in press) for hydrodynamic models. FaSTMECH is one computational model within MD_SWMS and was developed at the USGS (Nelson and McDonald, 1997; Thompson and others, 1998; Lisle and others, 2000, Nelson and others, 2003; McDonald, Nelson, and Bennett, in press; McDonald, Nelson, Kinzel, and Conaway, in press). FaSTMECH includes a 2-dimensional, vertically averaged model and a sub-model that calculates vertical distribution of the primary velocity and the secondary flow about the vertically averaged flow. This so-called 2.5-dimensional approach has been shown to adequately simulate the velocity field, bed shear stress, and resulting patterns of erosion and deposition where secondary flows are significant without the complexity of a fully 3-dimensional model.

Minimum data requirements for the model include channel geometry, streamflow at the upstream boundary, and water-surface elevation at the downstream boundary. Physical assumptions of the model are that (1) flow is steady, (2) flow is incompressible, (3) flow is hydrostatic (vertical accelerations are neglected), and (4) turbulence is adequately treated by relating Reynolds stresses to shear using an isotropic eddy viscosity (Nelson and others, 2003). Additional information on the interface and the model used for this study can be found in McDonald and others (2001), McDonald, Nelson, and Bennett (in press), McDonald, Nelson, Kinzel, and Conaway (in press), Nelson and others (2003), and Nelson and Smith (1989a).

Computational Grid and Bathymetric Interpolation

The computational grid used in FaSTMECH is a curvilinear orthogonal coordinate system with a user-defined centerline. The grid centerline is defined interactively to approximate mean flow streamline of the modeling reach (Nelson and others, 2003). The computational grid used to model the Kootenai River was 17,525 m in length with 3,505 nodes in the downstream direction and 800 m in width with 161 nodes in the cross-stream direction, forming an approximately 5.0- by 5.0-m grid (fig. 13).

Measured topography is mapped to the coordinates of the computation grid through a “nearest-neighbor” method. A search bin is defined with a downstream length and cross-stream width that forms a curved rectangle whose geometry follows the local grid curvature and is centered on the node coordinate being mapped. By choosing the cross-stream and streamwise extent of the search bin judiciously, the user can tune the interpolation to treat situations where slopes in the cross-stream direction are steeper than those in the streamwise direction, which is frequently true in alluvial rivers. Surveyed points within the bin are used to interpolate survey data to the node. If the search bin does not contain any surveyed points, the search bin is doubled in dimension until one or more surveyed points are found. Elevation of the points within the bin are weighted by distance from the survey point to the computational node and averaged to obtain a value for each node of the computational grid. This approach works well where the channel banks are nearly parallel to the computational grid centerline. This is effectively true for most of the modeling reach except around Shorty Island, where the Kootenai River diverges into two channels and their banks trend at angles across the centerline of the model grid. This was overcome by first separating the channel for the purposes of topographic interpolation into two separate reaches: the main channel and a secondary channel around Shorty Island. A curvilinear grid following the secondary channel around Shorty Island, with a 5.0-m spacing in the downstream and cross-stream dimensions near the grid centerline, was created to map the topography in this region (fig. 13). Surveyed topography was mapped to this grid based on a search bin with a length of 45.0 m in the downstream direction and a width of 3.0 m in the cross-stream direction. For the main channel,

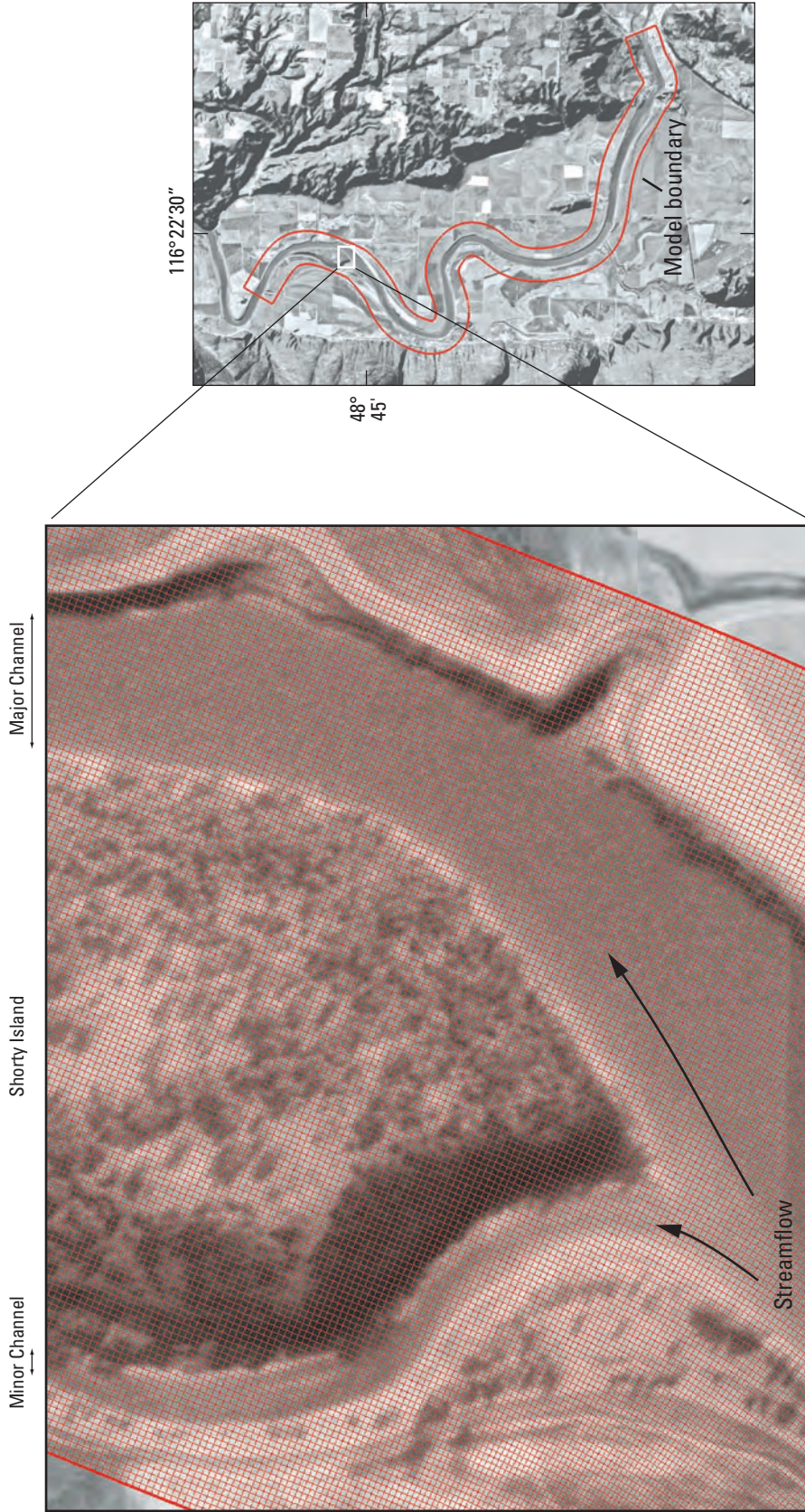


Figure 13. Nodes forming an approximately 5.0-by-5.0-meter grid in the multidimensional flow model at the upstream end of Shorty Island in the white sturgeon critical-habitat reach of the Kootenai River near Bonners Ferry, Idaho.

the surveyed data was separated into three separate reaches for the purposes of topographic interpolation: (1) between RKM 245.9 and RKM 237.5 in the upper part of the modeling reach, where multi-beam bathymetric data were collected during 2004 and single-beam bathymetric data collected during 2002 and 2003; (2) between RKM 231.9 and RKM 237.5 in the center of the modeling reach, where only single-beam bathymetric data were collected during 2002-03; and (3) between RKM 231.9 and RKM 228.4 near Shorty Island, where multi-beam bathymetric data were collected during August 2004 in addition to the single-beam bathymetric data collected during 2002 and 2003. Surveyed topography was mapped to 5.0-m grids created for each of these three regions using a search bin with lengths of 25.0, 45.0, and 20.0 m for reaches (1), (2), and (3), respectively, in the downstream direction, all with a width of 3.0 m and a weighting exponent of 1.5. The resulting topography mapped to all four grids (one for the Shorty Island secondary channel and three from the main channel) were combined with the original measured topography to form a densely spaced set of topographic data, thereby filling in some sparse areas in the surveyed data. The dense topographic data then were used to map the topography to the actual computational grid (a 5.0-m by 5.0-m grid at the centerline of the coordinate system) using a search bin of 5.0 m in length and width and a weighting exponent of 1.5. Although this overall process seems complicated, it was the simplest way to deal with interpolation to the model coordinate system, taking into account variations in the channel planform and density of the surveyed topographic data. Model coordinates and elevations are in the NAD 83 datum, Idaho Transverse Mercator projection, and NAVD 88, respectively.

Streamflow Velocity at the Upstream Model Boundary

Streamflow velocity at the upstream boundary of the model grid have a significant effect on the simulation of flow for roughly the upper kilometer of the modeling reach. Specified velocity boundary conditions at the upstream model boundary were based on available streamflow measurements made at a cross section at the U.S. Highway 95 Bridge using a Price AA current meter (fig. 14). A streamflow of 1,260 m³/s was measured on June 7, 1996, by making 35 current meter measurements in the cross section. A streamflow of 776 m³/s was measured on April 16, 2002, by making 33 current meter measurements in the cross section. The cross-section medians of the vertically averaged velocities for measurements made on April 16, 2002, and June 7, 1996, were 0.71 and 0.78 m/s, respectively. Field measurements show that the highest velocities and largest streamflows are focused between the mid channel and left bank (facing downstream). Vertically averaged velocities at each measurement point across the

channel for the 1996 and 2002 streamflow measurements were combined to produce an average upstream-velocity boundary condition and then normalized so that the distance and velocity magnitude ranged from 0.0 to 1.0. For all flow scenarios the model takes the normalized velocity distribution, stretches it to fit the wetted length of the specified boundary in the model and then amplifies the normalized velocity to satisfy the prescribed streamflow for the model run. The cross-stream velocity at the upstream model boundary was assumed to be zero, in good agreement with observations.

Water-Surface Elevation at the Downstream Model Boundary

In addition to the streamflow-velocity condition at the upstream boundary, the model requires a water-surface elevation (stage) at the downstream end of the modeled reach. Boundary conditions for water-surface elevation at the downstream model boundary typically were computed by interpolation of the water-surface elevation at the Bonners Ferry gaging station (12309500) and Klockmann Ranch gaging station (12314000). In some cases, the lower boundary conditions were set using the 1-dimensional model described by Berenbrock (2005).

During model runs, including calibration, channel curvature at the downstream model boundary caused recirculation currents at the model boundary, which is problematic, given that the momentum flux and water-surface elevation downstream of the model reach were unknown. To address this common problem, the MD_SWMS grid extension module was used to extend and gradually straighten the grid in the downstream direction by 60 nodes over a distance of 300 m to eliminate recirculation regions at the downstream end of the model reach. The grid extension does not alter the flow solution in the region of interest. The alternative would have been to survey additional topography to allow the downstream end of the model reach to be located in a region without recirculation, but this would have been costly and would not have had any effect on the model solutions.

Model Calibration

Calibration is the process of adjusting model parameters within reasonable limits to obtain the best fit of the model results to measured data. This process involves repeatedly adjusting a parameter, running the model, and inspecting differences between model results and measured data with the objective of minimizing the difference. In this study, calibration consisted of comparing the differences between simulated and observed water-surface elevations at selected sites, and adjusting the drag coefficient to match observed slopes.

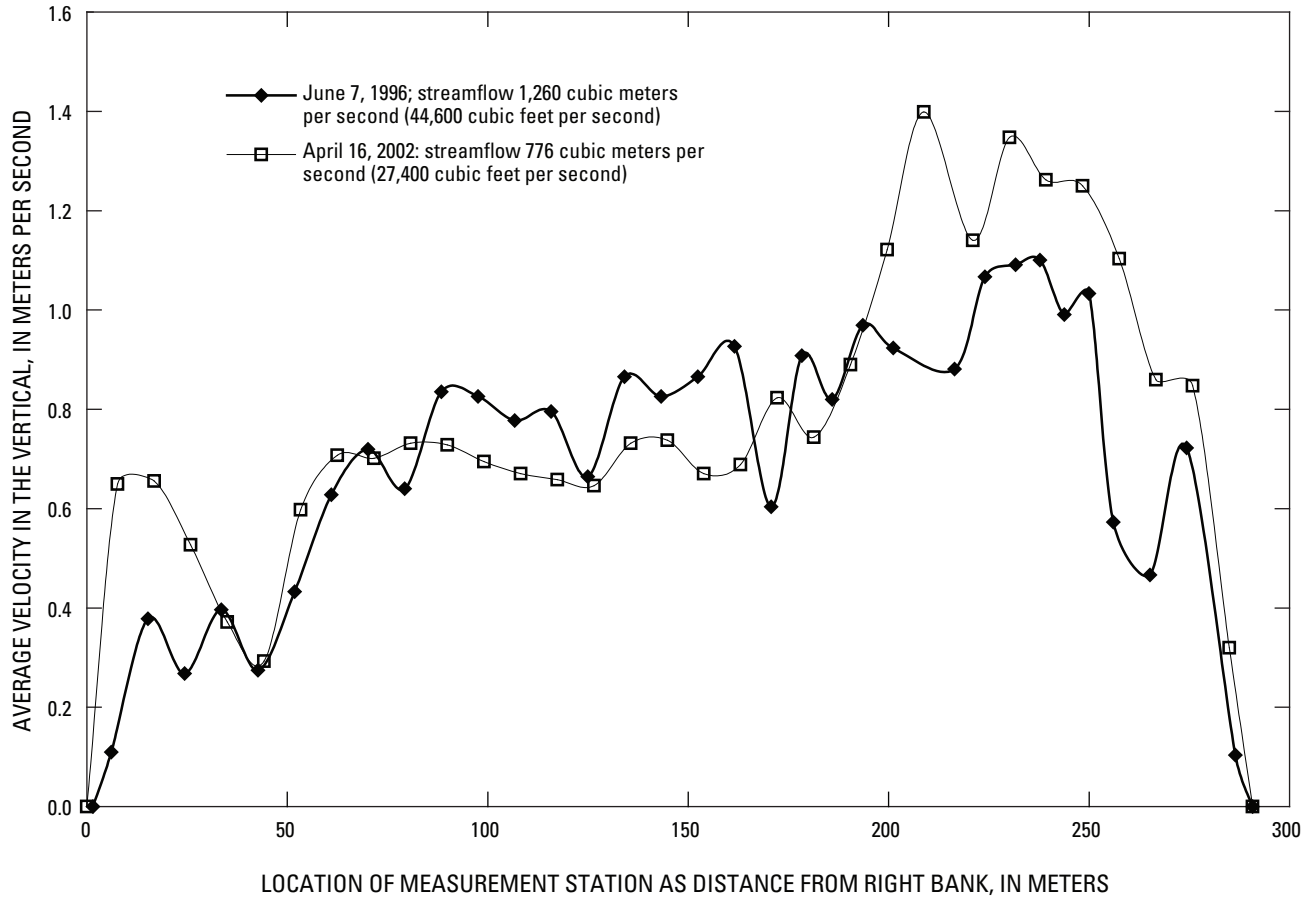


Figure 14. Streamflow-velocity measurements at the upstream model boundary on the white sturgeon critical-habitat reach of the Kootenai River at Bonners Ferry, Idaho, June 1996 and April 2002.

The model was calibrated to 14 historical streamflow conditions (table 2) that ranged from 157 to 2,540 m³/s. Selection of historical streamflow conditions used for model calibration was based on two criteria: (1) historical streamflows should be evenly distributed between 141.6 m³/s and 2,548.9 m³/s so the model could be adequately calibrated over the range of flow in the river; and (2) because MD_SWMS functions as a steady-state model, the historical streamflow and water-surface elevation should be stable for a minimum of 24 hours so river conditions approximate steady flow. Criterion (2) assumed that streamflow should be stable for a minimum of 24 hours at the Porthill stage-discharge

gaging station (12322000) for calibration measurements prior to October 2002 and at the Tribal Hatchery stage-discharge gaging station (12310100) for calibration measurements since October 2002. In addition, criterion (2) assumed that water-surface elevation should be stable for a minimum of 24 hours at the Klockmann Ranch stage gaging station (12314000) and the Bonners Ferry stage gaging station (12309500). The model was calibrated by adjusting the drag coefficient until simulated water-surface slope through the modeling reach matched the measured water surface. Physically, this process is equivalent to ensuring that the roughness used in the model accurately simulates the head loss in the channel over long reaches.

24 Simulation of Flow and Sediment Mobility Using Multidimensional Model, Kootenai River near Bonners Ferry, Idaho

Table 2. Calibration summary for the multidimensional hydraulic flow model for the white sturgeon critical-habitat reach of the Kootenai River, near Bonners Ferry, Idaho.

[Method of computing stage: C, stage is based on water-surface elevation recorded at streamflow gaging stations located upstream and downstream and of the modeling reach; M, stage is simulated from a 1-dimensional hydraulic model. **Computed Lateral Eddy Viscosity:** $0.01 \times \text{average depth} \times \text{average velocity}$.

Abbreviations: m³/s, cubic meter per second; ft³/s, cubic foot per second; m, meter; ft, foot; m/s, meter per second; ft/s, foot per second; –, no data]

Date	Streamflow		Water-surface slope	Method of computing stage	River stage (m)					River stage (ft)		
					Downstream boundary	Tribal Hatchery gage (12310100)			Upstream boundary		Downstream boundary	Upstream boundary
	(m ³ /s)	(ft ³ /s)			Computed stage	Computed stage	Model output	Computed stage	Model output	Computed stage	Computed stage	Model output
06-23-1967	2,540	89,700	0.000042	C	541.37	–	–	542.12	542.10	1,776.24	1,778.70	1,778.63
05-16-1969	2,540	89,700	.000049	C	540.62	–	–	541.49	541.48	1,773.77	1,776.63	1,776.60
05-30-1969	2,270	80,200	.000040	C	540.15	–	–	540.86	540.88	1,772.23	1,774.56	1,774.63
06-29-1967	1,920	67,800	.000033	C	540.07	–	–	540.66	540.66	1,771.97	1,773.91	1,773.91
05-22-1969	1,660	58,615	.000036	C	538.68	–	–	539.32	539.32	1,767.41	1,769.51	1,769.51
06-11-1997	1,400	49,400	.000029	C	538.17	–	–	538.67	538.68	1,765.74	1,767.38	1,767.41
07-03-2002	1,340	47,300	.000032	M	537.56	–	–	538.13	538.15	1,763.73	1,765.60	1,765.67
06-24-2002	1,050	37,100	.000028	C	536.89	–	–	537.38	537.38	1,761.54	1,763.14	1,763.14
06-13-2003	855	30,200	.000029	M	536.21	536.56	536.55	536.73	536.71	1,759.31	1,761.01	1,760.95
12-20-2002	779	27,500	.000036	C	535.10	535.53	535.55	535.77	535.76	1,755.66	1,757.86	1,757.83
07-02-2003	592	20,900	.000025	M	535.03	535.32	535.32	535.50	535.47	1,755.43	1,756.98	1,756.88
08-13-2003	535	18,900	.000032	C	535.27	535.65	535.64	535.87	535.86	1,756.22	1,758.19	1,758.16
05-05-2003	317	11,200	.000034	C	533.02	533.33	533.34	533.67	533.66	1,748.84	1,750.97	1,750.94
11-15-2002	157	5,540	.000030	M	532.50	532.62	532.59	533.10	533.12	1,747.13	1,749.10	1,749.17

Date	Model drag coefficient (dimensionless)			Lateral eddy viscosity		Average river depth		Average streamflow velocity	
	River kilometer 245.8 to 228.4	River kilometer 228.4 to 244.5	River kilometer 245.8 to 244.5	Model	Computed	(m)	(ft)	(m/s)	(ft/s)
	06-23-1967	0.0023	–	–	0.170	0.170	14.5	47.6	1.17
05-16-1969	.0022	–	–	.175	.175	14.5	47.6	1.21	4.0
05-30-1969	.0018	–	–	.160	.161	14.0	45.9	1.15	3.8
06-29-1967	.0021	–	–	.145	.149	13.5	44.3	1.10	3.6
05-22-1969	.0020	–	–	.130	.105	11.7	38.4	.90	3.0
06-11-1997	.0020	–	–	.100	.092	10.6	34.8	.87	2.9
07-03-2002	.0022	–	–	.090	.090	10.0	32.8	.90	3.0
06-24-2002	.0026	–	–	.080	.076	9.5	31.2	.80	2.6
06-13-2003	.0031	–	–	.054	.054	8.0	26.2	.67	2.2
12-20-2002	.0032	–	–	.048	.048	7.4	24.3	.65	2.1
07-02-2003	.0035	–	–	.036	.036	6.6	21.6	.55	1.8
08-13-2003	.0043	–	–	.032	.028	5.6	18.4	.50	1.6
05-05-2003	.0055	–	–	.021	.021	5.6	18.4	.37	1.2
11-15-2002	–	0.0040	0.0150	.010	.010	4.3	14.2	.23	.8

Model Boundary Conditions for Calibration Runs

Boundary conditions used during model calibration include (1) streamflow and water-surface elevations at the upstream model boundary, and (2) water-surface elevations at the downstream boundary. Streamflow conditions less than 878 m³/s were based on measurements at the Tribal Hatchery gaging station (1231010) for the period of record since October 2002 and streamflow conditions between 878 and 2,540 m³/s were computed as streamflow at the Porthill gaging station (1232200) minus Boundary Creek gaging station (12321500) for May 23, 1967, to July 3, 2002. Fourteen boundary conditions for water-surface elevation at the downstream model boundary (table 2) were determined for the calibration runs. Flows greater than 1,340 m³/s were computed by interpolation of the water-surface elevation at the Bonners Ferry gaging station (12309500) and Klockmann Ranch gaging station (12314000). Water-surface elevation boundary conditions for streamflows 1,340 m³/s and less were obtained from a steady 1-dimensional hydraulic model of the Kootenai River developed by Berenbrock (2005). One-dimensional model results were unavailable for higher flows, but the interpolation method should be adequately accurate.

Drag Coefficient

The model was calibrated by adjusting the roughness, as parameterized by drag coefficient, until the simulated average water-surface elevation at the upstream end of the model reach matched the water-surface elevation determined from the gaging station at Bonners Ferry. For flows during the Tribal hatchery (12310100) gaging station operation, modeled water-surface elevation also was compared with measurements at that location (fig. 2). Because the downstream water-surface elevation was set as a model boundary condition, this process ensured that the reach-averaged water-surface slope simulated by the model matched the measurements. Local roughness values are defined primarily by grain-size distribution and, when bedforms are present, the amplitude and wavelength of the bedforms. Between Ambush Rock and Shorty Island the channel bottom consists of fine sand and some lacustrine clay, and between the U.S. Highway 95 Bridge and Ambush Rock the river bottom consists predominantly of gravel, cobble, and sand. To account for these differences the drag coefficient was partitioned into regions of constant drag above and below Ambush Rock when modeling streamflow equal to or less than 170 m³/s. In the absence of spatially detailed measurements of bedforms and grain-size, a constant drag coefficient was used in each of these regions.

Results

Model calibration was considered acceptable when the difference between model-simulated and observed water-surface elevations at both the Tribal Hatchery gaging

station (12310100) and the upstream model boundary at Bonner's Ferry gaging station (12309500) were minimized. Results of the calibration are presented in table 2. Differences in model-simulated and observed water-surface elevations at both gaging stations were less than or equal to ± 0.03 m. Data from the Tribal Hatchery gaging station showed that, for the low-flow calibration streamflow of 157 m³/s, partitioning the drag coefficient into regions of constant drag above and below Ambush Rock significantly improved the comparison of model to the measurements.

Model calibration (fig. 15) resulted in drag coefficients that ranged from 0.004 for low-flow conditions of 157 m³/s to 0.0023 for pre-dam high-flow conditions of 2,540 m³/s. The drag coefficient for the sandy reach between Ambush Rock and Shorty Island increased sharply, from 0.004 to 0.006, as streamflow increased from 157 to 317 m³/s. For the straight reach between the U.S. Highway 95 Bridge and Ambush Rock, the drag coefficient decreased sharply from 0.015 to 0.0055 as flow increased from 157 to 317 m³/s. For flows greater than 157 m³/s, there was no clear justification for using more than a single value of the drag coefficient, because model results were not significantly better than results obtained using a single value. At greater streamflows, the drag coefficient was constant throughout the model, decreasing gradually from 0.0055 to 0.0022 as streamflow increased from 317 to 1,340 m³/s, then remaining about constant as streamflow increased to 2,540 m³/s. Model calibration suggests that bedforms have a large effect on the drag coefficient at streamflows less than about 595 m³/s: friction along the riverbed is increased at low streamflows due to formation of tall dunes, and friction decreases at higher streamflows because the dunes tend to wash out.

The model incorporates a lateral eddy viscosity to represent lateral momentum exchange due to turbulence or other variability that is not generated at the bed (see Nelson, 2003). The model's lateral eddy viscosity (*LEV*) parameter was computed for each model calibration condition using equation (1) defined as:

$$LEV = 0.01 * u_{avg} * y_{avg}, \quad (1)$$

where

LEV is lateral eddy-viscosity coefficient, in square meters per second,

u_{avg} is average velocity, in meters per second, and

y_{avg} is average depth, in meters.

The computed *LEV* value was applied uniformly throughout the modeling reach for each calibration streamflow. *LEV* consistently increased with increasing streamflow (fig. 15) and ranged from 0.010 to 0.175 for streamflow ranging from 157 to 2,540 m³/s.

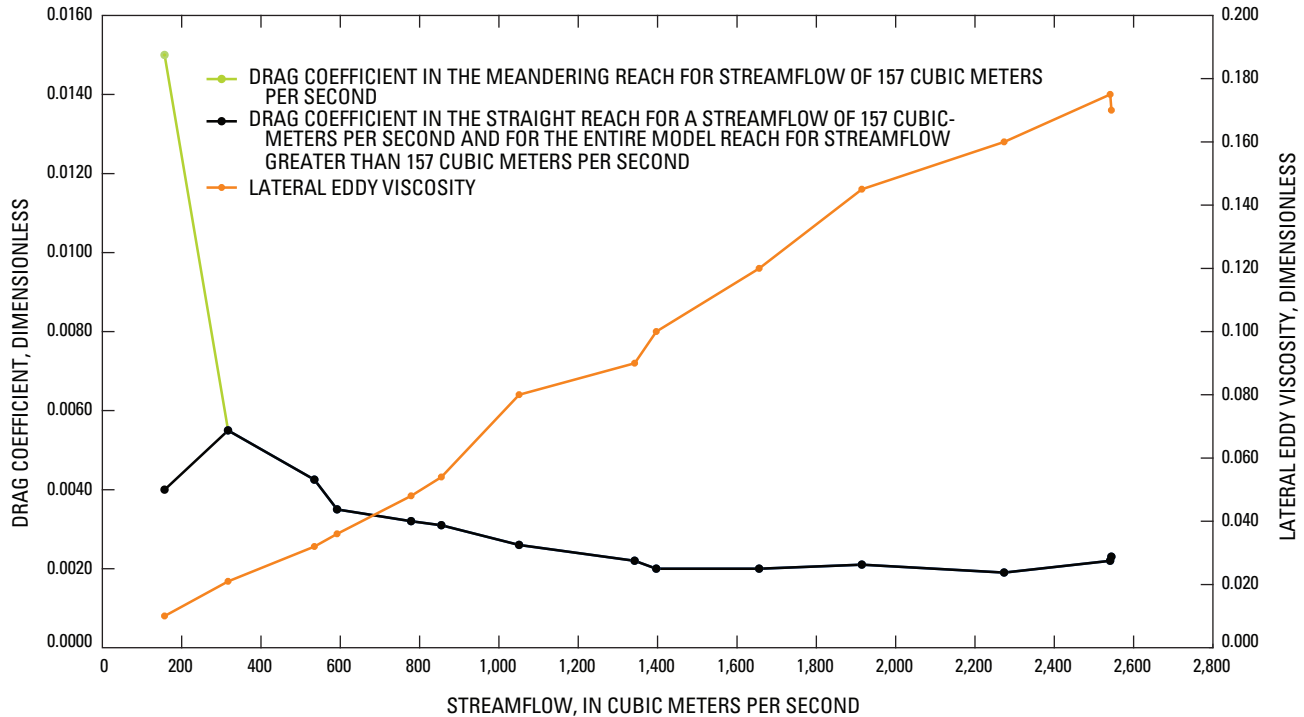


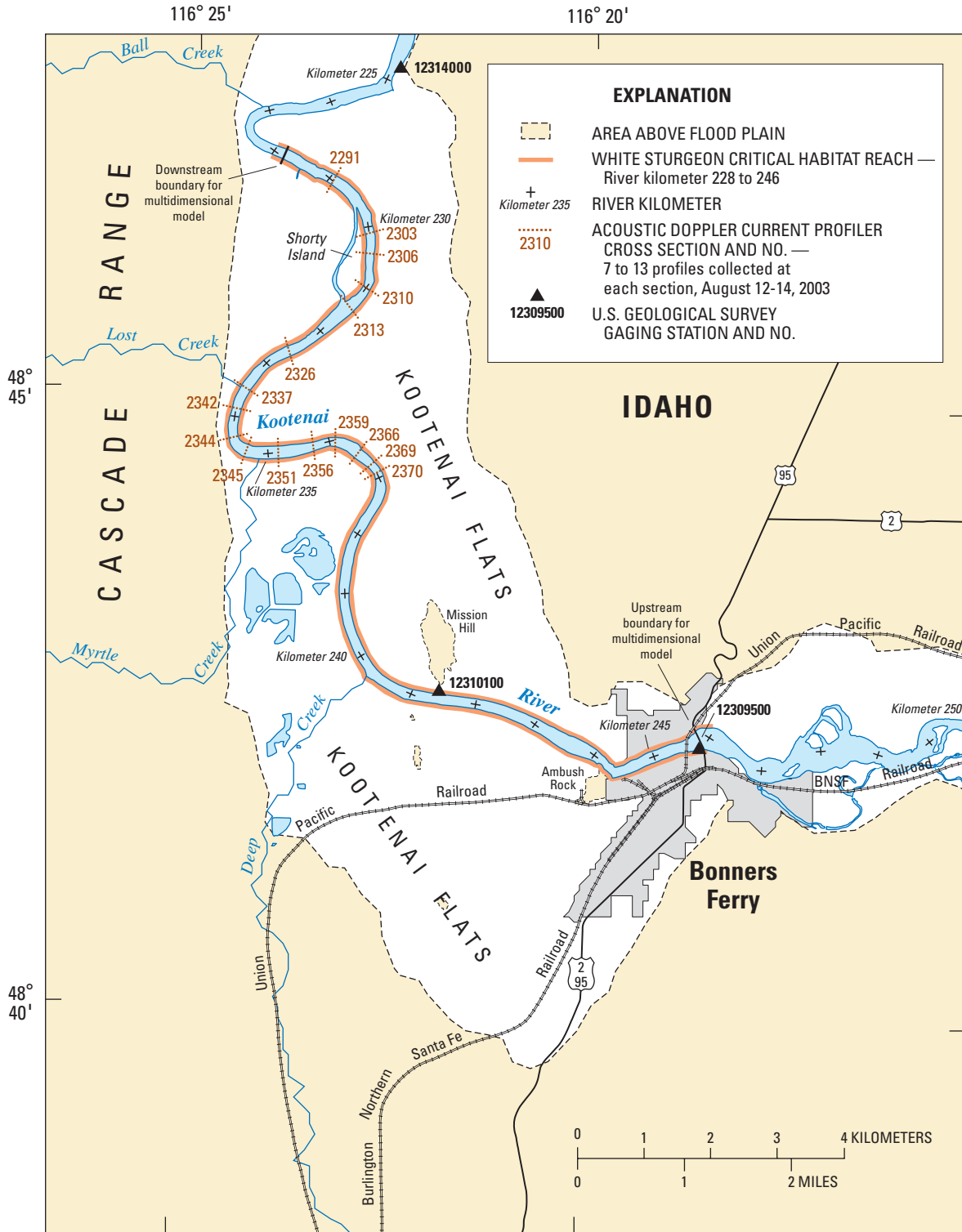
Figure 15. Drag and lateral eddy-viscosity coefficients for the calibrated multidimensional flow model of the white sturgeon critical-habitat reach of the Kootenai River near Bonners Ferry, Idaho.

Model Validation

The model was validated by comparing simulated flow velocities with flow velocities measured at 15 cross sections between RKM 229.1 and 236.9 during steady streamflow that averaged 538 m³/s on August 12-14, 2003 (figs. 9 and 16). Flow velocities were measured by an ADCP that was interfaced with a Trimble mapping-grade GPS receiver and Fugawi navigational software (<http://www.fugawi.com/docs/navframe.html>). The 15 river cross sections were measured multiple (7-13) times to obtain average velocities suitable for comparison to the model results. Measured data were processed into cross sections of vertically averaged velocity and vertical distributions of velocity (vertical slice) to test the 2- and 2.5-dimensional model components, respectively. Procedures for processing raw ADCP data are described in general form by Dinehart (2003) and in Appendix A.

The model simulates both the magnitude and structure of flow across the section reasonably well (fig. 17), with a few notable exceptions. The model slightly under-simulated the magnitude and location of peak velocities in cross sections at the apex of bends in the river, as in Section 2344. This is a common result for models that are not fully 3-dimensional, and can be attributed to the lack of secondary flow feedback on primary velocity distribution.

Streamflow simulations for the first two sections in the main channel around Shorty Island (2313 and 2310) are notably poor. One possible explanation is that specifying a constant drag coefficient is inappropriate in this reach. Bedforms in the straight, somewhat shallow reach just upstream of Shorty Island likely exert a drag on flow and effectively steer and magnify the flow near the right side of the channel looking downstream, as shown in Section 2313. To investigate this possibility, a hyperbolic tangent function was used to create a smooth transition from one value to another (fig. 18). Using this function resulted in a smooth variation in drag coefficient from 0.015 at the shallowest depths to 0.001 at depths greater than 10 m. The smooth roughness transition crudely simulates dunes about 2 m high in water less than 5 m deep and decrease in height until they are nonexistent in water greater than about 10 m deep. The hyperbolic tangent function was used only to illustrate the potential importance of dunes in setting the drag coefficient; it was not used in the model for any other purpose. A comparison of measured velocities with velocities simulated using a constant drag coefficient and a variable drag coefficient suggest that the model results could be improved through better understanding of the spatial distribution of dunes and their sizes (fig. 19).



Base from U.S. Geological Survey digital data, 1:100,000, 1983
 Universal Transverse Mercator projection, Zone 13

Figure 16. Location of acoustic Doppler current profiler cross sections for validating the multidimensional flow model for the white sturgeon critical-habitat reach of the Kootenai River near Bonners Ferry, Idaho.

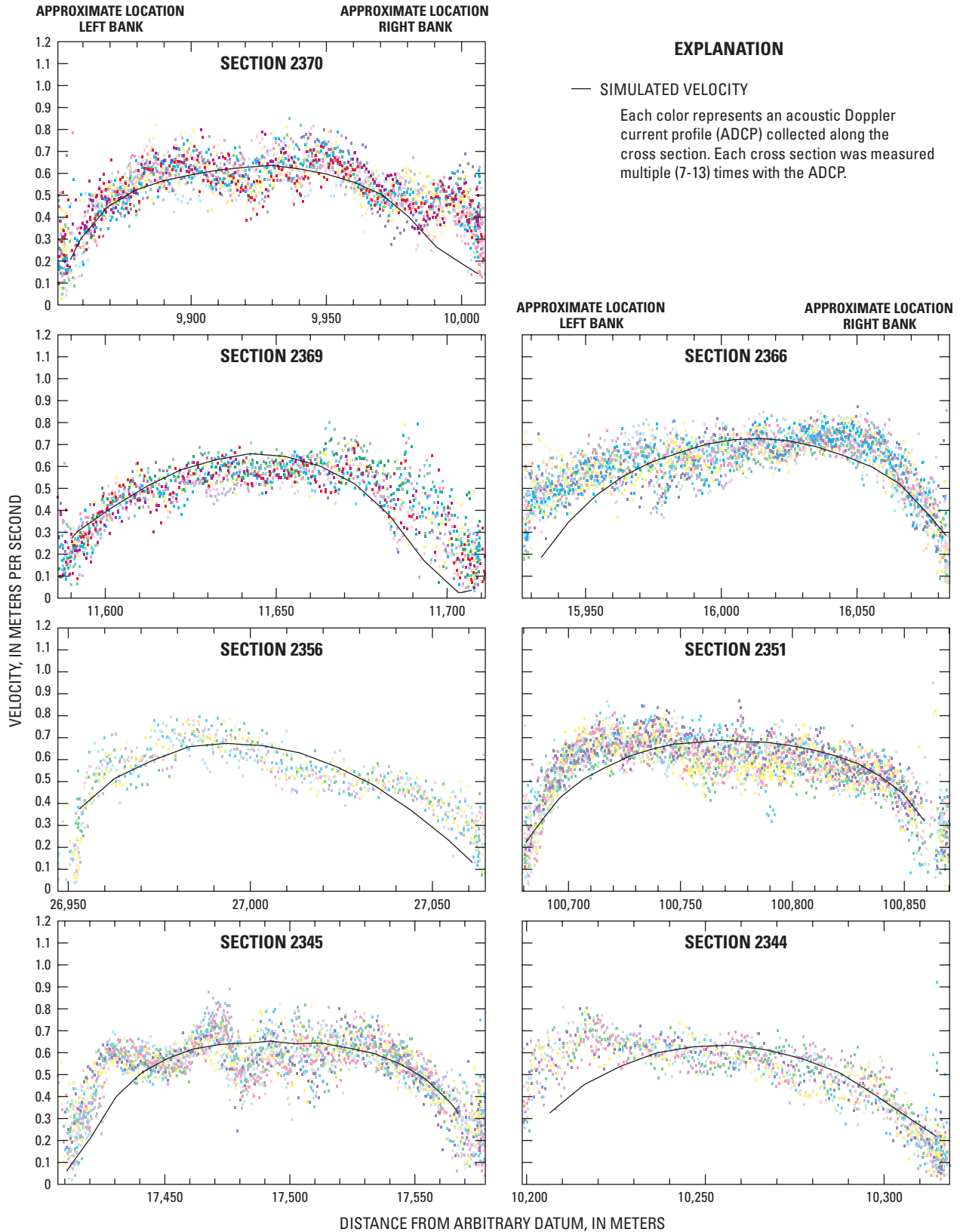


Figure 17. Measured cross sections of vertically averaged velocities and corresponding simulated velocities on the white sturgeon critical-habitat reach of the Kootenai River near Bonners Ferry, Idaho, for a steady flow that averaged 538 cubic meters per second on August 12–14, 2003. (As many as 13 velocity profiles were measured at each cross section. Locations of cross sections shown in [figure 16](#).)

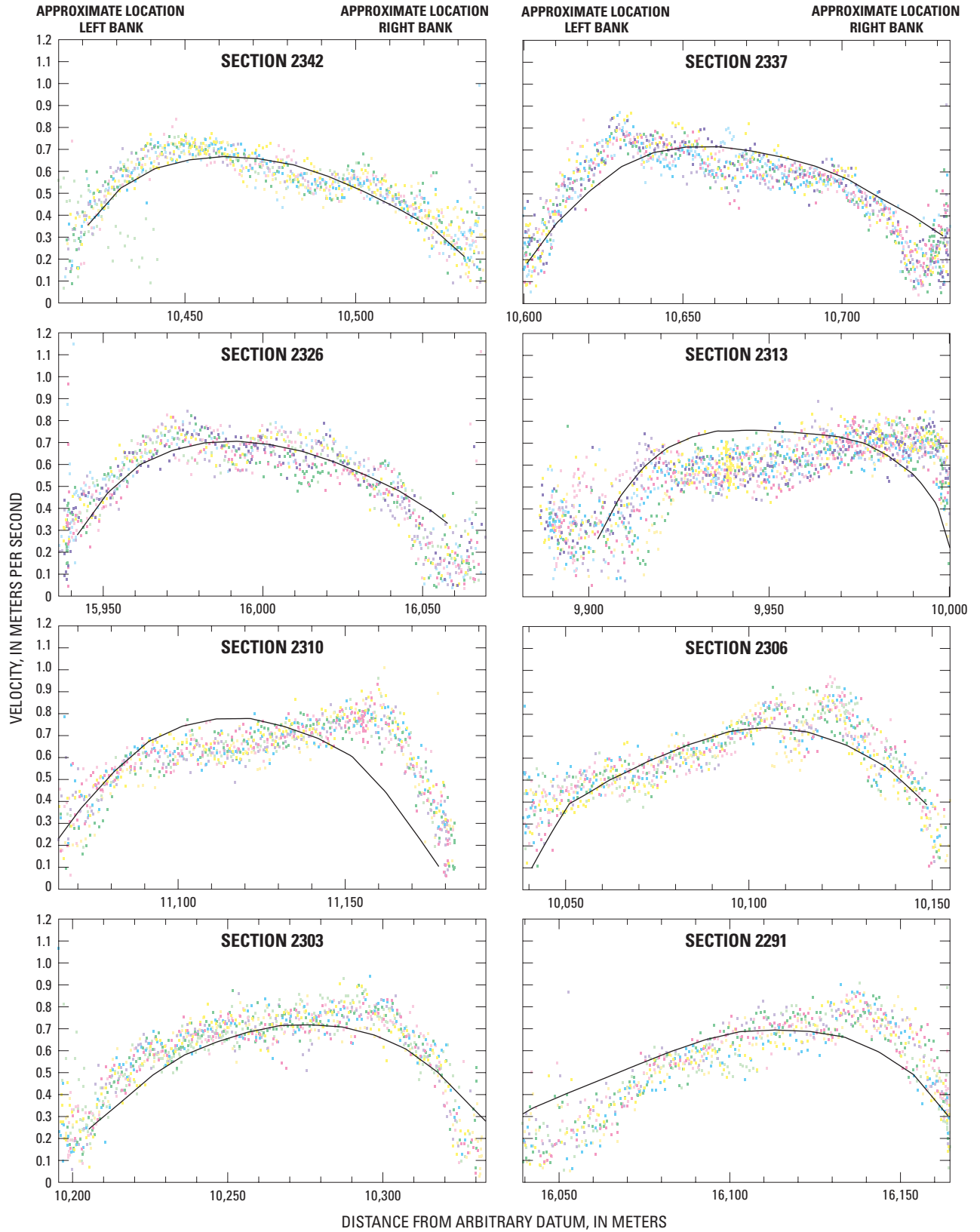


Figure 17. Continued.

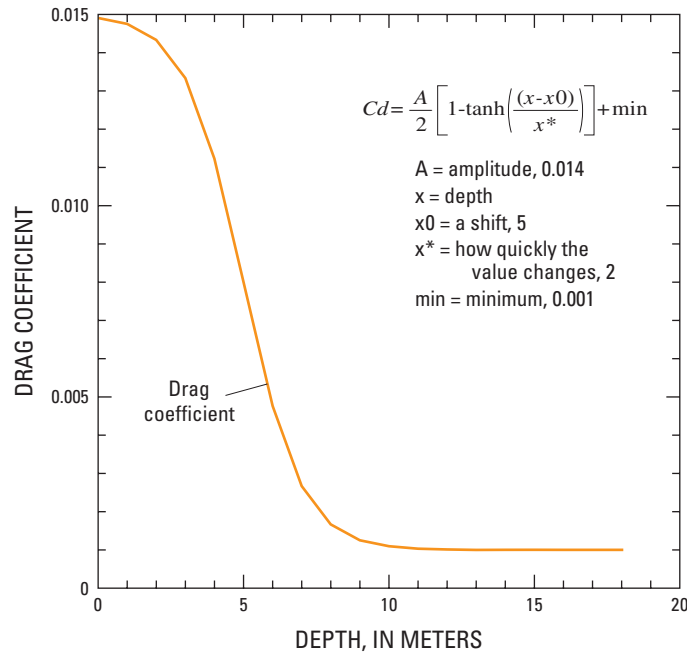
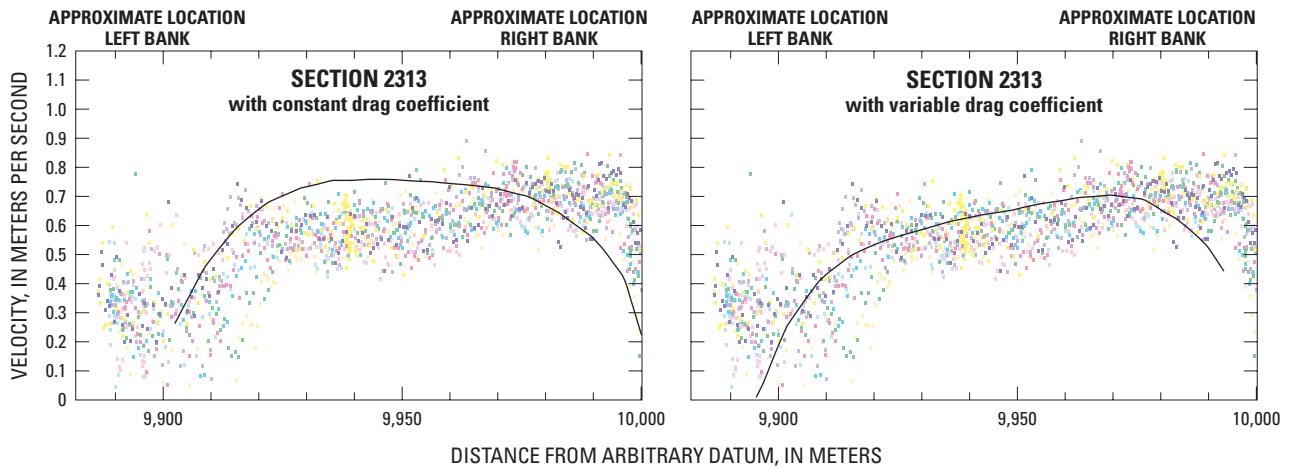


Figure 18. Functional dependence of the drag coefficient on depth, used to improve simulated vertically averaged velocity at cross section 2313 on the Kootenai River near Bonners Ferry, Idaho. The function uses a hyperbolic tangent to vary the drag coefficient smoothly from 0.015 at shallow depths to 0.001 at depths greater than 10 meters. The function is shown in the inset, along with the values used for each parameter.



EXPLANATION

— SIMULATED VELOCITY

Each color represents an acoustic Doppler current profile (ADCP) collected along the cross section. Each cross section was measured multiple (7-13) times with the ADCP.

Figure 19. Measured vertically averaged velocity and simulated vertical velocity based on a constant drag coefficient and variable drag coefficient for cross-section 2313 on the white sturgeon critical-habitat reach of the Kootenai River near Bonners Ferry, Idaho, for a steady flow that averaged 538 cubic meters per second on August 12–14, 2003. (Location of cross section shown in [figure 16](#).)

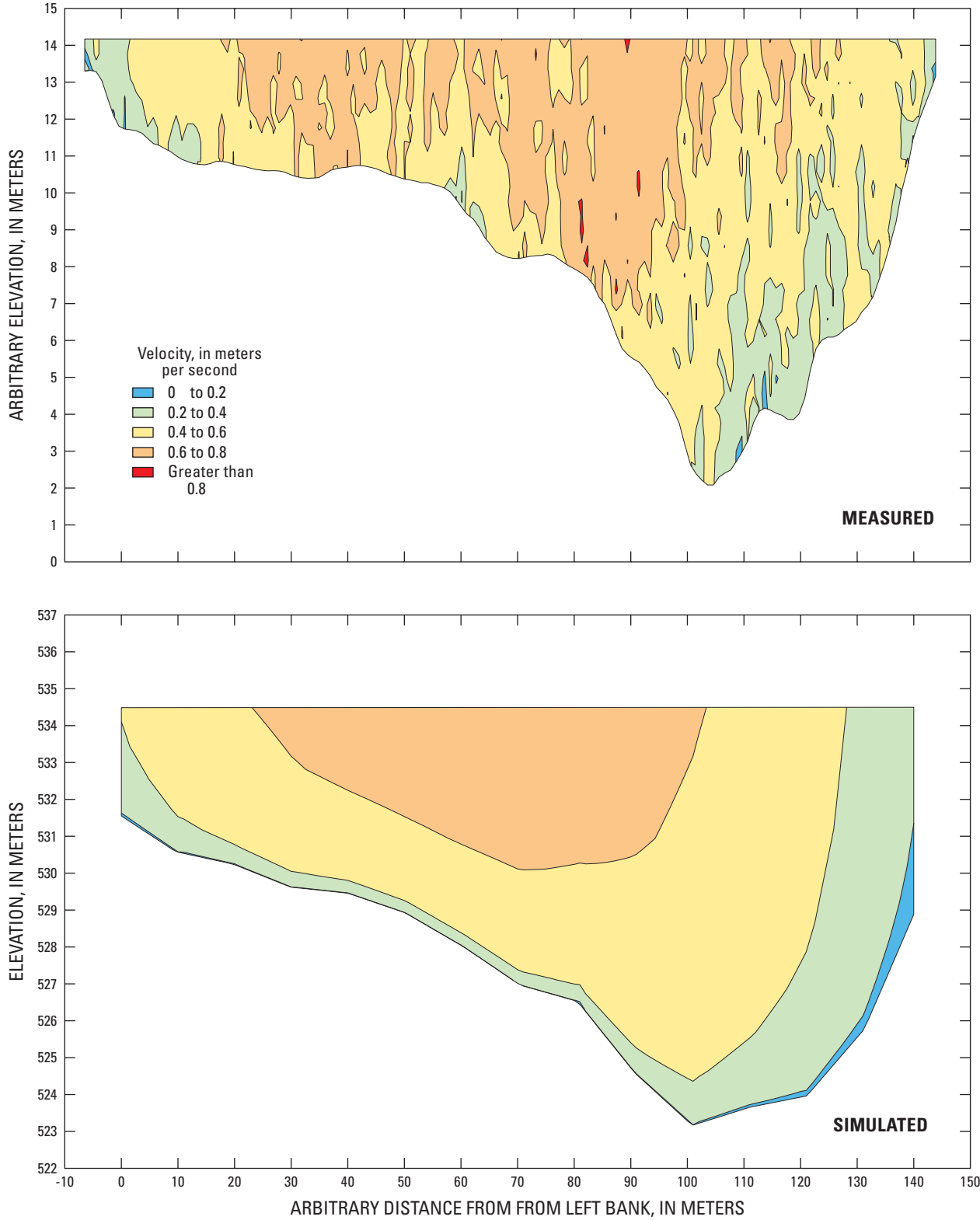
Validation of the model also included comparing measured and simulated vertical structure of downstream and cross-stream velocities for the 15 cross sections. Measured and simulated vertical structures for section 2370 are provided as an example (fig. 20). Downstream velocity is the flow component perpendicular to the measured cross section and cross-stream velocity is the flow component parallel to the measured section. These profiles were assembled by first straightening each measured cross section, as described in Dinehart and Burau (2003; in press). The ensemble-averaged velocity structure then was obtained by interpolating all measured cross sections onto a vertical grid spanning the channel and oriented, as nearly as possible, perpendicular to mean flow direction. Measuring velocities in a large number of ADCP cross sections was intended to increase the possibility that the velocity structure represents average flow. The fact that the contours for measured velocity show extensive variability compared to those of simulated velocity (fig. 20) reflects, in part, both the natural variability of flow due to turbulence and smaller scale features that cannot be resolved by the model and the possibility that the number of measured profiles was inadequate for obtaining a true average. The differences in topography between the measured section and the modeled section are due to: local variation in topography, the presence of dunes, some smoothing of the banks due to discretization of the topography, and the fact that modeled topography was measured at a different time than the topography determined from the ADCP measurements.

Differences in depths are as much as 2 m, which is consistent with the dune amplitudes, and differences in width are on the order of 5 m, which is comparable to the grid spacing.

For downstream and cross-stream velocity, the streamflow simulations represent both the magnitudes and structure of flow reasonably well, including the position of the velocity maxima and the strength of the cross-stream flow (fig. 20). Similar results are found for all cross sections, with the exception of sections 2313 and 2310, as discussed previously.

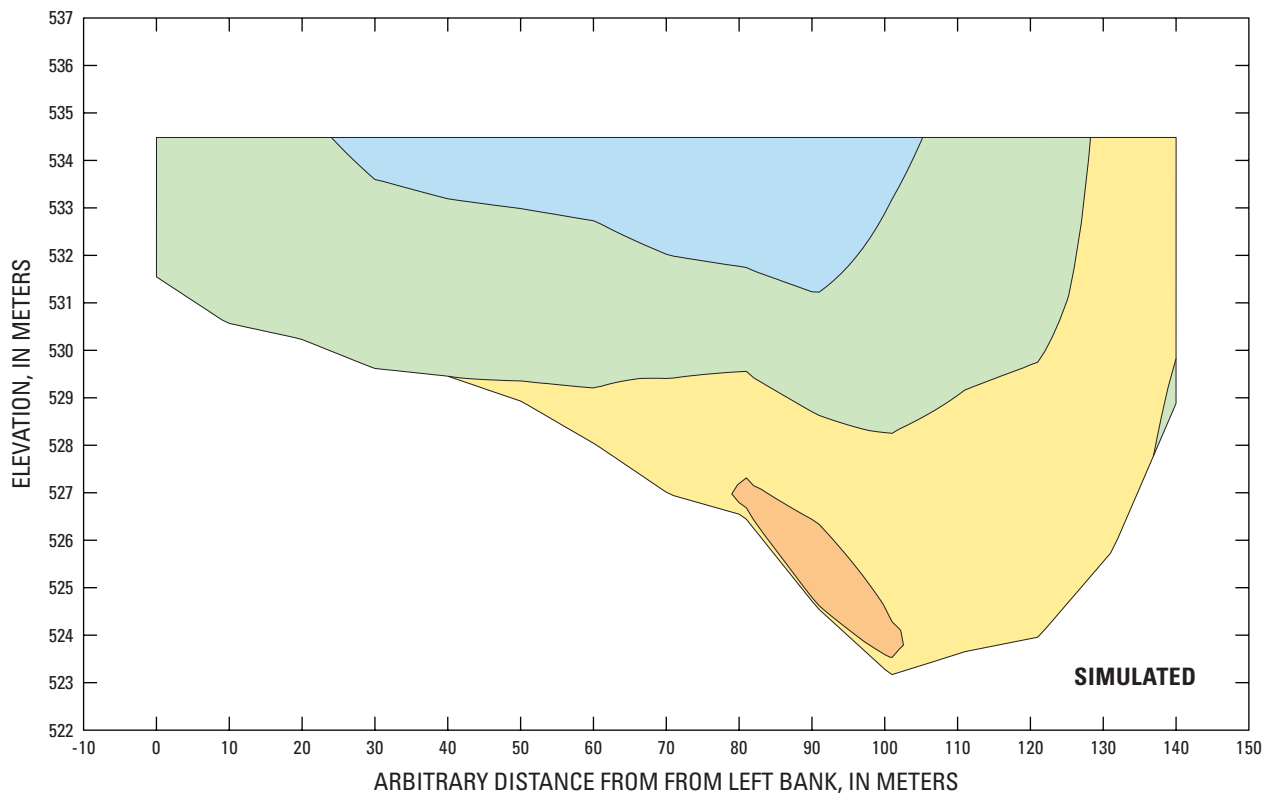
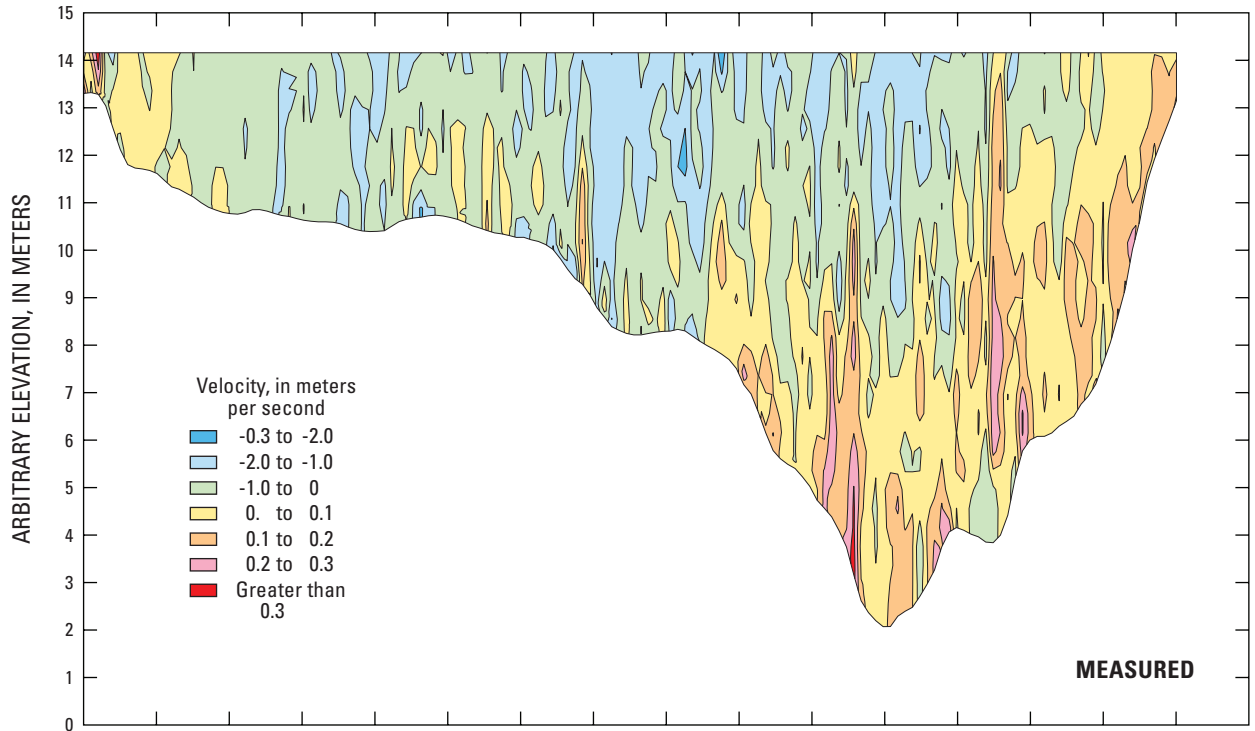
Model Sensitivity Analysis

Sensitivity analysis of the model consisted of decreasing and increasing the calibrated drag coefficient by 75 and 125 percent during streamflow simulation runs of 170, 566, 1,130, 1,700, and 2,270 m³/s. The analysis includes reporting median and maximum river water-surface elevation, velocity, and boundary shear stress for the entire population of wet model nodes (table 3). Varying calibrated drag coefficient by 75 and 125 percent changed the median water-surface elevation on average by 0.05 m. Model-simulated velocities were not sensitive to the choice of drag coefficient. Model-simulated shear stress changed proportionally with the drag coefficient. The sensitivity analysis highlights the importance of first calibrating the model to the roughness, mainly to accurately simulate shear stress.



A. DOWNSTREAM VELOCITY

Figure 20. Measured and simulated vertical profiles of downstream velocity and cross-stream velocity at section 2370 on the white sturgeon critical-habitat reach of the Kootenai River near Bonners Ferry, Idaho, for a steady flow that averaged 538 cubic meters per second on August 12–14, 2003. (Location of cross section shown in [figure 17](#).)



B. CROSS-STREAM VELOCITY

Figure 20. Continued.

Table 3. Sensitivity analysis and results of the multidimensional flow model for the white sturgeon critical-habitat reach of the Kootenai River near Bonners Ferry, Idaho, for five streamflows.

[Streamflow for river model simulation: The model is constructed with a variable drag coefficient for the 170-cubic-meter-per-second flow-management scenario: a drag coefficient of 0.015 is specified for the reach between the model's upstream boundary and Ambush Rock, and 0.004 is specified for the reach between Ambush Rock and the model's downstream boundary. Sensitivity analyses of the calibrated drag coefficient were made at 75 and 125 percent of the drag coefficient value. Reported median and maximum values are based on the population of all wet nodes in the model. **Abbreviations:** m³/s, cubic meter per second; ft³/s, cubic foot per second; m, meter; ft, foot; Med., median; Max., maximum; m/s, meter per second; ft/s, foot per second; newtons/m², newtons per square meter]

Streamflow for river model simulation		Drag coefficient value	Depth				Velocity				Shear stress (newtons/m ²)		Water-surface elevation			
			(m)		(ft)		(m/s)		(ft/s)		Med.	Max.	(m)		(ft)	
(m ³ /s)	(ft ³ /s)		Med.	Max.	Med.	Max.	Med.	Max.	Med.	Max.	Med.	Max.	Med.	Max.	Med.	Max.
170	6,000	0.0040	4.46	19.98	14.63	65.55	0.25	1.07	0.82	3.51	0.25	19.05	533.18	533.54	1,749.36	1,750.54
		.0150														
		.0030	4.45	19.97	14.60	65.52	.19	1.30	.62	4.27	.19	17.05	533.18	533.49	1,749.36	1,750.38
		.0113														
566	20,000	.0050	4.46	20.00	14.63	65.62	.31	1.09	1.02	3.58	.31	22.50	533.19	533.59	1,749.40	1,750.71
		.0188														
		.00400	6.14	22.08	20.15	72.44	.57	1.20	1.87	3.94	1.28	5.80	534.99	535.30	1,755.30	1,756.32
		.00300	6.10	22.01	20.01	72.21	.57	1.30	1.87	4.27	.98	5.10	534.95	535.21	1,755.17	1,756.02
1,130	40,000	.00500	6.17	22.16	20.24	72.71	.56	1.19	1.84	3.90	1.58	7.02	535.03	535.38	1,755.43	1,756.58
		.00260	7.97	24.39	26.15	80.02	.79	1.41	2.59	4.63	1.65	5.18	537.25	537.61	1,762.72	1,763.90
		.00195	7.94	24.32	26.05	79.79	.80	1.43	2.62	4.69	.82	4.74	537.21	537.54	1,762.59	1,763.67
		.00325	8.00	24.46	26.25	80.25	.79	1.37	2.59	4.50	2.03	6.07	537.29	537.69	1,762.85	1,764.16
1,700	60,000	.00200	9.33	26.10	30.61	85.63	.95	1.53	3.12	5.02	1.80	4.68	538.95	539.39	1,768.30	1,769.74
		.00150	9.31	26.08	30.55	85.57	.95	1.56	3.12	5.12	1.34	3.66	538.92	539.34	1,768.20	1,769.57
		.00300	9.37	26.23	30.74	86.06	.94	1.49	3.08	4.89	2.63	7.59	539.01	539.50	1,768.49	1,770.10
2,270	80,000	.00200	10.43	27.76	34.22	91.08	1.03	1.80	3.38	5.91	2.16	6.48	540.53	540.97	1,773.48	1,774.92
		.00150	10.40	27.64	34.12	90.69	1.00	1.84	3.28	6.04	1.52	5.06	540.50	540.89	1,773.38	1,774.66
		.00250	10.47	27.85	34.35	91.38	1.04	1.77	3.41	5.81	2.68	7.83	540.58	541.07	1,773.64	1,775.25

Simulation of Flow and Sediment Mobility in the White Sturgeon Critical-Habitat Reach

The model was used to simulate water-surface elevation, depth, velocity, bed shear stress, and sediment mobility in the Kootenai River for streamflows of 170, 566, 1,130, 1,700, and 2,270 m³/s. The range of simulated streamflows was selected to span river conditions typical of those before and since the construction of Libby Dam. The three lowest streamflows represent a range of conditions that have occurred throughout the historical record. The highest streamflow (2,270 m³/s) represents a discharge that is approximately equal to the annual median peak streamflow (2,237 m³/s) prior to emplacement of Libby Dam in 1972. Streamflows greater than 566 m³/s were increased incrementally by 570 m³/s.

For each of the five streamflows simulated using the model, it was necessary to set a boundary condition for water-surface elevation at the lower end of the modeled reach (table 4). This was determined by searching the historical record of mean daily streamflow for periods when the streamflow of interest was approximately steady for a few days. The 170 m³/s and 566 m³/s streamflows were based on the 2002-03 record from the Tribal Hatchery gaging station (12310100) in the model reach. The 1,130, 1,700, and 2,270 m³/s streamflows were based on the pre-Libby Dam era, when streamflow was much higher. Mean daily streamflow for the modeled reach was calculated as that at the Porthill gaging station (12322000) minus tributary inflow from Boundary Creek gaging station (12321500) during the pre Libby-dam era between 1965 and 1971. The Klockmann Ranch gaging station (12314000) and the Bonners Ferry gaging station (12309500) have no water-surface elevation-discharge relation.

Table 4. Upstream and downstream boundary conditions in the multidimensional flow model for the white sturgeon critical-habitat reach of the Kootenai River near Bonners Ferry, Idaho.

[Streamflow at upper model boundary: Computed as streamflow at Porthill gaging station (12322000) minus streamflow at Boundary Creek gaging station (12321500). Abbreviations: m³/s, cubic meter per second; ft³/s, cubic foot per second; m, meter; ft, foot]

Streamflow for model simulations		Streamflow at upstream model boundary						Water-surface elevation at downstream model boundary					
		Median		Minimum		Maximum		Median		Minimum		Maximum	
(m ³ /s)	(ft ³ /s)	(m ³ /s)	(ft ³ /s)	(m ³ /s)	(ft ³ /s)	(m ³ /s)	(ft ³ /s)	(m)	(ft)	(m)	(ft)	(m)	(ft)
170	6,000	170	6,006	163	5,750	178	6,280	532.97	1,748.59	532.50	1,747.05	533.38	1,749.93
566	20,000	547	19,300	535	18,900	592	20,900	534.71	1,754.30	534.27	1,752.85	535.03	1,755.35
1,130	40,000	1,130	40,000	1,120	39,500	1,145	40,400	536.98	1,761.75	536.06	1,758.73	538.02	1,765.16
1,700	60,000	1,710	60,300	1,680	59,200	1,719	60,700	538.65	1,767.22	538.65	1,767.22	539.48	1,769.95
2,270	80,000	2,270	80,000	2,250	79,300	2,285	80,700	540.22	1,772.38	539.50	1,770.01	540.92	1,774.67

As noted in the discussion of downstream water-surface elevation conditions for the calibration runs, water-surface elevation at the downstream model boundary for each streamflow simulated with the model is a linear interpolation of the water-surface elevation as recorded at the Bonners Ferry gaging station and the Klockmann Ranch gaging station (12314000). For each of the streamflows, 10-17 periods of approximately steady mean daily streamflow were identified and the water-surface elevation at the downstream model boundary was interpolated for each period. The water-surface elevation boundary condition then was identified as the median of all the calculated values. Table 4 presents the median, minimum, and maximum mean daily streamflow and water-surface elevation boundary condition for each of the five simulations.

Modeling results for the five streamflows provide insight into the spatial variability of water-surface elevation, depth, velocity, and shear stress (table 3). Median and maximum river depth, velocity, and shear stress are computed for all wet nodes in the model for each of the five simulated streamflows. In addition, for each of the five simulated streamflows, the average, maximum, and standard deviation of water-surface elevation, depth, velocity, and sediment mobility were calculated at 174 cross sections of the river channel, positioned every 100 m along the length of the model reach.

A few simple simulations are presented below to demonstrate how the model can be used to link physical characteristics of streamflow to biological or other habitat data. Some measures of depth, velocity, and substrate composition generally are considered when assessing sturgeon spawning habitat (Parsley and others, 1993). Habitat suitability curves developed for white sturgeon in the Lower Columbia River (Parsley and Beckman, 1994) were used to characterize conditions in the Kootenai River spawning habitat. Requirements for Kootenai River white sturgeon spawning habitat may vary from that in the Lower Columbia River; however, both rivers are highly-regulated systems. Discussions of the model simulation include relating the model results to observed patterns of spawning and egg locations, specifically

the number of spawning events per unit of effort (SEPUE), to illustrate how model results can be combined with biological data or other assessments of habitat quality.

Water-Surface Elevation Profiles and Free-Flowing and Backwater Streamflow

The modeling results do not support the hypothesis presented by Paragamian and others (2001) that the relative location of free-flowing and backwater streamflow may play a role in influencing white sturgeon spawning patterns. In view of this hypothesis, simulation of the water-surface elevation profiles over a range of streamflows is important. Model results for the five simulated streamflows and spawning event locations are presented here. Water-surface elevations vary by about 7 m between the lowest and highest streamflow simulations. Average slope of the water surface increased as streamflow increased (fig. 21), with slopes from lowest to highest simulated streamflow of 0.000014, 0.000028, 0.000033, 0.000037, and 0.000041 m³/s, respectively. The 170-m³/s streamflow simulation has the gentlest slope for the entire modeling reach; however, the slope of the water surface is markedly steeper (0.0002) than slopes associated with streamflow simulations over a 600-m reach downstream of the U.S. Highway 95 Bridge between RKM 245.4 and 246. The greater slope indicates water is free flowing in this short reach for this low streamflow; whereas, backwater conditions exist for the four larger streamflows. This occurs because water levels in Kootenay Lake tend to be low during periods of low streamflow and high during periods of higher streamflow. Since 1994, white sturgeon spawning was detected at egg-mat monitoring stations only in 2001, at RKM 245.7 and 245.1, in the straight reach between Ambush Rock and the U.S. Highway 95 Bridge (Paragamian and others, 2002). During 2001, spawning occurred further upstream than any other time during 1994-2001, at the same time, free-flowing streamflow was further downstream than any other spawning event during the same period. These spawning events occurred during flows between 179 and 188 m³/s, which are similar to the 170-m³/s streamflow simulation.

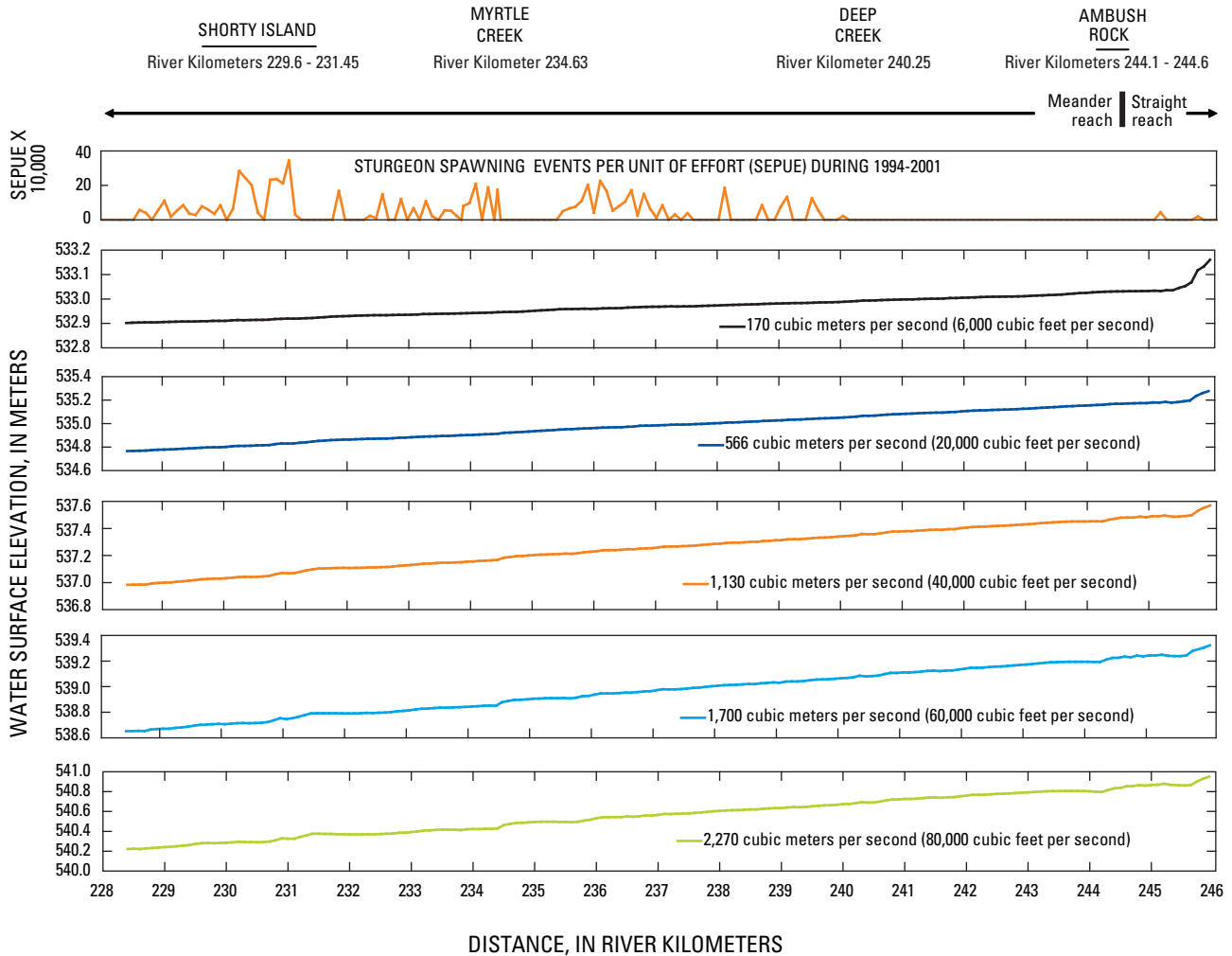


Figure 21. Simulated average water-surface elevation for five streamflows at cross sections positioned every 100 meters along the white sturgeon critical-habitat reach of the Kootenai River near Bonners Ferry, Idaho, and spawning event locations.

River Depth

The model simulated median and maximum river depth for all wet nodes (table 3). For the lowest and highest streamflow simulations (170 and 2,270 m³/s) these variables ranged from 4.5 to 10.4 m and from 20.0 to 27.8 m, respectively. The model also simulated average and maximum water depth for the five streamflows at cross sections every 100 m along the modeled reach (fig. 22). The river depth is shallowest in the upper one-half kilometer or so of the straight reach. In this area, the average depth for the lowest and highest streamflow simulations is 2.5 and 8.7 m and the maximum depth is 4.3 and 12.0 m. Below Ambush Rock, in the meandering reach, the average depth is 6.8 and 14.6 m and the maximum river depth is 15.6 and 23.1 m.

The river channel is locally deep in several areas along the model reach (fig. 22). The deepest point in the channel is at Ambush Rock, where the maximum river depth is 19.8 m for the lowest simulated flow and 27.5 m for the highest simulated flow. Other deep areas are at the outside of the

channel where the channel curvature is highest in the S-shaped meander near Myrtle Creek. The deep area near RKM 240.6 is associated with a bedrock outcrop on the left bank just upstream of the mouth of Deep Creek. A lateral recirculation eddy forms downstream of the outcrop and a deep hole with a depth ranging from 10.2 to 17.9 m is in the main channel adjacent to the eddy. Another deep hole is associated with a lateral recirculation eddy at RKM 229.8, along the right bank near the downstream end of Shorty Island, with a maximum depth of 13.6 to 20.9 m.

Egg collection on the Kootenai River during the past 12 spawning seasons shows that sturgeon eggs tend to accumulate in the thalweg, where depths can exceed 14 m (Vaughn Paragamian, U.S. Fish and Wildlife Service, oral commun., 2005). Parsley and Beckman (1994) presented microhabitat criteria curves showing that the depths for spawning white sturgeon in the Lower Columbia River range from 3.5 to 25 m. Habitat suitability in the straight reach ranges from poor to excellent and in the meandering reach is generally excellent (fig. 22). Although a comparison of simulated

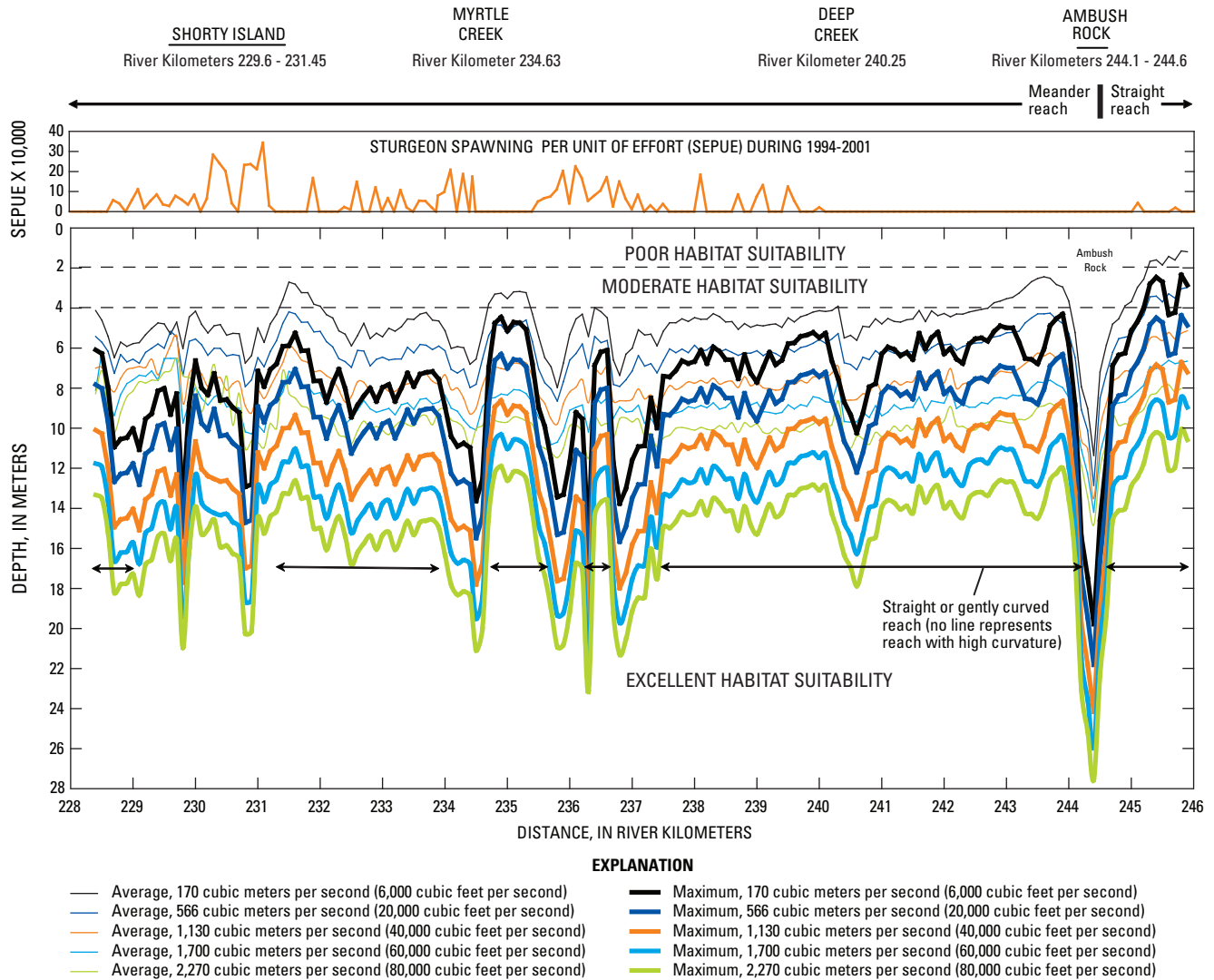


Figure 22. Simulated average and maximum depth for five streamflows at cross sections positioned every 100 meters along the white sturgeon critical-habitat reach of the Kootenai River near Bonners Ferry, Idaho, and spawning event locations. Spawning habitat suitability were developed for the white sturgeon in the Lower Columbia River (Parsley and Beckman, 1994). Requirements for Kootenai River white sturgeon spawning habitat may vary from that of the Lower Columbia River.

river depth and sturgeon spawning event locations per unit effort (egg locations) in the critical-habitat reach indicate that egg locations are preferentially found in deeper areas (fig. 22), careful analysis suggests that this is only a weak positive correlation (McDonald and others, 2004). Eggs are only slightly more likely to be found in deeper parts of the river. This correlation becomes slightly stronger if simulation results upstream of Ambush Rock (in the straight reach) are neglected.

Streamflow Velocity

The model simulates both streamwise and cross-stream velocity components at 15 points in the vertical for every horizontal grid point in the model reach, so providing a simple synopsis of all the information is difficult. However,

a general description of the river velocity structure can be developed by examining variation of median and maximum values of simulated velocity for all model nodes (table 3), as was done for the discussion of flow depth. The model also simulated average and maximum velocity for cross-sections located every 100 m along the model reach (fig. 23). Median and maximum velocity ranged from 0.25 and 1.07 m/s for the lowest streamflow to 1.0 and 1.8 m/s for the highest streamflow (table 3). The spatial variation in velocity across the river channel has been quantified using the standard deviation of velocity at cross sections positioned every 100 m along the length of the model reach. Standard deviation of velocity increases more than four-fold as streamflow increases from the lowest to the highest streamflow simulations (fig. 24), from an average of 0.09 to 0.43 m/s for the streamflow simulation of 170 and 2,270 m³/s.

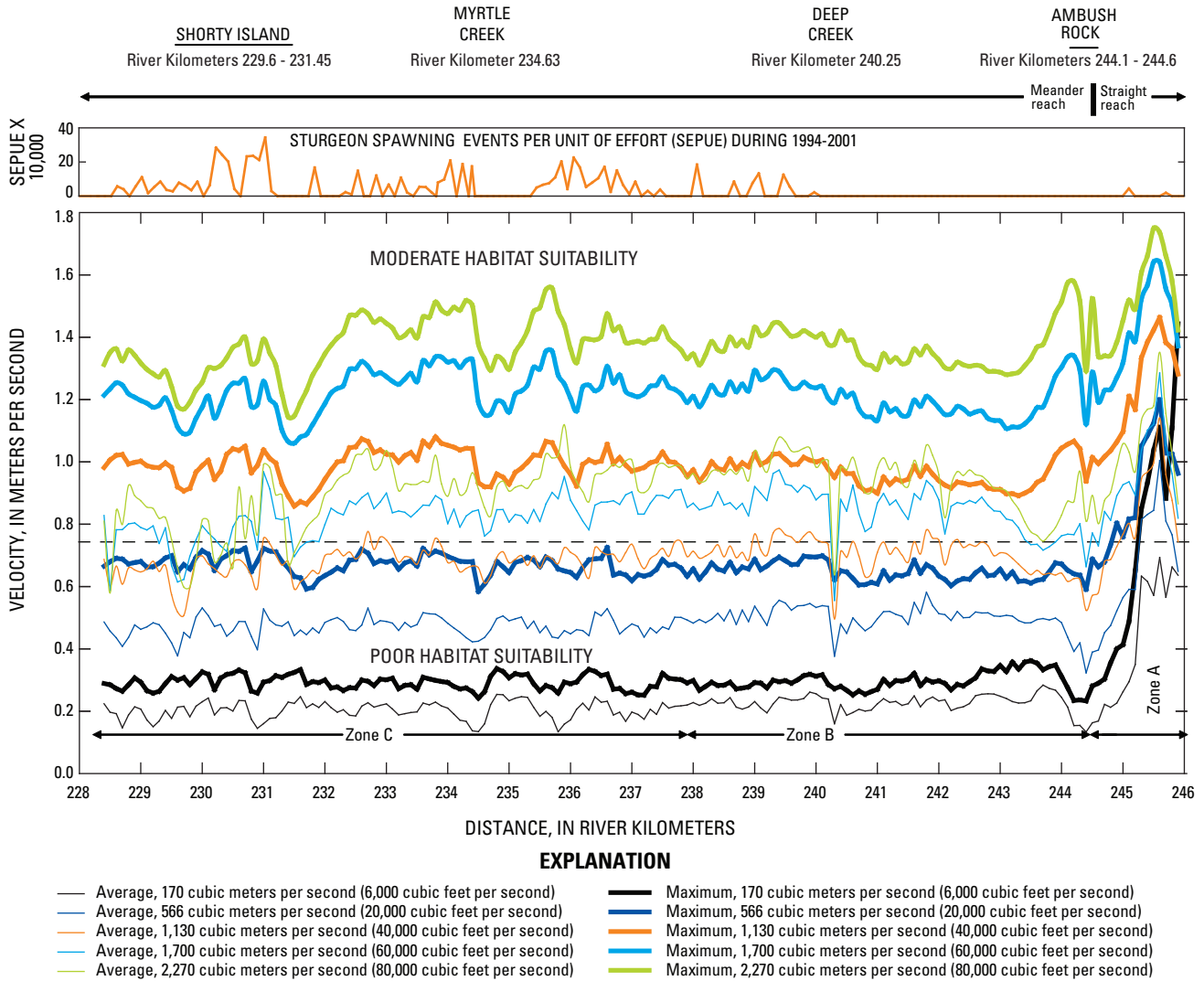


Figure 23. Simulated average and maximum velocity for five streamflows at cross sections positioned every 100 meters along the white sturgeon critical-habitat reach of the Kootenai River near Bonners Ferry, Idaho, and spawning event locations. Spawning habitat suitability were developed for the white sturgeon in the Lower Columbia River (Parsley and Beckman, 1994). Requirements for Kootenai River white sturgeon spawning habitat may vary from that of the Lower Columbia River.

The model reach can be divided into three velocity zones on the basis of the difference and variability of maximum simulated velocity along the length of the model reach (fig. 23). Zone A, between the upstream model boundary and Ambush Rock, is a region of high velocity. Maximum velocities in zone A generally are higher than those in the rest of the model reach, but the differences decrease with increasing streamflow (fig. 24). Zone B, between Ambush Rock and the first sharp meander below the mouth of Deep Creek at RKM 237.5, has less variable maximum streamflow velocities compared to the rest of the model reach. One notable exception is near the deep hole and lateral recirculation eddy above Deep Creek mentioned earlier. Zone C, downstream of zone B and extending to the downstream

model boundary at RKM 228.4, shows variations in the maximum velocity that increase with increasing streamflow. The greatest variability in velocity shown by the standard deviation (fig. 24) is a reflection of the complex channel geometry through the S-shaped meander and flow divergence around Shorty Island. The greatest occurrence of white sturgeon spawning is in zone C (fig. 24).

Studies on the Columbia River indicate that sturgeon seek areas of high velocity for spawning (Parsley and others, 1993). In other studies, lake sturgeon were found to spawn in tributary rapids (Auer, 1996; LaHaye and others, 1992). Spawning habitat suitability for streamflow velocity in the model is evaluated here using the research of Parsley and Beckman (1994). In the meander reach, the average velocity

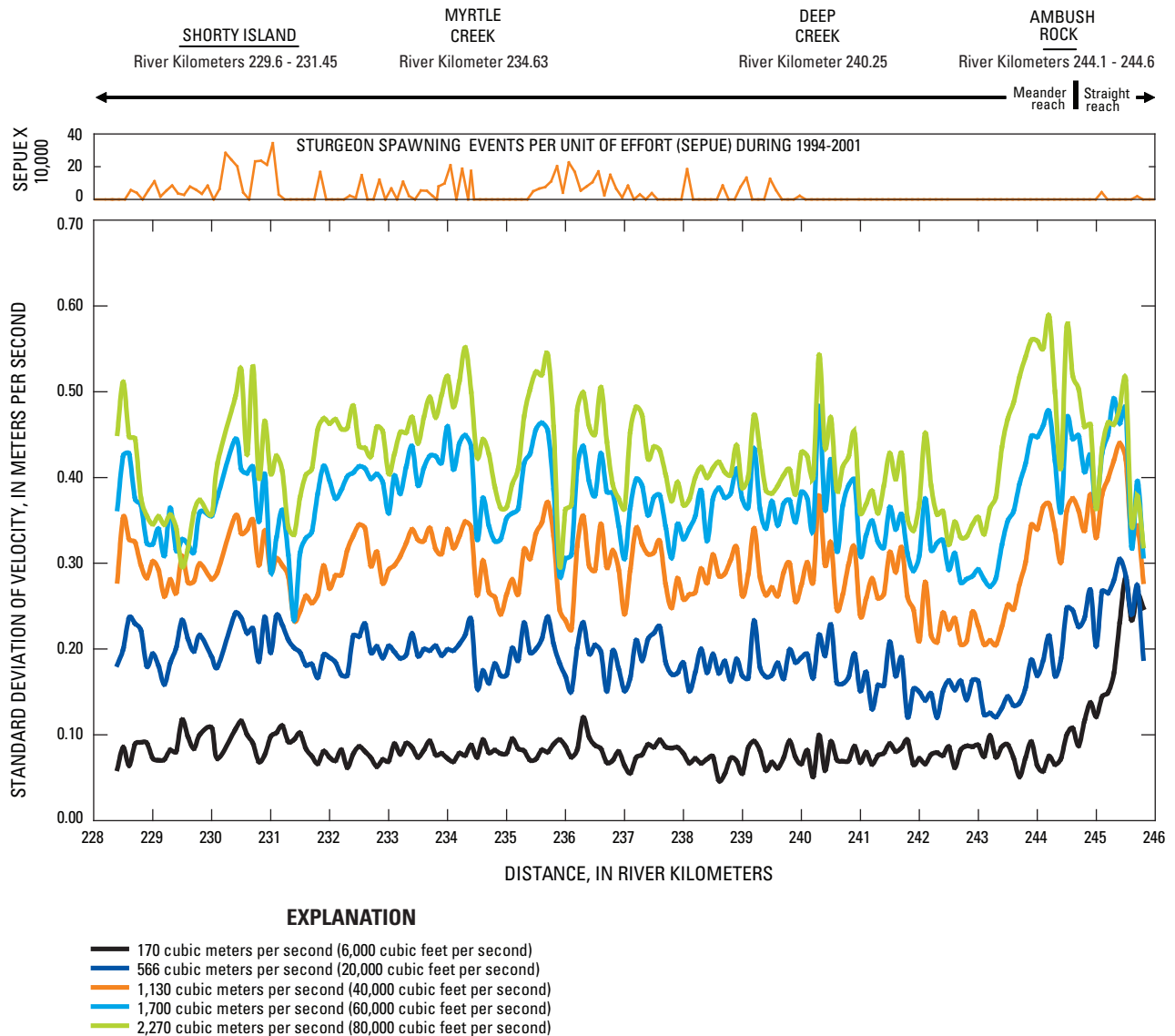


Figure 24. Standard deviation of simulated velocity for five streamflows at cross sections positioned every 100 meters along the white sturgeon critical-habitat reach of the Kootenai River near Bonners Ferry, Idaho, and spawning event locations.

at streamflows of 1,700 and 2,270 m^3/s is classified moderate except for parts of the reach at Shorty Island, where velocity is classified poor; streamflows of 1,130 m^3/s and less are classified poor. In the straight reach, the average velocity at all streamflows is classified poor to moderate except at a streamflow of 170 m^3/s , which is classified poor throughout the reach (fig. 23).

Streamflow velocities equal to or greater than 1.0 m/s are believed to greatly reduce or eliminate predation of white sturgeon eggs (Bob Hallock, U.S. Fish and Wildlife Service, oral commun., 2005) and based on the modeling results,

the velocities seldom are equal or greater than 1.0 m/s . The simulated average velocity in the main channel at Shorty Island, where white sturgeon most frequently spawn (Paragamian and others, 2002), does not approach 1.0 m/s until streamflow is 2,270 m^3/s , and this only occurs near RKM 231.1 (figs. 23 and 25). Streamflow of this magnitude only occurred prior to the Libby Dam era. However, maximum simulated velocity in the spawning reach is greater than 1.0 m/s for flows equal to and greater than a streamflow of 1,130 m^3/s . During the Libby Dam era there have been very few spawning seasons with streamflow of 1,130 m^3/s or greater.

SIMULATED VELOCITY STRUCTURE IS CONTINUED DOWNSTREAM ON THE OPPOSING PAGE.

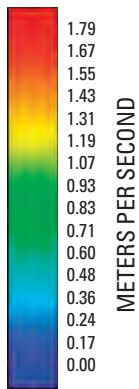


A. SIMULATED STEAMFLOW, 170 CUBIC METERS PER SECOND.



B. SIMULATED STEAMFLOW, 566 CUBIC METERS PER SECOND.

Figure 25. Distribution of simulated velocity for five streamflows in the white sturgeon critical-habitat reach of the Kootenai River near Bonners Ferry, Idaho. (Showing velocity at the same scale for all river-management scenarios for the sake of comparison means that some detail is lost for the lower streamflow scenarios.)



A. SIMULATED STREAMFLOW, 170 CUBIC METERS PER SECOND.—Continued



B. SIMULATED STREAMFLOW, 566 CUBIC METERS PER SECOND.—Continued

Figure 25. Continued.

SIMULATED VELOCITY STRUCTURE IS CONTINUED DOWNSTREAM ON THE OPPOSING PAGE.

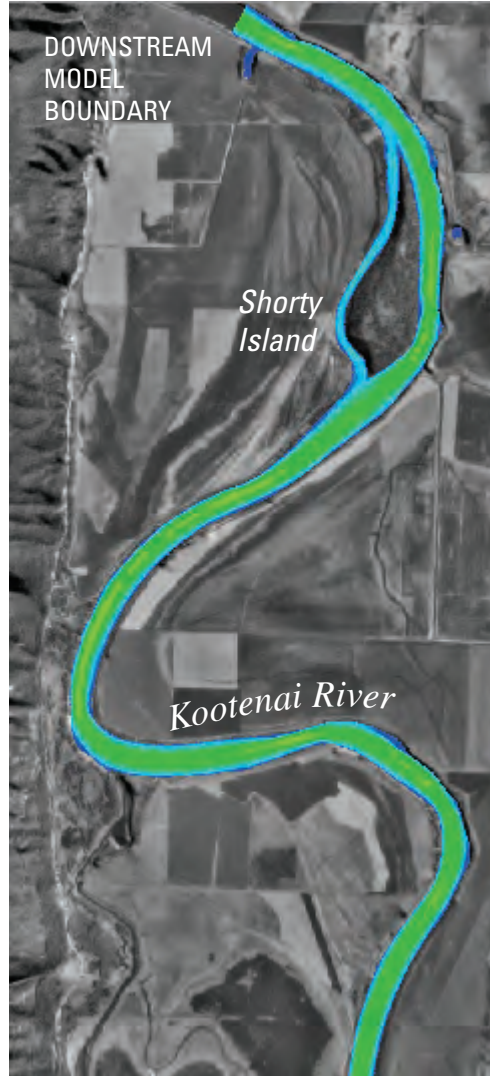
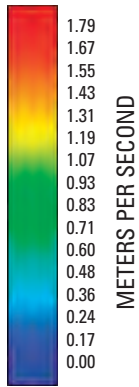


C. SIMULATED STEAMFLOW, 1,130 CUBIC METERS PER SECOND.

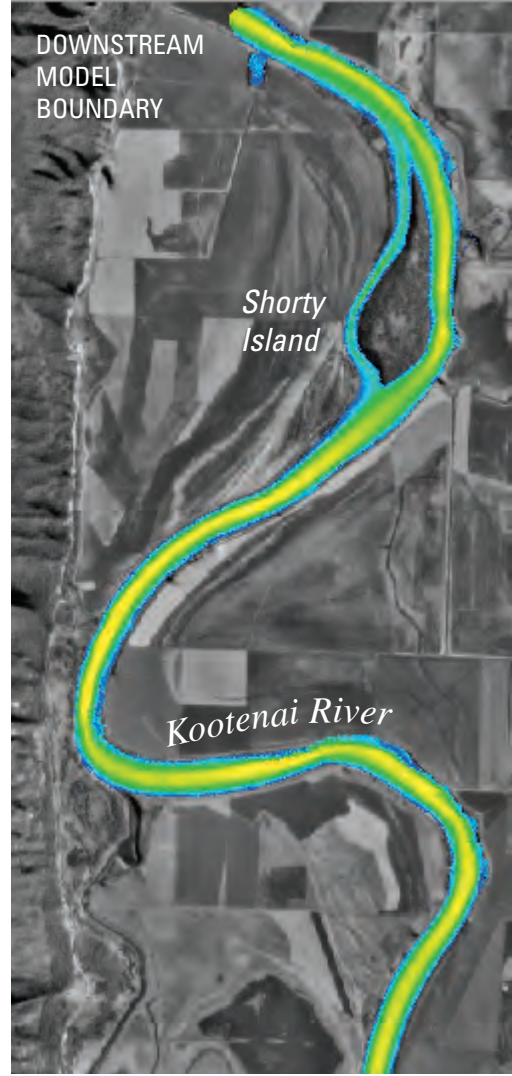


D. SIMULATED STEAMFLOW, 1,700 CUBIC METERS PER SECOND.

Figure 25. Continued.



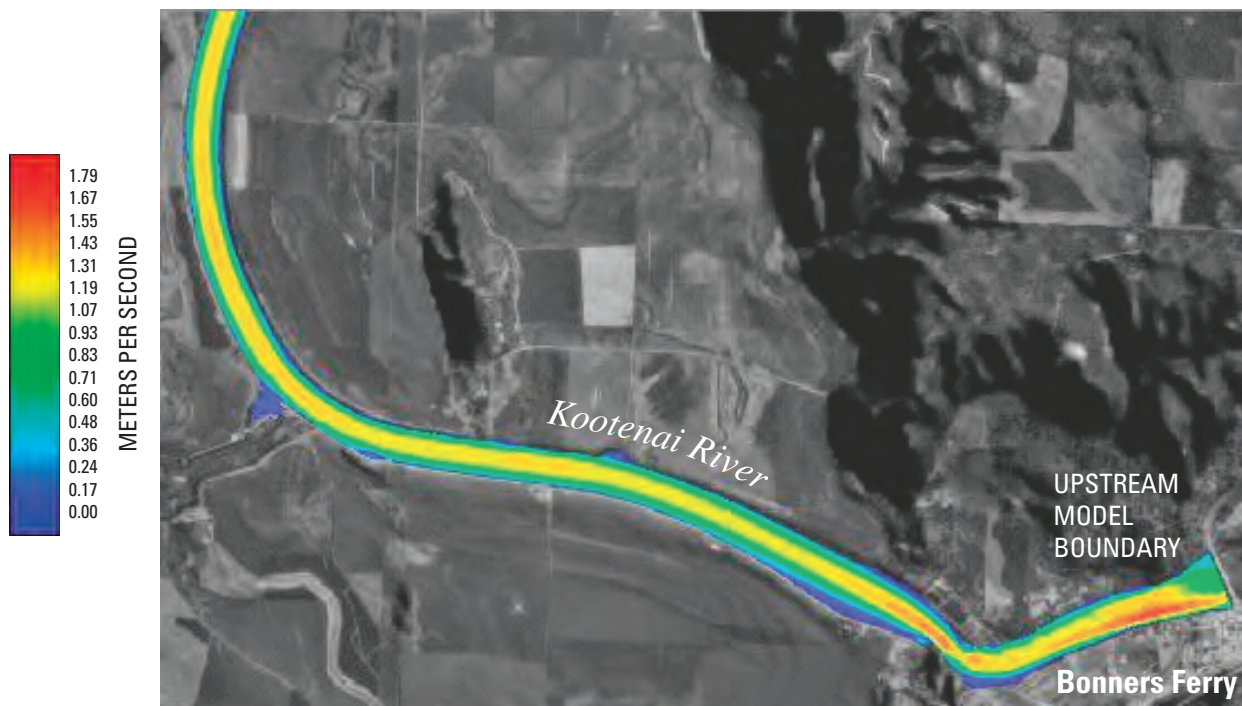
C. SIMULATED STREAMFLOW, 1,130 CUBIC METERS PER SECOND.—Continued



D. SIMULATED STREAMFLOW, 1,700 CUBIC METERS PER SECOND.—Continued

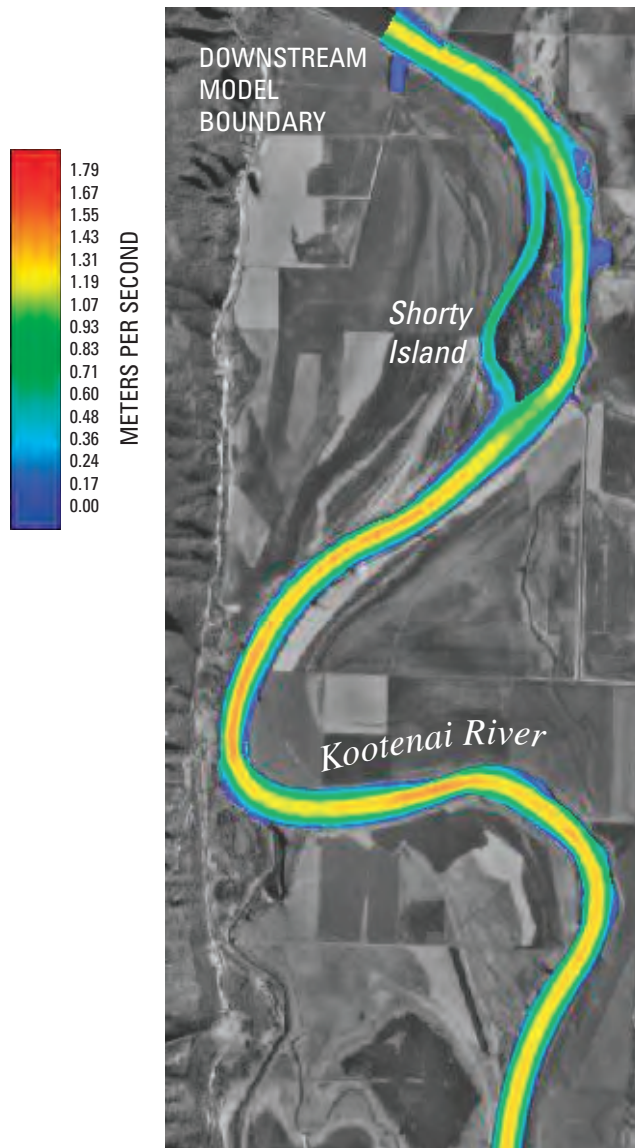
Figure 25. Continued.

SIMULATED VELOCITY STRUCTURE IS CONTINUED DOWNSTREAM ON THE OPPOSING PAGE.



E. SIMULATED STEAMFLOW, 2,270 CUBIC METERS PER SECOND.

Figure 25. Continued.



Recently collected LIDAR data indicates the elevation of Shorty Island is lower than that used on the multidimensional model. Inundation of Shorty Island may be substantially greater than shown in this simulation of high flow pre-Libby Dam conditions.

E. SIMULATED STREAMFLOW, 2,270 CUBIC METERS PER SECOND.—Continued

Figure 25. Continued.

Sediment Mobility

The model-simulated bed shear stress was used to assess sediment mobility over a range of streamflows from 170 to 2,270 m³/s for several particle sizes representative of the meandering reach below Ambush Rock and the straight reach above Ambush Rock. The ability of flow to move sediment most often is related to the shear stress of flow at the bed. Sediment movement occurs at a threshold or critical shear stress (Julien, 2002). FaSTMECH calculates bed shear stress as follows:

$$Tb = \rho Cd(u^2 + v^2), \quad (2)$$

where the variables are defined as follows:

- Tb is boundary shear stress, in newtons per square meter,
- ρ is fluid density, in kilograms per cubic meter,
- Cd is non-dimensional drag coefficient,
- u is vertically averaged streamwise velocity, in meters per second, and
- v is vertically averaged cross-stream velocity, in meters per second.

In sand-bedded channels where bedforms are present, such as the Kootenai River white sturgeon critical-habitat reach, the total boundary shear stress needs to be partitioned as calculated by the flow model into a form drag component due to bedforms and a skin friction component due to the sediment surface (McLean, 1992). In other words, resistance to flow, or drag coefficient, is the sum of resistance due to bedforms when present and resistance due to sediment grains making up the bed. Resistance to flow due to sediment grains is responsible for the movement of sediment. The component of shear acting on the grains can be calculated from the total shear stress as follows (Bennett, 1995, equation 9; Smith and McLean, 1977; and, Nelson and others, 1993):

$$\tau'_o / \tau = 1 / ((1 + C_d / 2K^2(\Delta / \lambda) \ln^2(0.368\Delta / z_o)), \quad (3)$$

where the variables are defined as follows:

- τ'_o is grain shear stress,
- τ is total boundary shear stress, derived from MD_SWMS output,
- C_d is drag coefficient for bedforms, typically has a value of 0.2,
- K is von Karman's constant,
- Δ is bedform wavelength, user defined,
- λ is bedform wavelength, user defined, and
- z_o is roughness height, user defined.

For all flows modeled in the sand-bedded reach, the fraction of the total bed shear stress that is due to the grain shear stress was calculated and used to assess the sediment mobility. Critical shear stress for grain motion is based on Shields (1936) using equation (4).

$$\tau_c = D_s \gamma_s \theta^*, \quad (4)$$

where:

- τ_c is critical shear stress for grain motion, newtons/m²,
- D_s is grain diameter, in meters,
- γ_s is sediment density, and
- θ^* is dimensionless Shields parameter.

[Table 5](#) summarizes the dimensionless Shields critical shear stress and critical shear stress values for a range of sediment sizes. Sediment mobility for a given grain size occurs when the boundary shear stress exceeds the critical shear stress.

Table 5. Sediment grade scale and critical shear stress for determining approximate condition for sediment mobility at 20 degrees Celsius.

[Sediment mobility for a given grain size occurs when the boundary shear stress exceeds the critical shear stress. It is important to note that this only determines whether or not a given grain size is mobile. **Abbreviations:** mm, millimeter; newtons/m², newtons per square meter; >, greater than. **Source:** Pierre Julien (1998, table 7.1)]

Class name	Diameter (mm)	Shields critical shear stress (dimensionless)	Critical shear stress (newtons/m ²)
<i>Boulder</i>	>2,048	0.054	1,790
Large	>1,024	.054	895
Medium	>512	.054	447
Small	>256	.054	223
<i>Cobble</i>			
Large	>128	.054	111
Small	>64	.052	53
<i>Gravel</i>			
Very coarse	>32	.05	26
Coarse	>16	.047	12
Medium	>8	.044	5.7
Fine	>4	.042	2.71
Very fine	>2	.039	1.26
<i>Sand</i>			
Very coarse	>1	.029	.47
Coarse	>.5	.033	.27
Medium	>.25	.048	.194
Fine	>.125	.072	.145
Very fine	>.0625	.109	.11
<i>Silt</i>			
Coarse	>.031	.165	.083
Medium	>.016	.25	.065

This analysis determines whether or not a given grain size is mobile, but does not calculate potential for erosion or deposition, which is determined by the divergence or convergence in the sediment transport rate, which is not addressed in this report.

Grain shear stress within the straight reach was set equal to the total shear stress. Grain shear stress within the meandering reach for three of the five streamflow simulations was simulated by specifying a dune amplitude and bedform wavelength equivalent to the average dune geometry that was observed during 2002 (table 1). The dune amplitude and wavelength specified in the model for the 170-m³/s streamflow simulation are 0.66 m and 20.4 m, for the 566-m³/s streamflow simulation are 0.45 m and 18.7 m, and for the 1,130-m³/s streamflow simulation are 0.2 m and 13.1 m, respectively. For the 1,700- and 2,270-m³/s streamflow simulations the bedforms were assumed to have washed out, as discussed earlier. Calculations based on the Rouse number, which can be used to describe the relative importance of transport mode (bedload versus suspended load) suggest that at the highest flows the transport is dominated by suspended load transport and support the assumption that dunes wash out. Therefore, the bedform drag component of the total boundary shear stress is considered negligible for the highest flows, so total boundary shear stress is equivalent to grain shear stress.

Quantification of sediment mobility provides preliminary insight into streamflow requirements for flushing silt and sand currently burying gravel and cobble substrate that could be used for spawning and egg incubation. Very-fine to fine gravel is mobile in the straight reach for all five streamflow simulations; however, at the lowest streamflow of 170 m³/s gravel is mobile in only the upper half of the reach (fig. 26).

Very coarse sand (b-axis diameter of >1.0 mm and <2 mm) is not mobile for about the lower third of the straight reach for the 170 m³/s streamflow simulation. Gravel becomes slightly more mobile at higher streamflows because the maximum grain shear stress increases as streamflow increases from the lowest to the highest streamflow simulations (fig. 26), from cross-sectional average values of 0.2 newtons per square meter (N/m²) to 5.0 N/m² and 2.3 N/m² to 6.2 N/m² for the streamflow simulations of 170 and 2,270 m³/s, respectively. However, gravel is most mobile for streamflow simulation of 170 m³/s at RKM 245.9.

In contrast to the straight reach, very fine gravel (b-axis diameter of >2 mm and <4 mm) is mobile in the meandering reach for only the three highest streamflow simulations of 1,130, 1,700, and 2,270 m³/s. Some gravel, cobble, and riprap are on the riverbed in the meandering reach, as noted earlier, but these sediments generally are in limited areas along the outside of meander bends where the streamflow velocities are higher. Some of these sediments do not occur naturally and are associated with dikes that line the river. The D₈₄ particle size of 0.33 mm in the meandering reach is medium sand and is not mobile at the lowest streamflow simulation. Sand in the meandering reach is more mobile at higher streamflows. Average and maximum grain shear stress increase more than an order of magnitude as streamflow increases from the lowest to the highest streamflow simulations (fig. 26), from 0.1 to 1.3 N/m² and 0.1 to 2.4 N/m² for streamflow simulations 170 and 2,270 m³/s. The contrast in sediment mobility between the meandering and straight reach shows that average and maximum grain shear stress for all five streamflow simulations is a factor of 2.5 and 2.7 greater in the straight reach compared to the meandering reach.

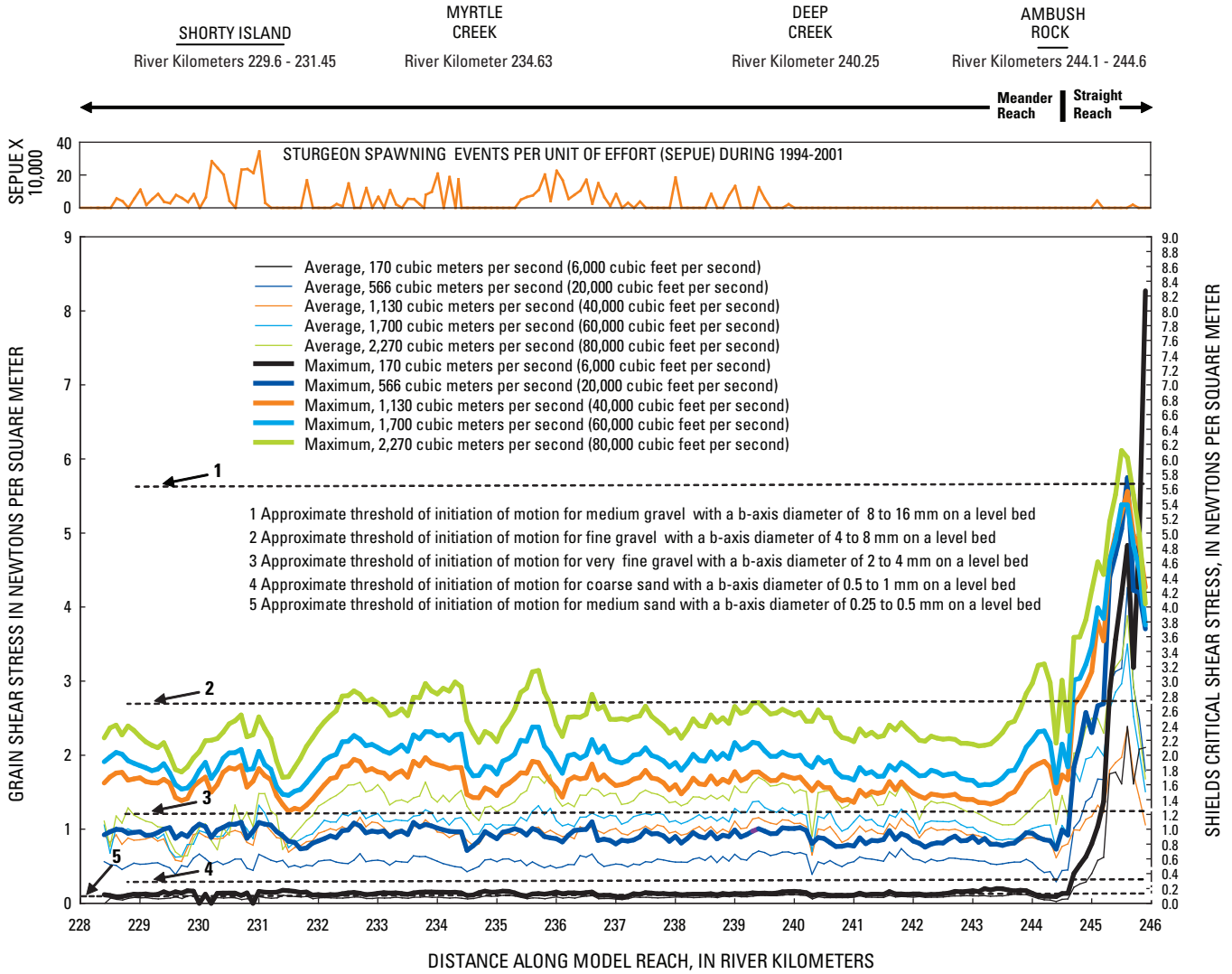


Figure 26. Simulated sediment mobility and critical shear stress for five streamflows at cross sections positioned every 100 meters along the white sturgeon critical-habitat reach of the Kootenai River near Bonners Ferry, Idaho, and spawning event locations.

Model Limitations

A fair evaluation of the applicability of the model to concerns about sturgeon spawning habitat requires consideration of potential modeling approach limitations, some of which are associated with the formulation of the model, and some of which are associated with limitations in the field data used to develop, calibrate, and validate the model. The model's ability to simulate the velocity flow field, bed shear stress, and sediment mobility is constrained largely by (1) the accuracy and level of channel geometry detail, especially regarding errors that could arise because topography was measured during varying streamflows, because different streamflows were used in the model, and because the accuracy of the current topology available for Shorty Island is not known, (2) the way the relation between streamflow and bedforms was characterized, and (3) the potential errors incurred by applying a steady-state model to unsteady flow situations. Several minor potential sources of error also are in the model. For example, flow dynamics adjacent to anthropogenic or natural vertical obstructions in the flow field would be better described using a fully 3-dimensional model. Similarly, the model treatment of turbulence is fairly simple because areas in the river with undulating and complex bathymetry most likely are areas where advection of turbulence and anisotropy in the turbulence field are important. Because of the complex computations, and the requirement to collect even more data, the beneficial return of an unsteady 3-dimensional, turbulence-resolving model probably is limited.

Although the model was calibrated to a maximum streamflow of 2,540 m³/s, the calibration streamflows greater than 1,400 m³/s represent the pre-Libby Dam era, so the modern channel bathymetry used in the model may not accurately reflect the bed morphology present during those flows. On the basis of stream gaging measurements, Barton (2004) reported that the closure of Libby Dam did not influence the long-term mean elevation of the riverbed beneath the Copeland cableway: 524.7 m (n = 599) is the median value during the pre-Libby Dam era from 1929 through 1971 and 524.7 m (n = 145) is the median value during the Libby Dam era from 1972 to 1993. The Copeland gaging station (12318500) is about 30.4 km below the downstream boundary of the model reach. Although strong evidence indicates that pre-dam and dam-era channel geometry generally are similar, the accuracy of streamflow simulations for pre-dam peak flows is expected to be less than streamflow simulations for dam-era peak flows.

Velocity conditions at the upstream boundary of the model grid have a profound effect on the flow simulation for roughly the upper 1 km of the modeling reach. Velocity conditions have been specified at the upstream boundary in the model based on field measurements taken at the boundary during streamflows of 776 m³/s and 1,260 m³/s.

Velocity boundary conditions likely will vary for streamflow conditions that are greater or less than streamflow during field measurements.

Summary

In support of the Kootenai River White Sturgeon Recovery Team, the USGS developed, calibrated, and validated a multidimensional model for streamflow in the critical-habitat reach of the Kootenai River near Bonners Ferry, Idaho. The results of a few simple streamflow simulations and demonstrations of how the model can be used to link physical characteristics of streamflow to biological or other habitat data are presented, as well as model limitations. The model potentially is a useful tool for quantifying quality and quantity of white sturgeon spawning and rearing habitat, as well as for evaluating proposed habitat enhancement measures.

During the field study, the channel geometry in the white sturgeon spawning reach was mapped with a horizontal accuracy of ± 0.051 m and a vertical accuracy of ± 0.041 m. In addition, the $\frac{1}{2}$ phi particle-size distribution of riverbed sediments was determined, the degradation and aggradation of the Kootenai River channel were measured at five sites, and the amplitude and wavelength of dunes and other bedforms were monitored at five sites for streamflows of 229, 663, 1,110, and 1,150 m³/s. The velocity structure of the river also was mapped in detail at 15 cross sections using an acoustic Doppler current profiler and mapping-grade global positioning system.

The USGS MultiDimensional Surface-Water Modeling System was used to construct a flow model for the critical-habitat reach of the Kootenai River, between river kilometers (RKM) 228.4 and 245.9. The model reach is subdivided into two reaches based on the primary sediment forming the river substrate: (1) a straight reach with a sand, gravel, and cobble substrate between the upstream model boundary (RKM 245.9) and the upstream end of Ambush Rock (RKM 244.6), and (2) a meandering reach consisting primarily of a sand substrate between the upstream end of Ambush Rock and the downstream model boundary. Near the downstream boundary, Shorty Island divides the flow into a main and a secondary channel. In addition, the model reach was divided into three velocity zones based on the velocity structure characteristics within each zone. The computational grid used to model Kootenai River was 17,525 m in length with 3,505 nodes in the downstream direction and 800 m in width with 161 nodes in the cross-stream direction, forming an approximately 5.0- by 5.0-m grid.

The model was calibrated to 14 historical streamflow conditions ranging from 157 to 2,540 m³/s. Model calibration indicated that bedform-induced form drag is a significant fraction of the flow resistance in the Kootenai River for

streamflow less than about 595 m³/s. Friction along the riverbed is increased at low streamflows due to formation of tall dunes, and friction decreases at higher streamflows because the dunes tend to wash out.

The model was validated by comparing simulated flow velocities with flow velocities measured at 15 cross sections between RKM 229.1 and 236.9 during steady streamflow that averaged 538 m³/s on August 12-14, 2003. The model simulates the magnitude and structure of flow across the section reasonably well, with a few notable exceptions. The model slightly under-simulated the magnitude and location of peak velocities in cross sections at the apex of bends in the river. This is a common result for models that are not fully 3-dimensional, and can be attributed to the lack of secondary flow feedback on primary velocity distribution. Streamflow simulations for the first two sections in the main channel around Shorty Island (2313 and 2310) are notably poor. Validation of the model also included comparing measured and simulated vertical structure of downstream and cross-stream velocities for the 15 cross sections. For downstream and cross-stream velocity, the streamflow simulations represent both the magnitudes and structure of flow reasonably well, including the position of the velocity maxima and the strength of the cross-stream flow.

The model's ability to simulate the velocity flow field, bed shear stress, and sediment mobility is constrained largely by (1) the accuracy and level of channel geometry detail, especially regarding errors that could arise because topography was measured during varying streamflows and because different streamflows were used in the model, and because the accuracy of the current topology available for Shorty Island is not known, (2) the way the relation between streamflow and bedforms was characterized, and (3) the potential errors incurred by applying a steady-state model to unsteady flow situations. Although strong evidence indicates that pre-dam and dam-era channel geometry generally are similar, the accuracy of streamflow simulations for pre-dam peak flows is expected to be less than streamflow simulations for dam-era peak flows. Velocity conditions at the upstream boundary of the model grid have a profound effect on the flow simulation for roughly the upper 1 km of the modeling reach. Velocity conditions have been specified at the upstream boundary in the model based on field measurements taken at the boundary during streamflows of 776 m³/s and 1,260 m³/s. Velocity boundary conditions may vary for streamflow conditions that are greater or less than streamflow during field measurements.

The MultiDimensional Surface-Water Modeling System model was used to simulate the water-surface elevation, depth, velocity flow field, bed shear stress, and sediment mobility for the study reach in the Kootenai River for the same range of streamflows used in calibration. Spawning events per unit of effort during 1994-2001 in the white sturgeon critical-habitat reach are graphically presented along with modeling results. A few simple simulations demonstrate how the model

can be used to link physical characteristics of streamflow to biological or other habitat data. Some measures of depth, velocity, and substrate composition generally are considered when assessing sturgeon spawning habitat. Habitat suitability curves developed for white sturgeon in the Lower Columbia River were used to characterize conditions in the Kootenai River spawning habitat. Requirements for Kootenai River white sturgeon spawning habitat may vary from that in the Lower Columbia River; however, both rivers are highly regulated.

The modeling results do not support the hypothesis that the relative location of free-flowing and backwater streamflow may play a role in influencing white sturgeon spawning patterns. During 2001, spawning occurred further upstream than any other time during 1994-2001, at the same time, free-flowing streamflow was further downstream than any other spawning event during the same period. The 2001 observations appear not to support the hypothesis that the upstream extent of sturgeon spawning is set by the location of the backwater transition.

Egg collection on the Kootenai River during the past 12 spawning seasons shows that sturgeon eggs tend to accumulate in the thalweg, where depths can exceed 14 m. Habitat suitability in the straight reach ranges from poor to excellent and in the meandering reach is generally excellent. Although a comparison of simulated river depth and sturgeon spawning event locations (egg locations) in the critical-habitat reach indicate that egg locations are preferentially found in deeper areas, careful analysis suggests that this is only a weak positive correlation. Eggs are only slightly more likely to be found in deeper parts of the river. This correlation becomes slightly stronger if simulation results upstream of Ambush Rock (in the straight reach) are neglected.

Studies on the Columbia River indicate that sturgeon seek areas of high velocity for spawning. In other studies, lake sturgeon were found to spawn in tributary rapids. Spawning habitat suitability for streamflow velocity in the model was evaluated. In the meander reach, the average velocity at streamflows of 1,700 and 2,270 m³/s is classified moderate except for parts of the reach at Shorty Island, where velocity is classified poor; streamflows of 1,130 m³/s and less are classified poor. In the straight reach, the average velocity at all streamflows is classified poor to moderate except at a streamflow of 170 m³/s, which is classified poor throughout the reach.

Streamflow velocities equal to or greater than 1.0 m/s are believed to greatly reduce or eliminate predation of white sturgeon eggs. The simulated average velocity in the main channel at Shorty Island, where white sturgeon most frequently spawn, does not approach 1.0 m/s until streamflow is 2,270 m³/s, and this only occurs near RKM 231.1. However, maximum simulated velocity in the spawning reach is greater than 1.0 m/s for flows equal to and greater than a streamflow of 1,130 m³/s.

Quantification of sediment mobility provides preliminary insight into streamflow requirements for flushing silt and sand currently burying gravel and cobble substrate that could be used for spawning and egg incubation. Very-fine to fine gravel is mobile in the straight reach for all five streamflow simulations; however, at the lowest streamflow of 170 m³/s gravel is mobile in only the upper half of the reach. Very coarse sand is not mobile for about the lower third of the straight reach for the 170 m³/s streamflow simulation. Gravel becomes slightly more mobile at higher streamflows. In contrast to the straight reach, very fine gravel (b-axis diameter of 2.0 mm) is mobile in the meandering reach for only the three highest streamflow simulations of 1,130, 1,700, and 2,270 m³/s.

References Cited

- Barton, G.J., 2004, Characterization of channel substrate, and changes in suspended sediment transport and channel geometry in white sturgeon spawning habitat in the Kootenai River near Bonners Ferry, Idaho, following the closure of Libby Dam: U.S. Geological Survey Water-Resources Investigations Report 03-4324, 102 p.
- Barton, G.J., and Ireland, S., 2000, Simulation of sediment transport in white sturgeon spawning habitat and assessment of the feasibility of enhancing spawning substrate, Kootenai River, Idaho: Columbia Basin Fish and Wildlife Authority, accessed August 4, 2005, at <http://www.cbfwa.org/FWProgram/ResultProposal.cfm?PPID=MC2002000024009>
- Barton, G.J., Moran, E.H., and Berenbrock, C., 2004, Surveying cross sections of the Kootenai River between Libby Dam, Montana, and Kootenay Lake, British Columbia, Canada: U.S. Geological Survey Open-File Report 2004-1045, 34 p.
- Bennett, J.P., 1995, Algorithm for resistance to flow and transport in sand-bed channels: *Journal of Hydraulic Engineering*, v. 121, no. 8, p. 578-590.
- Bennett, J.P., 2001, Mixed-size sediment transport model for networks of one-dimensional open channels: U.S. Geological Survey Water-Resources Investigations Report 01-4054, 41 p.
- Berenbrock, Charles, 2005, 1D Simulations of hydraulic characteristics in the white sturgeon spawning habitat of the Kootenai River near Bonners Ferry, Idaho: U.S. Geological Survey Scientific Investigations Report 2005-5110, 30 p.
- Berenbrock, Charles, and Bennett, J.P., 2005, Simulation of flow and sediment transport in the white sturgeon spawning habitat of the Kootenai River near Bonners Ferry, Idaho: U.S. Geological Survey Scientific Investigations Report 2005-5173, 43 p.
- Collier, M., Webb, R., and Schmidt, J.C., 1996, Dams and rivers—primer on the downstream effects of dams: U.S. Geological Survey Circular 1126, 94 p.
- Dinehart, R.L., 2003, Spatial analysis of ADCP data in streams, in Workshop on Sediment Monitoring Instrument and Analysis Research: Flagstaff, Ariz., September 2003, Proceedings U.S. Geological Survey, 8 p.
- Dinehart, R.L., and Burau, J.R., 2003, Repeated surveys by acoustic Doppler current profiler for flow and sediment dynamics in Delta Cross Channel, in Proceedings of the CALFED Science Conference: Sacramento, Calif., January 2003: CALFED Bay-Delta Program, p. 43.
- Dinehart, R.L., and Burau, J.R., in press, Repeated surveys by acoustic Doppler current profiler for flow and sediment dynamics in a tidal river: *Journal of Hydrology*.
- Duke, S., Anders, P., Ennis, G., Hallock, R., Hammond, J., Ireland, S., Laufle, J., Lauzier, R., Lockhard, L., Marotz, G., Paragamian, V., and Westerhol, R., 1999, Recovery plan for Kootenai River white sturgeon (*Acipenser transmontanus*): *Journal of Applied Ichthyology*, v. 15, p. 157-163.
- Henderson, F.M., 1966, Open channel flow: Upper Saddle River, New Jersey, Prentice-Hall, Inc., 522 p.
- Julien, P.Y., 1998, Erosion and sedimentation: Cambridge University Press, 280 p.
- Julien, P.Y., 2002, River mechanics: Cambridge University Press, 434 p.
- Lisle, T.E., Nelson, J.M., Pitlick, J., Madej, M.A., and Barkett, B.L., 2000, Variability of bed mobility in natural, gravel-bed channels and adjustments to sediment load at local and reach scales: *Water Resources Research*, v. 26, no. 12, p. 3743-3755.
- McDonald, R.R., Bennett, J.P., and Nelson, J.M., 2001, The USGS multi-dimensional surface water modeling system, in Proceedings, 7th U. S. Interagency Sedimentation Conference: Reno, Nev., p. I-161-I-167.
- McDonald, R.R., Nelson, J.M., Barton, G., and Paragamian, V., 2004, Flow and sediment-transport modeling of Kootenai River White Sturgeon spawning habitat: *Eos Transactions, American Geophysical Union*, v. 85, no. 47, Abstract H53B-1239.
- McDonald, R.R., Nelson, J.M., and Bennett, J.P., in press, Multi-dimensional surface-water modeling system user's guide: U.S. Geological Survey Techniques and Methods, book 6, chap. B2.
- McDonald, R.R., Nelson, J.M., Kinzel, P.J., Conaway, J., in press, Modeling surface-water flow and sediment mobility with the Multi-Dimensional Surface Water Modeling System (MD_SWMS): U.S. Geological Survey Fact Sheet 2005-3078.
- McLean, S.R., 1992, On the calculation of suspended load for noncohesive sediments: *Journal of Geophysical Research*, v. 97(C4), p. 5759-5770.

- Nelson, J.M., Bennett, J.P., and Wiele, S.M., 2003, Flow and sediment-transport modeling, *in* Kondolf, G.M., and Piegay, H., eds., *Tools in fluvial geomorphology*: England, Wiley, p. 539-576.
- Nelson, J.M., and McDonald, R.R., 1997, Mechanics and modeling of flow and bed evolution in lateral separation eddies: Bureau of Reclamation, Glen Canyon Environmental Studies Report, 69 p.
- Nelson, J.M., McLean, S.R., and Wolfe, S.R., 1993, Mean flow and turbulence fields over two-dimensional bed forms: *Water Resources Research*, v. 29, no. 12, p. 3935-3963.
- Nelson, J.M., and Smith, J.D., 1989a, Flow in meandering channels with natural topography, *in* Inkeda, S., and Parker, G., eds., *River meandering*: Washington, D.C., American Geophysical Union Water Resources Monograph, v. 12, p. 69-102.
- Nelson, J.M., and Smith, J.D., 1989b, Evolution and stability of erodible channel beds, *in* Inkeda, S., and Parker, G., eds., *River meandering*: Washington, D.C., American Geophysical Union Water Resources Monograph, v. 12, p. 311-377.
- Northcote, T.G., 1973, Some impacts of man on Kootenay Lake and its salmonids: Ann Arbor, Mich., Great Lakes Fishery Commission Technical Report no. 25, 25 p.
- Parsley, M.J., and Beckman, L.G., 1994, White sturgeon spawning and rearing habitat in the lower Columbia River: *North American Journal of Fish Management*, v. 14, p. 812-827.
- Parsley, M.J., Beckman, L.G., and McCabe Jr., G.T., 1993, Spawning and rearing habitat used by white sturgeon in the Columbia River downstream of McNary Dam: *Transactions of the American Fisheries Society*, v. 122, p. 217-227.
- Paragamian, V.L., Barton, G.J., and Ireland, S., 2001, Have we found the pre-Libby Dam spawning location of Kootenai River white sturgeon? [abs.], *in* Proceedings, Idaho Chapter of the American Fisheries Society Annual Meeting: February 22-24, 2001, Boise, Idaho, p. 1.
- Paragamian, V.L., Beamesderfer, R.C., and Ireland, S.C., 2005, Status, population dynamics, and future prospects of the endangered Kootenai River white sturgeon population with and without hatchery intervention—Spawning locations and movement of Kootenai River white sturgeon: *Transactions of the American Fisheries Society*, v. 134, 14 p.
- Paragamian, V.L., Wakkinen, V.D., and Crews, G., 2002, Spawning locations and movement of Kootenai River white sturgeon: *Journal of Applied Ichthyology*, v. 18, 9 p.
- Shields, A., 1936, Application of similarity principles and turbulence research to bed-load movement: *Berlin, Mitteilungen der Preuss, Versuchsanst fur Wasserbau und Schiffbau*, no. 26, 10 p.
- Simons, D.B., and Richardson, E.V., 1961, Forms of bed roughness in alluvial channels, *in* Proceedings of the American Society Civil Engineers: May 1961, v. 87, no. HY3, p. 87.
- Smith, J.D., and McLean, S.R., 1977, Spatially averaged flow over a wavy surface: *Journal of Geophysical Research* v. 84, no. 12, p. 1735-1746.
- Snyder, E.B., and Minshall, G.W., 1996, Ecosystem metabolism and nutrient dynamics in the Kootenai River in relation to impoundment and flow enhancement of fisheries management: Idaho State University, Stream Ecology Center, variously paginated.
- Tetra Tech, Inc., 2003, Kootenai River geomorphic assessment: Seattle, Washington, 114 p.
- Thompson, D.M., Nelson, J.M., and Wohl, E.E., 1998, Interactions between pool geometry and hydraulics: *Water Resources Research*, v. 34(12), p. 3673-3681.
- U.S. Fish and Wildlife Service, 1999, Recovery plan for the Kootenai River population of the white sturgeon (*Acipenser transmontanus*): Portland, Oregon, variously paginated.
- U.S. Fish and Wildlife Service, 2000, Biological opinion on effects to listed species from operation of the Federal Columbia River Power System: Portland, Oregon, variously paginated.

Appendix A. Processing Acoustic Doppler Current Profiler Data

Spatial Mapping of Bed Elevation

The acoustic Doppler current profile (ADCP) measures a separate distance to the riverbed along each of four transducer beams. The four bed elevations at the point of beam contacts were computed using a custom algorithm (Dinehart and Burau, 2005). Points of bed elevation, accumulated over ADCP survey paths, were sufficient and widespread enough to allow useful extraction of a bathymetric surface. Each crossing path was offset from a previous path, which generated a distribution of bed-elevation points through the cross section. A bathymetric surface was created by interpolation of 1,000 points or more to a rectangular grid enclosing the range of crossing paths.

Velocity Ensembles

The ADCP velocity ensembles were filtered and smoothed by a series of algorithm passes (Dinehart and Burau, 2005). One pass removed statistical outliers of velocity-vector components at the bottom of each ensemble. Another pass numerically smoothed velocity data in two steps. Vector components exceeding the ensemble mean by 2.5σ (standard deviation) were first replaced directly by an average of nearest neighbors, removing extreme outliers that originate with velocity ambiguity of the ADCP. This operation was followed by a centered, three-point average applied to all interior components of velocity ensembles, using the formula,

$$u_b = 0.24u_{b-1} + 0.5u_b + 0.25u_{b+1} \quad , \quad (1)$$

where u_b signifies a vector component u , v , or w at an interior bin, and b ranges from $N=2$ to $N=$ (number of bins -1).

The irregular paths followed in ADCP surveys produced a curvilinear mesh of velocity ensembles when plotted in the channel reach. The sampled velocity ensembles were realigned and interpolated to regular grids for averaging different ensembles at similar positions. Previous studies of ADCP surveys have shown that secondary flows can be resolved by averaging multiple crossings of bends (Dinehart and Burau, 2005).

To derive a linear grid of averaged ADCP velocity vectors, it was necessary to translate the irregular positions of velocity ensembles in survey paths to the same linear cross section. Therefore, a procedure of “section straightening” was used to translate velocity ensembles spatially to a straight line. A mean crossing line was fit through a set of crossing paths to ensure that ensembles were translated minimally over measured bathymetry. The position of each ensemble was translated to the crossing line. The distance L from a distant start point of the crossing line (x_s, y_s) to each ensemble location (x_e, y_e) was calculated and applied with the angle θ of the crossing line above the x -axis in the form,

$$\begin{aligned} x_1 &= x_s + \cos(\theta)L \\ y_1 &= y_s + \sin(\theta)L \quad , \end{aligned} \quad (2)$$

to yield translated points x_1 and y_1 for each ensemble. Although some velocity ensembles were translated by several meters, the distance of translation was usually less than 10 percent of the channel width.

Grid Interpolation and Averaging

Flow-field ADCP data collected by repeated crossings were interpolated to 2-dimensional cross-sectional grids. The grids were constructed to match the bathymetric surface and water-surface elevations of the surveyed cross sections. A rectangular grid with specified i - j dimensions was created and then modified to match the cross-sectional bathymetry and vertical-spacing requirements. Lateral nodes across the channel were ordered by the i increment. Distances between i nodes approximated the original spacing of velocity ensembles. This usually yielded cell widths of 0.5 to 1 meter (m). Vertical j nodes at each i increment were extended to the bed from the water-surface elevation. Cell heights were set to approximate the original bin height (0.25 m) used during ADCP surveys.

The number of j nodes in a grid was calculated from the maximum depth in the cross section and the cell height. To maintain constant cell heights over irregular bathymetry in an ordered grid, extra j nodes were assigned closely spaced elevations within 0.3 m of the lower bathymetric boundary. This configuration was chosen to (1) maintain uniform vertical spacing of vector components over the measured range of velocity, and (2) isolate the extra j nodes within the near-bed region that was unmeasurable by ADCPs. By interpolating ADCP crossings to 2-dimensional cross-sectional grids, the random sequence of distances between ensembles was

replaced by regular intervals of velocity profiles. The velocity vectors were interpolated in Tecplot by an inverse-distance algorithm of the form

$$\phi_d = \frac{\sum w_s \phi_s}{\sum w_s}, \quad (3)$$

where ϕ_d and ϕ_s are the variable values at the grid nodes and in the ensembles, respectively. The weighting function, w_s , was set equal to $1/D^{3.5}$, where D is the distance between the random ensemble point and the target grid point. The algorithm weights a number of nearby vectors (source vectors) to derive a new vector value at each interpolated-grid node (target node). Each vector at a target node was interpolated from six source vectors chosen by an equipartite arrangement around the target node. This arrangement prevented the algorithm from selecting source vectors on only one side of the target node, or only source vectors within the same ensemble. With the high spatial density of source vectors and the low number used for interpolation, target vectors represented only the nearest ensembles of the source mesh.

To average multiple ADCP surveys, multiple grids of identical dimensions were created. Velocity vectors in each ADCP survey were interpolated to a single grid by weighting several source vectors to each target node. Vectors from all interpolated grids were then averaged at corresponding grid nodes. The ensembles of any ADCP survey are spaced variably because boat speed varies. If the set of ADCP surveys was averaged directly to a single grid, slow crossings would be weighted more than rapid crossings.

Therefore, an interpolation step was required first to yield a time-averaged velocity field with statistical validity. Inverse-distance interpolation of ADCP data provided only a first approximation of mean velocity fields because turbulent structures across velocity ensembles remained in the processed ADCP surveys.

From the central limit theorem, the standard deviation of many averaged crossings is expected to approach the population standard deviation. Averaging of N crossings at straight reaches showed that standard deviations of cross-stream and vertical velocities were proportional to $1/N^{0.5}$, and trended toward zero at large N . For vector components with a near-zero mean over time (cross-stream and vertical velocities), averages of multiple crossings approached their means rapidly with about six crossings (Randall Dinehart, U.S. Geological Survey, written commun., 2004), using the ADCP settings specified earlier. Standard deviations of streamwise components were less reduced because they reflected vertical and lateral variations in velocity profiles across the channel.

After averaged grids were prepared from multiple ADCP surveys, the vector components at each i node were averaged over the vertical.

References

- Dinehart, R.L., and Burau, J.R., in press, Repeated surveys by acoustic Doppler current profiler for flow and sediment dynamics in a tidal river: *Journal of Hydrology*.

Manuscript approved for publication, October 20, 2005

Prepared by the U.S. Geological Survey Publishing staff

Tacoma Publishing Service Center

Bill Gibbs

Debra Grillo

Ginger Renslow

Bobbie Jo Richey

Judy Wayenberg

For more information concerning the research in this report, contact the

Director, Idaho Water Science Center

230 Collins Road

Boise, ID 83702

<http://id.water.usgs.gov>



Barton and others

**Simulation of Flow and Sediment Mobility Using a Multidimensional Flow Model for the
White Sturgeon Critical-Habitat Reach, Kootenai River near Bonners Ferry, Idaho**

SIR 2005-5230